UNIVERSITY OF SOUTHERN QUEENSLAND

Depth of Anaesthesia Assessment Based on Time and Frequency Features of Simplified Electroencephalogram (EEG)

A Dissertation Submitted by

Tianning Li

Master, University of Adelaide, 2012
Bachelor, Nanjing University, 2009

For the award of

Doctor of Philosophy

2015

Abstract

Anaesthesiology is a medical subject focusing on the use of drugs and other methods to deprive patients' sensation for discomfort in painful medical diagnosis or treatment. It is important to assess the depth of anaesthesia (DoA) accurately since a precise assessment is helpful for avoiding various adverse reactions such as intraoperative awareness with recall (underdosage), prolonged recovery and an increased risk of postoperative complications for a patient (overdosage). Evidence shows that the depth of anaesthesia monitoring using electroencephalograph (EEG) improves patient treatment outcomes by reducing the incidences of intra-operative awareness, minimizing anaesthetic drug consumption and resulting in faster wake-up and recovery. For an accurate DoA assessment, intensive research has been conducted in finding "an ultimate index", and various monitors and DoA algorithms were developed. Generally, the limitations of the existing DoA monitors or latest DoA algorithms include unsatisfactory data filtering techniques, time delay and inflexible.

The focus of this dissertation is to develop reliable DoA algorithms for accurate DoA assessment. Some novel time-frequency domain signal processing techniques, which are better suited for non-stationary EEG signals than currently established methods, have been proposed and applied to monitor the DoA based on simplified EEG signals based on plenty of programming work (including C and other programming language). The fast Fourier transform (FFT) and the discrete wavelet transforms are applied to pre-process EEG data in the frequency domain. The nonlocal mean, mobility, permutation entropy, Lempel-Ziv complexity, second order difference plot and interval feature extraction methods are modified and applied to investigate the scaling behaviour of the EEG in the time domain. We proposed and developed three new indexes for identifying, classifying and monitoring the DoA. The new indexes are evaluated by comparing with the most popular BIS index. Simulation results demonstrate that our new methods monitor the DoA in all anaesthesia states accurately. The results also demonstrate the advantages of proposed indexes in the cases of poor signal quality and the consistency with the anaesthetists' records. These new indexes show a 3.1-59.7 seconds earlier time response than BIS during the change from awake to light anaesthesia and a 33-264 seconds earlier time response than BIS during the change from deep anaesthesia to moderate anaesthesia.

Certification of Dissertation

I certify that the ideas, experimental work, results, analyses, software and conclusions reported in this dissertation are entirely my own effort, except where otherwise acknowledged. I also certify that the work is original and has not been previously submitted for any other award, except where otherwise acknowledged.

Tianning Li — 29/11/2015

Signature of Candidate — Date

ENDORSEMENT

24/11/2015

Signature of Supervisors — Date

24/11/2015

Acknowledgement

My time at the USQ has been a great learning experience. I am extremely grateful to a number of people for their guidance and assistance.

Firstly I would like to express my gratitude to my Supervisor A/Professor Peng (Paul) Wen for his support, encouragement and patience. I am also grateful for his invaluable suggestions, discussion and confidence in my work.

I would like to thank A/Professor Armando Apan for his unparalleled encouragement, guidance and support, and A/Professor Yan Li for her guidance at the beginning of my PhD program. I would also like to acknowledge the technical and administrative support of the School of Mechanical and Electrical Engineering. Last but certainly not the least, my special gratitude goes to my parents, who have always been there for me and have shown consistent interest in my welfare.

List of related publications

The following papers, associated with the research contained in this dissertation, have been published or submitted for publication.

JOURNAL PAPERS

- **Li, T**, Wen, P & Jayamaha, S 2014, 'Anaesthetic EEG signal denoise using improved nonlocal mean methods', *Australasian Physical & Engineering Sciences in Medicine*, vol. 37, no. 2, pp. 431-437.

- **Li, T**, & Li, Y 2014, 'Depth of anaesthesia monitors and the latest algorithms', *Asian Pacific journal of tropical medicine*, vol. 7, no. 6, pp. 429-437.

- **Li, T**, Wen, P. 'Depth of Anaesthesia assessment using interval second order difference plot and permutation entropy techniques', Journal of the Institution of Engineering and Technology (IET) Signal Processing. Submitted on 3-4-2015 (Accepted).

CONFERENCE PAPER

- **Li, T,** Wen, P & Liu, G 2015, 'Depth of Anaesthesia Assessment using the second order different plot technique and feature evaluation method', In: CMECE 2015: International Conference on Mechanical, Electronics and Computer Engineering 24-26 Jan 2015, Zhuhai, China.

JOURNAL PAPER SUBMITTED

- **Li, T**, Wen, P. 'DoA Assessment Based on Timing Characteristics of EEG Beta Frequency Band.' Under review at the Journal of Biomedical Signal Processing and Control. Submitted on 25-7-2015.

Contents

List of Frequently used Acronyms and Abbreviations

AEP	Auditory Evoked Potential
BIS	Bispectrum Index
BS	Burst Suppression
BSR	Burst Suppression Ratio
CFAM	Central Function Analyzing Monitor
CSI	Cerebral State Index
CTV	Covariance with the Time Variable
DB	Daubechies Wavelet.
DFA	Detrended Fluctuation Analysis
DMA	Detrended Moving Average
DoA	Depth of Anaesthesia
DSP	Digital Signal Processing
DWT	Discrete Wavelet Transform
ECGs	Electrocardiograms
EEG	Electroencephalogram
EMG	Electromyogram
EOG	Electroocclugrams
FFT	Fast Fourier Transform
fMRI	functional Magnetic Resonance Imaging
IF	Interval Feature

IPE	Interval Permutation Entropy
ISOPE	Interval Second order difference plot
LCZ	Lempel-Ziv Complexity
LOC	Loss of Consciousness
MASP-NLM	Moving Adaptive Shape Patches- Nonlocal Mean
Mobility	Mobility
NLM	Nonlocal Mean
NLMWTD	Nonlocal Mean Wavelet Threshold Denoising
PCA	Patient Controlled Analgesia
PE	Permutation Entropy
PRDimp	Improved Percentage Distortion Ratio
PSD	Power Spectral Density
PSI	Patient State Index
RE	Response Entropy
SE	State Entropy
SNAP	Score of Neonatal Acute Physiology
SNRimp	Improved Signal to Noise Ratio
SODP	Second order difference plot
SQI	Signal Quality Indicator
USB	Universal Serial Bus
WE	Wavelet Entropy
WT	Wavelet Transform
WTD	Wavelet Threshold Denoising

List of Figures

List of Tables

1. INTRODUCTION

1.1. Depth of anaesthesia assessment

Anaesthesiology is a medical subject focusing on the use of drugs and other methods to deprive patients' sensation for discomfort in painful medical diagnosis or treatment. The anaesthesia depth is reflected in the change of the partial pressure of the anaesthetics in the brain (Nakamura, Sanjo, & Ikeda, 1999). Successful anaesthetic processes can be defined as patients achieving reversible loss of consciousness, no intraoperative awareness, and no reaction to pain stimuli.

It is extremely important to assess the depth of anaesthesia (DoA) accurately since a precise assessment is helpful for avoiding various adverse reactions such as intraoperative awareness with recall (underdosage), prolonged recovery and an increased risk of postoperative complications for a patient (overdosage). For patients, the intraoperative awareness is a terrible experience. It may cause serious mental illness. Although the incidence of intraoperative awareness has been reduced from 1-2% of the 1980s to the current 0.1%, there are still a lot of risks for some special procedures (such as caesarean section or heart surgery) or high-risk surgery patients. The incidence of intraoperative awareness may be over 40% for patients with multiple trauma or other special diseases (Ghoneim & Block, 1997; Myles et al., 2004).

The inhalation anaesthesia and intravenous anaesthesia are two main general anaesthesia. As for inhalation anaesthesia, experiences have shown that if the concentration of volatile gas in the blood is more than 50% of the minimum alveolar concentration, the intraoperative awareness will not happen. However, for some patients, it is more suitable to use intravenous anaesthesia. Nowadays, the existing general anaesthesia is normally using combined intravenous anaesthesia and inhalation anaesthesia to optimize the security and stability of operations.

Because of the individual patient differences, no clear explanations about the effects of narcotic drugs on the brain mechanism and also for other reasons, the accurate dose necessary to induce anaesthesia, assessing the DoA and determining the relationship of anaesthesia and consciousness are always persistent challenges for anaesthesiologists (Alfeeli & Agah, 2009). Therefore, more profound study about anaesthesia mechanisms and DoA algorithms is required to ensure patient safety, avoid intraoperative awareness, prevent narcotic drug overdose, reduce health care costs and reduce complications. The research for accurate DoA assessment is of great significance.

1.2. Real-time monitoring of depth of anaesthesia using EEG

It has been shown that there are reversible invariant electroencephalographic changes, independent of the drug used, and independent of the anaesthesia protocol (John, 2001). Determining the depth of anaesthesia using electroencephalography (EEG) is based on these changes related to increasing concentrations of anaesthetics in the blood. An intravenous agent propofol, for example, induces a continuum of neurophysiological changes, which reflect on the spectral properties of EEGs (Kortelainen, Koskinen, Mustola, & Seppänen, 2008). Unlike most clinical assessments such as systolic blood pressure, heart rate, sweating, lacrimation, limb movements, pulse and skin conductance, the DoA assessment based on EEG is more accurate because it is less impacted by the use of other drugs like muscle relaxants and vasodilators (Sebel et al., 2004).

Generally, the DoA assessment is based on the simplified forehead EEG signal analysis. There are two main ways to generate anesthesia index: Proactive monitoring (by stimulating the patient and then analyzing the activity of evoked potentials) and passive monitoring (by analyzing the EEG activity observed).

The EEG patterns change during anaesthesia. As the level of anaesthesia deepens, the EEG activity of high frequency bands decreases but the synchronous activity of low frequency bands enhances. The EEG signal becomes regular and the average of amplitude increase. The synchronization of EEG from frontal area and top area of head reduces. As the anaesthesia level deepens further, the amplitude and frequency of EEG signals are both reduced and the burst suppression phenomenon occurs. Therefore, it is advocated that the EEG signal can provide a reliable basis for the measurement of hypnosis or anaesthesia (Zikov, Bibian, Dumont, Huzmezan, & Ries, 2006). Evidence shows that the depth of anaesthesia monitoring using EEG improves patient treatment outcomes by reducing the incidences of intraoperative awareness, minimizing anaesthetic drug consumption and resulting in faster wake-up and recovery (Bowdle, 2006; Chen, Li, Xiong, Bao, & Li, 2010).

However, the high nonlinearity and nonstationarity make the processing of EEG and derivation of DoA hard. In addition, each individual patient is different, for instance, the degree of stimulation and pain induced by surgery are different and the use of concomitant analgesic drugs produce different results. Therefore, developing an accurate DoA index is a big challenge.

The traditional EEG analysis methods can be classified into time domain analysis methods and frequency domain analysis methods.

General time domain analysis methods are based on amplitude, mean, variance, kurtosis and so on. These methods are relatively simple and can only show a basic understanding of EEG signals.

Frequency domain analysis methods include the Fourier transform methods, Wavelet transform methods, Hilbert-Huang transform methods and so on. The EEG frequency values obtained by frequency domain analysis methods certainly have the physical

meanings and can be used for DoA assessments. In addition, there are also different nonlinear methods in EEG signal processing and DoA algorithm developments. They include entropy, complexity, detrended moving-average, Isomap-based estimation, detrended moving-average, Bayesian methods and so on. However, there is still a lack of consensus as to which physiological features constitute anaesthesia, and no general hypotheses exists for the mechanism of anaesthesia (Urban & Bleckwenn, 2002).

In the past few decades, many commercial DoA monitors are available. Among these DoA monitors, the Bispectral index (BIS) monitor, produced by the American Aspect company, is the most famous and widely used one. However, even for the BIS monitors, the warning from the Aspect company is "not recommended the anaesthetists simply rely on BIS monitor during surgery" ("Service information manual, Aspect Medical Systems, Inc.,") .

It has been reported that problems exist with the BIS monitor such as false alarm, time delay and fuzzy values (Liang, Li, & Li, 2009). In addition, electromyogram (EMG) and other high-frequency electrical artifacts interfere with EEG interpretation. Data processing time produces a lag in the computation of the DoA monitoring index. The EEG effects of anaesthetic drugs are not good predictors of movement in response to surgical stimulus and the currently available monitoring algorithms do not account for all anaesthetic drugs. Generally, the limitations of the existing BIS DoA monitor and DoA algorithms include unsatisfactory data filtering techniques, time delay and inflexible and low noise immunity problems.

1.3. Research objectives

This research aims to develop new methods to monitor the DoA in real time based on EEG data recorded during operations using the time-frequency domain analysis techniques. The objectives of this research are:

1. Develop reliable data filtering techniques to denoise recorded EEG signals;

2. Extract EEG features in time and frequency domains and to develop reliable DoA indexes:

- in the time and frequency domain using the fast Fourier transforms, mobility, permutation entropy and Lempel-Ziv complexity methods;
- in the time and frequency domain using the fast Fourier transforms, second order difference plot methods;
- in the time and frequency domain using the fast Fourier transforms, interval feature extraction, modified second order difference plot and modified permutation entropy methods;

3. Identify patient’s anaesthetic state in the case of poor signal quality;

4. Improve the time lag in DoA computation;

5. Evaluate and compare the proposed DoA indexes and their performance.

1.4. Outcomes and results

In this study, the EEG signals from the forehead are employed to monitor the DoA using both the time domain and frequency domain analysis methods. The fast Fourier transforms (FFT) and the discrete Wavelet transforms (DWT) are applied to pre-process EEG data in the frequency domain. The mobility (M), permutation entropy (PE), Lempel-Ziv complexity (LZC), second order difference plot (SODP) and interval feature extraction methods are applied to study the scaling behaviour of the EEG in the time domain. The conceptual framework of this study is presented in Figure 1.1 and Figure 1.2. Based on these above techniques, four new methods (one denoising method and three DoA indexes) are proposed and developed for monitoring the DoA and the outcomes are listed below.

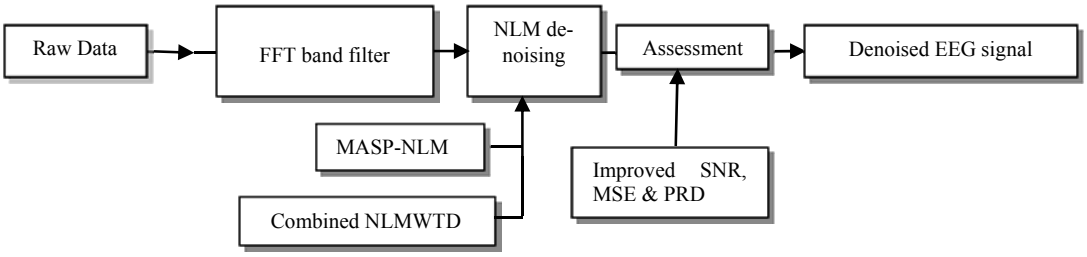

Figure 1.1: EEG signal filtering

To obtain satisfactory data filtering results, a modified nonlocal mean method was developed to denoise the raw EEG data. As a patch-based method, the nonlocal mean method (NLM) method calculates the weighted sum of a patch. The weight of each point is determined by the similarity between the points of the own patch and its neighbour. Based on the weighted sum, the noise is filtered out. After filtering some low frequency noise of raw data by the FFT band filter, the NLM method was applied for EEG signal denoising for the first time. The denoising results are compared with that of the popular sym8 and db16 Wavelet threshold denoising (WTD) methods. On average, the NLM achieves 2.70dB increase in improved signal to noise ratio (SNRimp) and 0.37% drop in improved percentage distortion ratio (PRDimp) compared with WTD. A modified nonlocal mean method, the moving adaptive shape patches- nonlocal mean method (MASP-NLM), performs even better than the original NLM when the signals change dramatically. In addition, the performance of the combined NLMWTD method is also better than the original WTD method (0.50dB to 4.89dB higher in SNRimp), especially, when the signal quality is poor.

Three new indexes, which are developed based on the denoised signals, are developed and evaluated. All of them are able to continuously assess the DoA of patients while the quality of signal was poor and the popular BIS did not have any valid outputs.

It is shown in Figure 1.2 that EEG signals of different frequency bands were obtained using FFT band filter from denoised EEG data. Then the parameters such as Ms, LZCs, PEs and SODPs were calculated from the EEG signals of different frequency bands

using four feature extraction methods (mobility, Lempel-Ziv complexity, permutation entropy and second order difference plot methods). After that, these different parameters were selected to form parameter sets. Three new DoA indexes were designed based on these parameter sets. Eventually, the performances of new indexes were evaluated by comparing to the most popular BIS index and patients' clinical records.

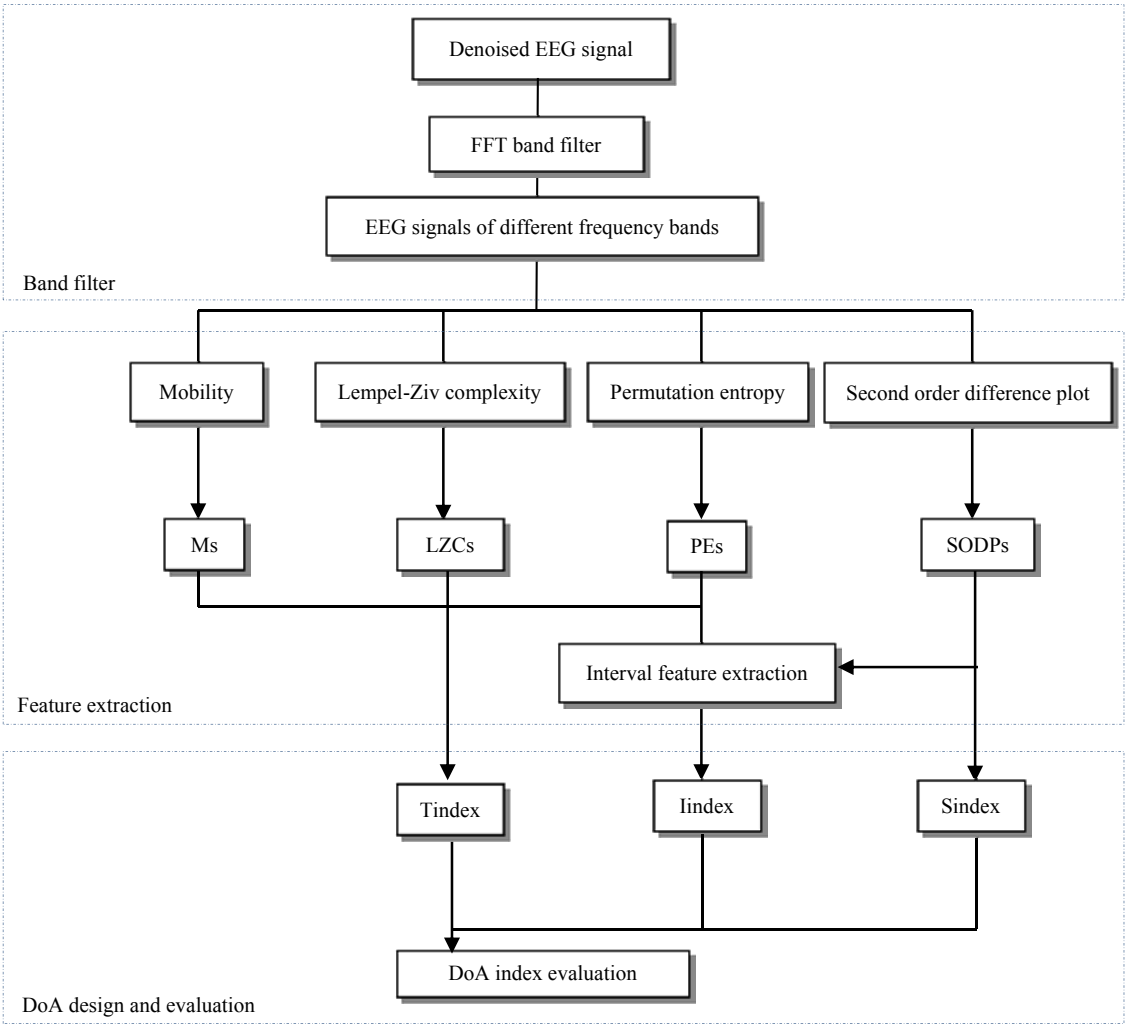

Figure 1.2: Diagram for methodologies of feature extraction and DoA index design

To improve the time lag in DoA computation, two new DoA indexes are developed. They are Tindex and Iindex which are designed based on parameters of M, SODP, PE and LZC.

The mobility is a timing characteristic calculated from the variance and the variances of the signal and the first derivative of the signals. As a graphical representation of successive rates against each other, the second order difference plot provides a rate of data variability. This technique has been used in EEG signal processing (Thuraisingham, Tran, Boord, & Craig, 2007) and classification (Pachori & Patidar, 2014). There the SODP and M parameters are used to assess the DoA for the first time.

The Lempel-Ziv complexity and permutation entropy were also applied to extract the feature from EEG signals in this study. As an effective method of measuring for characterizing the randomness of signals, the Lempel-Ziv complexity is a commonly used method in biomedical signal processing (McBride et al., 2014). The permutation entropy, based on symbolic dynamics, was also proposed to measure the complexity in an electroencephalographic series (Bandt & Pompe, 2002).

The these new indexes are evaluated and compared with measured BIS. The results show that there is a very close correlation between the proposed indexes and the BIS during different anaesthetic states.

The Iindex shows an earlier time response (3.1-59.7 seconds) than BIS during the change of anaesthetic states from consciousness to unconsciousness. The Tindex also shows a 33-264 seconds earlier time response than BIS from deep anaesthesia to moderate anaesthesia.

To enhance the flexibility of DoA index, the three new indexes are developed based on four different parameters which are calculated from different EEG frequency bands. All of the three indexes show better performance than BIS index in case of poor signal quality.

The noise immunity problems of existing DoA assessment methods are noted in this research. In some cases, the popular BIS index does not have any valid outputs or shows incorrect DoA results because of noise. However, the new indexes can accurately assess the patients' anaesthetic states according to the clinical records.

In addition, the interval feature method was applied to increase the robustness of DoA algorithms. The features derived from different signal segments, called "interval features", are able to lead to high classification accuracy (Rodríguez, Alonso, & Maestro, 2005). Using the interval feature method, it is possible to only extract more features from the same signals but also obtain interval features from different lengths. The new Iindex is designed based on the interval second order difference plot (ISODP) and interval permutation entropy (IPE) techniques. ISODP and IPE make the new DoA index smoother than the BIS index and clearly respond to the change of index trends which can be seen from most cases of this study.

1.5. Presentation of the dissertation

The dissertation consists of seven chapters. The development of a reliable DoA index is the focus of this study. Chapters 4-7 illustrate various time and frequency domain analysis methods and their applications in the accurate assessment of DoA.

Chapter 1 introduces the depth of anaesthesia assessment and significance, real-time monitoring depth of anaesthesia using EEG, research objectives, outcomes and thesis outline.

Chapter 2 provides a comprehensive literature overview about the DoA assessment which includes anaesthesia and clinical practice, DoA monitors and EEG, basic methods and techniques, limitations of existing DoA monitors and DoA assessment methods, and potential improvements.

Chapter 3 describes BIS system configuration and EEG data acquisition. It includes data acquisition, equipment settings, data format and normalization and signal quality.

Chapter 4 presents a modified nonlocal mean denoising method. Its results are compared with that of the popular sym8 and db16 Wavelet threshold denoising methods. The results show that the NLM, on average, achieves 2.70dB increase in improved signal to noise ratio and 0.37% drop in improved percentage distortion ratio compared to the popular sym8 and db16 Wavelet threshold denoising methods. Two modified nonlocal mean methods, the moving adaptive shape patches-NLM and combined NLMWTD denoising methods, are also introduced and evaluated in this chapter.

Chapter 5 applies timing characteristics of EEG Beta frequency band to assess the DoA. The M, PE and LCZ parameters of Beta frequency bands (21.5-30Hz) are selected to form the parameter set and to design a new DoA index. The results demonstrate that the new index can clearly discriminate the awake, light anaesthesia, moderate anaesthesia, and deep anaesthesia states. The new index also shows a 33-264 seconds earlier time response than BIS during the change of anaesthetic states. In addition, the proposed index is able to continuously assess the DoA of patients while the quality of signal was poor and the BIS did not have any valid outputs.

Chapter 6 applies a regression technology-based parameter evaluation method to evaluate the correlation between the SODPs calculated from different frequency components in the EEG signal. The best parameter set of SODP is selected to design a new DoA index. The results show that there is a very close correlation between the proposed index and the BIS during different anaesthetic states. The proposed DoA index is able to continuously assess the DoA of patients and agree with the clinical records while BIS did not have any valid outputs.

Chapter 7 extends the SODP method to apply the interval second order difference plot and the interval permutation entropy techniques to assess the DoA. The new index shows an earlier time response (3.1-59.7seconds) than BIS during the change of anaesthetic states. In addition, the proposed index is able to provide valid DoA index while the quality of signal was poor and the BIS did not have any valid outputs.

Chapter 8 summarises the major outcomes and conclusions of this study. The chapter also presents the possible future work in this area based on this work.

2. BACKGROUND AND LITERATURE REVIEW

This chapter reviews the existing depth of anaesthesia monitors and their algorithms, identifies their problems. The latest research results show that their performance can be improved further using up-to-date computing techniques and neural research outcomes.

2.1. Anaesthesia and clinical practice

2.1.1. The process of anaesthesia

Anaesthesia is used to decrease sensitivity to pain of patients during surgeries. For different surgeries, general anaesthesia and local anaesthesia are applied to make patients partially or totally lose consciousness. Only general anaesthesia is concerned in this research. The three phases to general anaesthesia are induction, maintenance and emergence. The descriptions of anaesthetic type and process are introduced in the Table 2.1.

Table 2.1: Anaesthetic type and process (Tai Nguyen-Ky, 2011)

	Name	Descriptions
Type	**General anaesthesia**	It affects the whole body and leads to a loss of consciousness.
	Local anaesthesia	It temporarily blocks the sensation of pain in a certain part of the body while the patient remains awake
Process of general anaesthesia	**Induction**	The initial state of unconsciousness.
	Maintenance	Keeping patient unconscious.
	Emergence	Patient emerges from unconscious into awake.

There are four parts for a typical anaesthetic procedure: premedication, induction, maintenance and recovery. Pharmacological methods are used for the whole medical procedures of general anaesthesia.

2.1.2. Anaesthetic medicines

From 1840 to 1860, Nitrous oxide, Ether and Chloroform were introduced as anaesthetic drugs. At the end of the 1890s, Ethylchloride was used for the first time. After 1920, the species of anaesthetic agents used increased quickly. The Ethlene, Vinethene, Pentobarbital, Cyclopropane, Trichlorethylene, Thiopental, Isopropenylvinylether, Propylmethylether, Meperidine, Fluroxene, Althesin, Ethylvinylether, Halothane, Methohexital, Droperidol, Methoxyflurane, Ketamine, Enflurane, Isoflurane, Etomidate, Fentanyl, Midazolam, Sevoflurane, Alfentanyl, Sufentanil, Propofol, Desflurane, Remifentanil and Xe were introduced as anaesthetic agents in succession in the 20th century (Urban & Bleckwenn, 2002). Nowadays, the Propofol, Parecoxib, midazolam, fentanyl and alfentanil are still widely used for modern general anaesthesia.

Anaesthetics are available in three formulations: gases (vapours), injections (intravenous anaesthetics) and external application. Generally, the gases and injections are used for general anaesthesia.

Table 2.2: Anaesthetic agent administration

Type	Descriptions
Injection	The drug is injected into muscle, vein (intravenously) or under the skin with a needle.
Gases	The drug is applied with a gas mask for inhalation.
External application	Creams, gels, liquids are applied directly onto the body tissues being treated.

The most commonly used anaesthetic protocol is to induce anaesthesia intravenously, then maintain it with anaesthetic gases (Tai Nguyen-Ky, 2011). The hypnotic, analgesic and muscle relaxant are typically applied together in general anaesthetics. Before different agents are combined for patients, several important factors need to be considered: their characteristics, their relative concentrations with respect to each other,

and bolus or continuously intravenous dose (Urban & Bleckwenn, 2002). For the patients in different cases, the type and doses of anaesthetic agents are decided by anaesthetists based on their experiences.

2.1.3. Anaesthesia and awareness

A precise assessment of DoA is helpful for avoiding various adverse reactions such as intraoperative awareness with recall (underdosage), prolonged recovery and an increased risk of postoperative complications for a patient (overdosage).

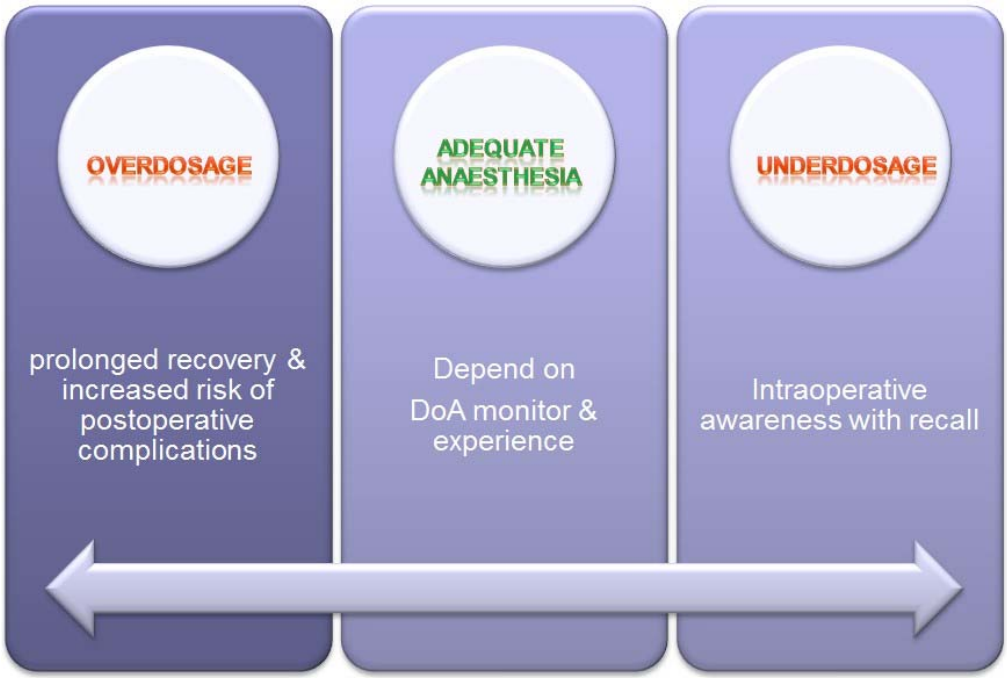

Figure 2.1: Significance of DoA assessment

Awareness in general anaesthesia most often refers to remembering events from the procedure and signifies inadequate anaesthesia. The figure below shows the relationship between consciousness and anaesthetic agents.

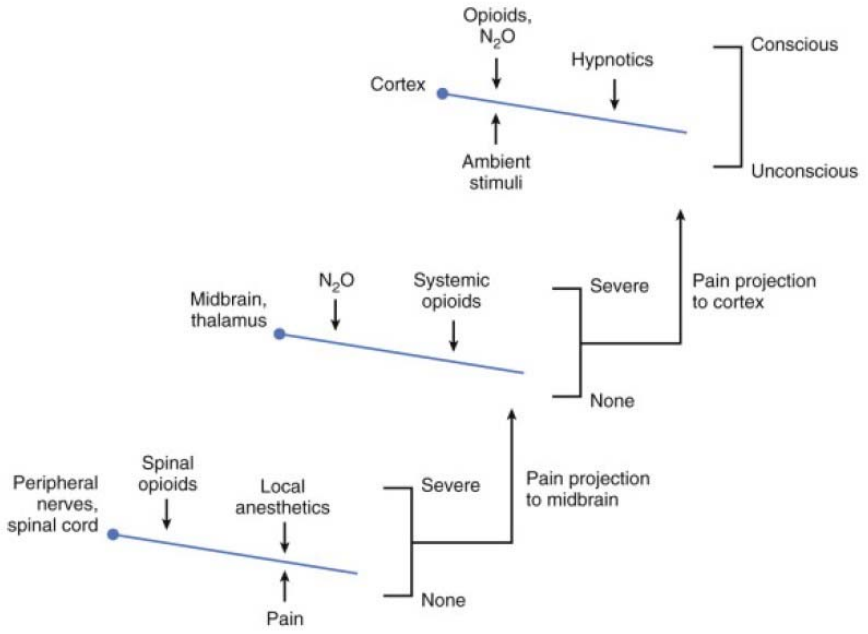

Figure 2.2: Hierarchical model of the interaction between pain and anaesthetic agents to achieve unconsciousness (Gelb, Leslie, Stanski, & Shafer, 2010).

The Hierarchical model introduced by Gelb et al. (2010) describes anaesthesia as a hierarchical system in which anaesthetic agents operate at three distinct levels in the nervous system. When a patient is under dosage, there is not enough anaesthetic or analgesic to prevent consciousness during the operation process. This leads to awareness during surgery (Brice, Hetherington, & Utting, 1970). Intraoperative awareness occurs in 0.1% of cases in low risk procedures (Jones & Aggarwal, 2001; Myles et al., 2004; Sandhu & Dash, 2009) and 4% of cases in high risk procedures (Tonner & Bein, 2006). Moreover, the incidence of intraoperative awareness may be over 40% for patients with multiple trauma, patients undergoing caesarean section or cardiac surgery and haemodynamically unstable patients (Davidson et al., 2005; Kuizenga, Wierda, & Kalkman, 2001; Mathews, Rahman, Cirullo, & Malik, 2005; Tai Nguyen-Ky, 2011).

When the intraoperative awareness happens, patients may feel the pain or pressure of operation, hear conversations, or feel they cannot breathe. As a result, the intraoperative awareness may cause severe postoperative psychosomatic dysfunction. Therefore, intraoperative awareness, which is caused by a failure to adequately anaesthetise, is treated as a medico-legal liability for anaesthetists (Lennmarken, Bildfors, Enlund, Samuelsson, & Sandin, 2002; Moerman, Bonke, & Oosting, 1993; Sandin, Enlund, Samuelsson, & Lennmarken, 2000; Sebel et al., 2004).

On the other hand, the over dosage may lead to a serious brain injury, nerve damage, paralysis, or a spinal cord injury of patients. It may also cause serious complications such as a heart attack; stroke or even death (One case reported during patient-controlled analgesia (PCA)) (Bøggild-Madsen & Cargnelli, 1978; Musshoff, Padosch, & Madea, 2005; Tai Nguyen-Ky, 2011).

A number of methods have been developed over the years to detect the level of consciousness and determine the depth of anaesthesia clinically. Most clinical assessments

are based on biophysical signs such as systolic blood pressure, heart rate, sweating, lacrimation, limb movements, pulse and skin conductance. However, the use of other drugs like muscle relaxants and vasodilators makes the interpretation of clinical signs harder, and cases of intraoperative awareness have been reported (Sebel et al., 2004). In addition, the clinical manifestations of individual patients are different. Therefore, those clinical methods do not achieve the desired accuracy in anaesthetic depth assessment (Nguyen-Ky, Peng Wen, & Yan Li, 2013b).

2.2. EEG and DoA monitors

2.2.1.Human brain and neural networks

The human brain, a complex structure, is a network with 100 billion units and 100 trillion connections. The neuron is a single brain cell which is the fundamental unit of the brain. The structure of a neuron is shown in Figure 2.3.

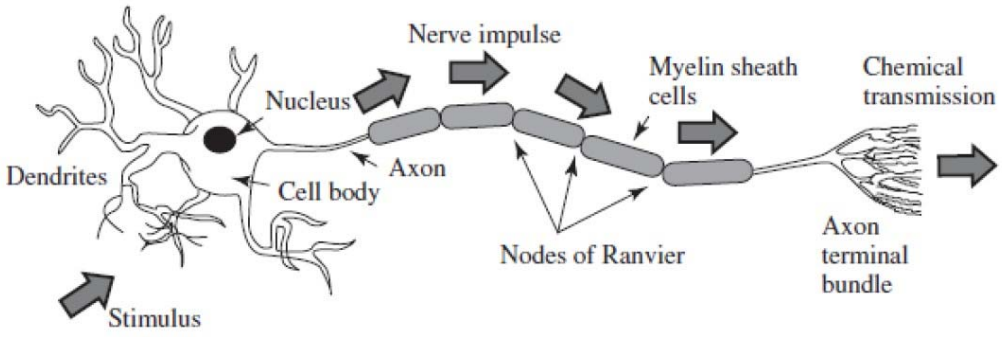

Figure 2.3: Structure of a neuron (Atwood & MacKay, 1989)

The electrical impulses and chemical secretions enable the neurons to communicate to each other. The electrical impulses have a specific amount of influences or weights on the neuron, and transport from one neuron to another. This kind of transmission activates the neuronal network and leads to a noticeable change in voltage. A special apparatus called electroencephalograph can be capture the changes in voltage, and shows continuous oscillating electric activities (Antognini, Carstens, & Raines, 2003; Atwood & MacKay, 1989; Bischoff, Schmidt, & am Esch, 2000; Nguyen-Ky, 2011; Saeid & Chambers, 2007).

2.2.2. EEG and DoA

As the amount of anaesthetic agent increase, the typical patterns of EEG signals show the characteristics that average amplitude increase and average frequency decline. It has been shown that there exists reversible invariant EEG changes, independent of the drug used, and independent of the anaesthesia protocol (John, 2001). Hence, it is advocated that the EEG signal can provide a reliable basis for deriving a surrogate measurement of hypnosis and anaesthesia (Zikov et al., 2006).

Determining the depth of anaesthesia using the EEG is based on the changes in signal characteristics related to increasing concentrations of anaesthetics in the blood. An intravenous agent propofol, for example, induces a continuum of neurophysiological changes, which reflect on the spectral properties of EEG (Kortelainen et al., 2008). However, the EEG signals are the signatures of neural activities (Sanei & Chambers, 2008), their great nonlinearity and nonstationarity make the EEG signals hard to assess. In addition, individual patients have variability and various factors, for instance, the degree of stimulation and pain induced by surgery and the use of concomitant analgesic drugs. Therefore, developing an accurate DoA index is indeed challenging work.

2.2.3. Instrumental monitoring

For an accurate DoA assessment, intensive research has been conducted in finding "an ultimate index", and various monitors were developed to assess the DoA, including central function analyzing monitor (CFAM) (Maynard & Jenkinson, 1984), Bispectral (BIS) monitor, Nacotrend monitor, Patient State Analyser 4000, Score of Neonatal Acute Physiology (SNAP) monitor, Auditory evoked potential (AEP) monitor, Entropy-Module, Cerebral State monitor (CSM), and Index of Consciousness (IoC) monitor. With the advanced DoA monitors, the incidences of awareness have been reduced from about 1–2% in the 1980s to about 0.1% in 2010 (Musizza & Ribaric, 2010).

The Narcotrend Monitor was first introduced by Narcotrend in 2000, Germany. Compared to the BIS, the Narcotrend seems to perform better during emergence as it regains its baseline value upon discontinuation of the drug effect (G. N. Schmidt et al., 2003). The Danmeter company designed the first generation of the AEP monitor in 2001 and then AEP-Monitor/2. The new version applied autoregressive models with exogenous input to detect the AEP and added spectral EEG parameters to build DoA index (Musizza & Ribaric, 2010). In 2002, Physiometrix introduced the PSA-4000, which also displays a dimensionless number: the Patient State Index (PSI). While the PSI is based on similar principles to the BIS (i.e., composite index based on spectral and bispectral parameters), it differs in that it focuses on the power shift of specific frequency components between the frontal cortex and the posterior lobes. In the same year, the Score of Neonatal Acute Physiology (SNAP) monitor, the first Personal Digital Assistant (PDA)-based DoA monitor, was introduce by Nicolet Biomedical Monitors. It assesses high and low frequency EEGs and outputs a SNAP index that ranges from 0 to 99 (awake) (Willmann, Springman, Rusy, & Daily, 2002).

The Morpheus medical company introduced the Index of Consciousness (IoC) monitor whose main algorithm is the symbolic dynamics method, which divides an EEG signal

into a finite number of partitions with certain symbols and uses the alternations of symbols to determine the dynamics of the EEG. Entropy index monitoring produced by Datex-Ohmeda in 2003 was based on the acquisition and processing of raw EEGs and facial electromyography signals by using entropy algorithms to produce two parameters: State Entropy (SE) and Response Entropy (RE) (Viertiö‐Oja et al., 2004). In 2004, Danmmeter devised the Cerebral State monitor (CSM). Its Cerebral State Index (CSI) is calculated using a fuzzy logic combination of four sub parameters of the EEG signals in time domain and frequency domain (Jensen, 2005). Besides, central function analysing monitor (CFAM) (Maynard & Jenkinson, 1984), which analyses EEG spectrum and amplitude, is rarely used because of the limitations of the early technologies.

Table 2.3: Comparison of DoA monitors summarized from (Musizza & Ribaric, 2010).

	BIS	**Narcotrend**	**PSA 4000**	**AEP-Monitor/2**	**Entropy Module**	**CSM**	**IoC**
Database included in the development of algorithm or for inference	Yes	Yes	Yes	No; index based on previous studies of the algorithm	No; index based on previous studies of the algorithm	No; index based on previous studies of the algorithm	No; index based on previous studies of the algorithm
Features or methods included in algorithm	Bispectral analysis, beta-ratio	SEF, median frequency, spectral entropy, relative δ, Θ, α, β, AR model	Several frequency domain features extracted from power spectrum	AEP, ARX model	Multiscale analysis, entropy, spectral entropy	α, β, α-β power ratios	Symbol dynamics analysis
Surrogate analysis	No	Yes	Yes	Yes	No	No	No
Burst suppression analysis	Yes	Yes	Yes	Yes	Yes	Yes	Yes
Index calculation	Weighted sum of sub-parameters	Classification function with plausibility analysis	Plausibility analysis with surrogate testing against BSR and arousal parameters	Modulation of index based on SNR and EMG	Entropy, no inference algorithm	Fuzzy logic inference system	Fuzzy logic inference system

In Musizza's research, a detailed comparison of different DoA monitors was reported (Musizza & Ribaric, 2010). They discussed the advantages and disadvantages of different monitors according to their algorithms at full length (See the summary in).

In this chapter, we analyse the performance of different DoA monitors in clinical use and the functions of the latest models.

2.2.3.1. BIS Index

The BIS index (A-2000 BIS monitor; Aspect Medical Systems Inc., Newton, MA) is a single index derived from a set of time domain and frequency domain measures (Pomfrett & Pearson, 1998). It is calculated from the following four parameters: (i) burst suppression ratio (BSR); (ii) quazi suppression index; (iii) relative β ratio and (iv) synch fast slow. BIS is presented as a numerical index ranging from 100 (awake) to 0 (isoelectric EEG). Values below 60 indicate that the patient is almost certainly unconscious. Generally, the anaesthesia states include awake, light anaesthetic, moderate anaesthetic and deep anaesthetic states. The awake states are corresponding to the BIS range from 80 to 100, the light anaesthetic states are corresponding to the BIS range from 60 to 80, the moderate anaesthetic states are corresponding to the BIS range from 40 to 60, and the deep anaesthetic states are corresponding to the BIS range from 10 to 40 (Nguyen-ky, Wen, & Li, 2013a).

Although the BIS monitor has received some critical press, it is an important reference or benchmark for a newly developed DoA index. According to DoA monitors industry reports (Aspect, 2013), up to August 2013, 90% of the famous brands have BIS modules and more than 3400 papers published are related to the BIS. The BIS monitors were and are still the most popular monitor in the market. The newest BIS models have four electrodes to obtain two channels of EEG signals. The filter results are improved by comparing the signals of two channels. However, Nguyen-Ky et al claimed that there were still some problems existing in the BIS monitors (Nguyen-ky, Wen, & Li, 2013a), including being redundant (Schneider, Schöniger, & Kochs, 2004); not responsive to some anaesthetic agents (Johansen, Sebel, & Sigl, 2000); not robust across patients (Hall & Lockwood, 1998) and time delay (Kuizenga et al., 2001).

2.2.3.2. Other indexes

The AEP-Monitor/2 applies the autoregressive model with the exogeneous input (ARX) model instead of moving time averaging (MTA) (old version) to calculate the Middle Latency Auditory Evoked Potentials (MLAEP). As a result, the time delay for data collection decreases from 45-120 seconds to 2-6 seconds. However, the limitations of the AEP-Monitor/2 are that the quality of signals from the passive electrode are not good; it is only suitable for the patients who are more than two years old; it cannot be used for patients who are impaired in hearing or have severe neurological dysfunction; it cannot be applied for ear-nose-throat surgeries; and not convenient in clinical use (Li & Li, 2014).

The Danmeter CSM monitor is equipped with Danmeter Neuro sensors (the same as AEP). It is portable and able to connect with a UP8000 monitor wirelessly and it can be applied in intensive care units (ICU) and infants' surgeries. However, some cases reveal that the CSI cannot reflect the real states of patients. The advantage of the Narcotrend monitor is that it is cheap. The disadvantages are that the monitor is too big to be applied in some small ICU or operating rooms; and the information obtained from the monitor is too complex to be understood timely.

The latest E-Entropy modules can be used for the monitors with a newer version software than L-ANE03(A) or L-CANE03(A). State entropy reflects the hypnotic effect of drugs on the cerebral cortex and RE serves as analgesic parameters. However, some research reveal that BIS was seen to respond better with State entropy and response entropy in some cases (Vanluchene, Struys, Heyse, & Mortier, 2004) and the increase of the difference between SE and RE shows that the motor neuron only responds to noxious simulation, but not directly indicates the analgesia per se (Takamatsu, Ozaki, & Kazama, 2006).

The SNAP 2 can detect the useful information in low frequency band and predict the recovery of consciousness in high frequency band at the same time. But it can only analyse and present one channel of raw EEG data and are not equipped with paediatric sensors as BIS monitors do.

2.3. Basic methods and techniques

2.3.1. Frequency domain methods

Frequency domain analysis examines the EEG signal based on the frequency spectrum of the signal. Fast Fourier transformation and Wavelet transformation are the most popular methods which transform data from time domain signal into frequency domain signal for DoA assessment. A fast Fourier transform is an efficient algorithm to compute the discrete Fourier transform (DFT) which decomposes signals into components of different frequencies. It can extract the features of amplitude, phase spectrum and angle of a signal.

Wavelet transformation normally includes integral Wavelet and orthonormal Wavelet transformations. The former one is usually used for Time-frequency analysis (TFA) and the later one enjoys a great popularity in the research of Multi-resolution analysis (MRA). Wavelet transforms are also classified into discrete wavelet transforms (DWTs) and continuous wavelet transforms (CWTs). Since Fourier transformation defines the presence of a particular frequency within a sample window, it has no time response or time resolution. However, Wavelet transformation is able to detect both time and frequency responses of finite duration signal components but with limited frequency content over their duration (Daubechies, 1992; Mallat, 1999; Tai Nguyen-Ky, 2011; Vetterli & Herley, 1992). In Zikov et al.'s results, the Daubechies Wavelet DB16 worked slightly better than other wavelet methods for identifying different states of anaesthesia (Zikov et al., 2006). The Daubechies Wavelets are characterized by a maximal number (A) of vanishing mo-

ments for the given support width N=2A. With each Wavelet type of Daubechies wavelets class, there is a low pass scaling function (called the father wavelet) which generates an orthogonal multi-resolution analysis.

$$£(x) = \sum_{k=0}^{N-1} a_k \, £(2x - k) \tag{2.1}$$

The high pass Wavelet function (mother wavelet) can be depicted based on scaling function.

$$m(x) = \sum_{k=0}^{M-1} b_k \, £(2x - k) \tag{2.2}$$

As Daubechies Wavelet is orthogonal Wavelet, there is a fixed relationship between the scaling coefficient (a) and Wavelet coefficient (b), that is

$$b_n = (-1)^n a_{N-1-n} \tag{2.3}$$

Symlet Wavelets are similar to Daubechies Wavelets, and the main differences are the mother Wavelet functions. Daubechies Wavelets D2-D20 (the index number refers to N) and Symlet Wavelets 2-8 are commonly used to carry out different feature extraction work.

Other methods such as Filter banks (Mertins), power spectral density (PSD), eigenvector-based method (R. Schmidt & Franks, 1986) are also used in DoA assessment.

2.3.2. Time domain methods

Most of the time domain analysis measures are statistical ones such as mean, variance and standard deviation (Musizza & Ribaric, 2010). For DoA assessment, the features such as amplitude, entropy, complexity autoregressive and burst suppression are extracted from the time of EEG signals. In most DoA algorithms, both frequency domain analysis methods and time domain analysis methods are employed.

2.3.3. Time-frequency and nonlinear methods

EEG changes during the induction of anaesthesia are nonlinear and need, therefore, to be processed with nonlinear methods. The methods based on nonlinear dynamics theory and information theory, such as entropy algorithm, have been applied (Bein, 2006; Bruhn, Lehmann, Röpcke, Bouillon, & Hoeft, 2001; Bruhn, Röpcke, Rehberg, Bouillon, & Hoeft, 2000; Cao, Tung, Gao, Protopopescu, & Hively, 2004; Fell, Röschke, Mann, & Schäffner, 1996; XL Li, Sleigh, Voss, & Ouyang, 2007; Viertiö‐Oja et al., 2004). The approximate entropy can serve as an index of degree of conscious states or DoA (Fan, Yeh, Chen, & Shieh, 2011). However, compared with the sample entropy, it is more suitable for long time series and less sensitive to the transformation of complexity (Wei et al., 2013). Multi-scale entropy (MSE) is also applied to identify the different states of patients (Liu et al., 2012).

The detrended moving-average (DMA) method is used to quantify correlation properties in nonstationary signals with underlying trends. It has been proposed to study the scaling properties of a time series (Arianos & Carbone, 2007; Nguyen-Ky, Wen, & Li, 2010; Xu et al., 2005). The Isomap-based estimation is designed to assess neurophysiological changes during anaesthesia and offers potentials for the development of more advanced systems for the depth of anaesthesia monitoring (Kortelainen, Väyrynen, & Seppänen, 2011a; Kortelainen, Vayrynen, & Seppanen, 2011b).

Empirical-mode decomposition (EMD) was proposed to explore the structure of EEG recordings (Li, Li, Liang, Voss, & Sleigh, 2008; Sweeney-Reed & Nasuto, 2007). The method can break a complicated signal into a series of oscillatory intrinsic mode functions (IMFs) embedded in the original signal (Chen et al., 2010). Li et al (2008) have successfully established an approach centering on Hilbert–Huang transform (HHT) and EMD to analyze the EEG data for the DoA measurement. Ensemble empirical-mode decomposition (EEMD), an adaptive time-frequency analysis method is particularly suitable for extracting useful information from noisy nonlinear or nonstationary signals. Unfortunately, since the EEMD is highly compute-intensive, the method is not suitable for real-time applications. Aiming to solving this problem, a parallelized EEMD method was developed using general-purpose computing on the graphics processing unit (GPGPU), namely, G-EEMD (Chen et al., 2010). The Multivariate empirical mode decomposition (MEMD) can efficiently eliminate the noises among EMD, EEMD and complementary ensemble empirical mode decomposition (CEEMD) (Wei et al., 2013).

As one of the most popular choices in the time-frequency-transformations, Wavelet transformation is also used for DoA assessment. In 2001, Wavelet decomposition of the EEG was adopted to assess the hypnotic state of anesthetised patients undergoing surgery. The results show that the technique could differentiate clearly between the anesthetised state and the awake "baseline" state (Bibian et al., 2001). Gifani et al (2005) claimed the depth of anaesthesia could be discriminated precisely using the detrended fluctuation analysis (DFA) on different scales of Wavelet coefficients and quantifying the relative drift between the lines generated by DFA. In 2006, Wavelet entropy (WE) was designed to characterize the dynamical properties of EEGs and the results show that the WE measure distinguished the awake and asleep state in anaesthesia with a high accuracy of 95% (Ye, Tian, & Weng, 2006). Stationary Wavelet transform (SWT) was used to analyse a single-channel (frontal) EEG signal to obtain a Wavelet-based anaesthetic value for central nervous system monitoring (WAVCNS). The results show WAVCNS offers faster tracking of transitory changes at induction and emergence, with an average lead of 15–30 seconds compared with the BIS. In addition the WAVCNS regains its pre induction baseline value when patients are responding to verbal command after emergence from anaesthesia (Zikov et al., 2006). Through the Wavelet analysis technique, a steady-state index was developed to obtain steady-state information of the system response (inputs-output) which is useful for modelling the drugs combined effect (Castro, Almeida, Amorim, & Nunes, 2009). Based on the features extracted using Wavelet analysis, a radial-basis function (RBF) network is trained to calculate the index for DoA assessment (Taslimi, Rabiee, & Shakouri, 2009). Nguyen-Ky et al. proposed a double Wavelet-based denoising algorithm to denoise the raw data, and proposed to assess DoA based on discrete Wavelet transform (DWT) and power spectral density (PSD) function (Nguyen-Ky et al., 2010,

2013a; Nguyen-Ky, Wen, Li, & Gray, 2011). The result shows that the proposed index reflected the patient's transition from consciousness to unconsciousness with the induction of anaesthesia in real time (Ghanatbari, Mehridehnavi, Rabbani, Mahoori, & Mehrjoo, 2010). They also applied the Wavelet transform on EEG signals to obtain a new index (namely WAI). In 2012, Liang et al. applied the Hurst exponent and wavelet transform in multiscale rescaled range analysis (MRRA) algorithms and received a satisfactory result (Liang et al., 2012).

Variational Bayesian framework was used to extract high order spectral features of EEG signals. The results show that, better classification can be achieved with higher order spectral features in two third of anaesthetic agents (Rezek, Roberts, Siva, & Conradt, 2005). In 2007, Rezek et al. (Rezek, Roberts, & Conradt, 2007) presented an autoregressive class of polyspectral models in the variation Bayesian framework. Their results showed that the estimated higher order spectra significantly improved DoA assessment. A Bayesian dynamical model for quantifying probability of response and probability of correct response simultaneously was applied to trinary behavioural data from ten human subjects undergoing general anaesthesia. This method served as an example of responses to auditory stimuli at varying levels of propofol anaesthesia ranging from light sedation to deep anaesthesia in human subjects (Wong et al., 2011). Kortelainen et al. developed an algorithm based on Bayesian Information Criterion (BIC) for the assessment of the switch-like change in the signal characteristics occurring just before the awakening (Kortelainen, Vayrynen, Jia, Seppanen, & Thakor, 2012). The result showed it detected the sudden change in the EEG related to the moment of awakening with a precision comparable to careful visual inspection. Based on the Bayesian method, the MAP was applied to denoise the wavelet coefficients based on a shrinkage function and the new Bayesian threshold showed better performance than the Larger Posterior Mode (LPM) one. The effect of sample n and variance r on the Maximum Posterior Probability (MPP) is studied. Compared with the BIS index, the new BDoA index could estimate the patient's hypnotic state in the case of poor signal quality (Nguyen-Ky et al., 2013a).

The main noise sources of EEG signals are external (environmental) noise and physiological noise. The external sources include the AC power line noise and electromagnetic noise from the equipment and recording rooms. The physiological noise such as EMG, ECG, EOG and skin potentials are hard to avoid during the recording process (Repovš, 2010). Although there is no accurate description (traits and magnitude) of the noise in EEG signals, three types of noise can be summed up from previous studies (Nguyen-Ky et al., 2011; Repovš, 2010; Ryynanen, Hyttinen, & Malmivuo, 2004; Zandi et al., 2011). They are Gaussian white noise, spiking noise and specific frequency noise. Normally, the frequencies below 0.01Hz (caused by sweating and drifts in electrode impedance) and those above 100 Hz (caused by contraction of muscles) are filtered out (Repovš, 2010). The noise from electricity lines (50 or 60 Hz) can also be eliminated by notch filters.

Conventionally, three steps are applied to obtain high quality denoised EEG signals. Firstly, external environmental noise should be eliminated using efficient methods during data recording process (Repovš, 2010). Secondly, based on known EMG, ECG and EOG data, algorithms (e.g., adaptive filtering (He, Wilson, & Russell, 2004) and blind source separation (Romero, Mañanas, & Barbanoj, 2008)) are developed to remove

these interferences from EEG signals. Thirdly, the other types of noise are eliminated using advanced denoising methods (e.g., signal averaging, filtering). Although most of the existing DoA monitors have artefact detection and removal modules, the denoising results are not satisfactory.

To eliminate the EMG, AC power line, electrode disturbance and other disturbances, the Wavelet transform noise rejection methods including Wavelet decomposition and reshape, Wavelet threshold values and the Wavelet max-module method were applied in EEG signal denoising (Yu, 2009). The newest outcomes include that an adaptive threshold technique to remove spikes and low-frequency noise from raw EEG data and the results revealed the output EEG signal is almost noiseless when using the hard threshold (Nguyen-Ky et al., 2011); a new Bayesian Wavelet threshold based on the Maximum a Posterior (MAP) is applied to denoise the wavelet coefficients (Nguyen-Ky et al., 2013a) and it performed better than the wavelet threshold based on Larger Posterior Mode (LPM) (Cutillo, Jung, Ruggeri, & Vidakovic, 2008). However, these methods are mainly based on the Fourier transform, their denoising results of EEG signals (which is not cyclical or steady) is not that good (L. Zhang, Wu, & Zhi, 2009). While the Hilbert-Huang Transform (HHT) shows better performance in EEG signal denoising, the empirical-mode decomposition, one important part of HHT, is highly compute-intensive and may lead to time delay in some cases.

To reduce the time delay, an adaptive window length technique in Nguyen-Ky et al.'s paper was applied to compute the optimum length of the sliding window and the results shown that the new index can reflect the changes between consciousness and unconsciousness during emergence from anaesthesia in nearer to real time (Nguyen-Ky et al., 2011). In Nguyen-Ky et al.'s later study, a new index BDoA was proposed based on the Maximum Posterior Probability (MPP) values, which performed better in detecting the anaesthesia states' change from awake to light, moderate and deep anaesthesia than the BIS index (Nguyen-Ky et al., 2013a).

To enhance the flexibility and robustness of a DoA index, a novel technology using the spectral features of EEG was presented for separating the anaesthetic effects of propofol and an ultrashort-acting opioid, remifentanil. The results show that the feature set was able to detect the impacts of propofol and classified whether remifentanil had been co-administered or not. As a result, the determination of the clinical state of the patient becomes more accurate (Kortelainen, Vayrynen, et al., 2011a).

Table 2.4: Summary of latest DoA algorithms.

Algorithms	Derivative algorithms	Reference
Entropy	Entropy	(Bein, 2006; Bruhn et al., 2001; Bruhn et al., 2000; Cao et al., 2004; Fell et al., 1996; Li et al., 2007; Viertiö‐Oja et al., 2004)
	Approximate entropy	(Fan et al., 2011)
	Sample entropy	(Wei et al., 2013)
	Multi-scale entropy	(Liu et al., 2012)
DMA	MDMA	(Nguyen-Ky et al., 2010)
Isomap-based estimation	Isomap-based estimation	(Kortelainen, Vayrynen, et al., 2011a)
EMD	Empirical-mode decom-position	(Li et al., 2008; Sweeney-Reed & Nasuto, 2007)
	EEMD	(Li et al., 2008)
	G-EEMD	(Chen et al., 2010)
	MEMD	(Wei et al., 2013)
	CEEMD	(Wei et al., 2013)
Wavelet	Wavelet	(Bibian et al., 2001) (Castro et al., 2009)
	DFA	(Gifani et al., 2005)
	Wavelet entropy	(Ye et al., 2006)
	WAVCNS	(Zikov et al., 2006)
	RBF	(Taslimi et al., 2009)
	DWT	(Ghanatbari et al., 2010; Nguyen-Ky et al., 2010, 2013a; Nguyen-Ky et al., 2011)
	MRRA	(Liang et al., 2012)
Bayesian	Bayesian	(Rezek et al., 2005)
	Variation Bayesian	(Rezek et al., 2007) (Wong et al., 2011)
	BIC	(Kortelainen et al., 2012)
	MAP	(Nguyen-Ky et al., 2013a)
	MPP	(Nguyen-Ky et al., 2013a)

2.4. Limitations of existing DoA monitors

Although the BIS monitor is the most popular one, it still received many criticisms. Other monitors based on different DoA algorithms improved the performance in dif-

ferent aspects. However, they are not widely used because of other limitations. According to the review of existing DoA monitors and their algorithms, the following research gaps in the field are identified:

2.4.1. Unsatisfactory filtering results

The filtering results were not satisfactory with existing methods and it's hard to accurately evaluate the denoising results for EEG signals. Electromyography (EMG), Electrocardiography (ECG) and Electrooculography (EOG) cannot be removed efficiently by existing filtering methods (Johansen, 2006). In addition, all existing monitors were susceptible to electromagnetic (EM) interference (Musizza & Ribaric, 2010). Therefore, an efficient denoising method is urgently needed, especially in the case of denoising poor quality signals.

2.4.2. Time delay

The BIS and other existing monitors showed a long time delay after a change in a state of consciousness. The burst-suppression ratio (BSR), one important parameter for all the existing monitors, normally only represents a portion of the isoelectric EEG of 60s (Musizza & Ribaric, 2010), thus existing monitors are hard to avoid time delay.

Table 2.5: Susceptibility to EM interference and time delay (Musizza & Ribaric, 2010)

	BIS	**Narcotrend**	**Entropy Module**	**CSM**
Susceptibility to EM interference	Moderate	Moderate	High	Moderate
Estimated time delay	63 s / 61 s	90 s /26 s	Data not available	106 s / 55s

2.4.3. Inflexibility

Since there is a wide variation in responses to the anaesthetic agents among individuals, the same effect-site concentrations, even if accurately approximated do not therefore induce similar EEG changes to all patients (Kortelainen, Vayrynen, et al., 2011a). The BIS monitor received criticisms, such as non-responsive to some anaesthetic agents (Johansen et al., 2000) and not robust across patients (Hall & Lockwood, 1998). In addition, it is not reasonable to attempt to measure DoA changes with a single, complex parameter, but rather using multiple parameters that properly describe all the phases of the continuum from awake to very deep anaesthesia state (Kortelainen, Vayrynen, et al., 2011a). Although most of the existing DoA algorithms used different multiple parameters to estimate DoA, the parameter selections were not flexible and

they were limited in some aspects, Therefore the existing DoA algorithms are not robust with the changes of agents or patients.

2.5. Summary

This chapter conducts a comprehensive review about existing DoA monitors and their algorithms. The latest research results show that there are still many improvements need to be made. The review shows that the main limitations of existing DoA monitors are:

- EMG and other high-frequency electrical artifacts are common and interfere with EEG interpretation.
- Data processing time produces a lag in the computation of the depth-of-anaesthesia monitoring index.
- The EEG effects of anaesthetic drugs are not good predictors of movement in response to surgical stimulus because the main site of action for anaesthetic drugs to prevent movement is the spinal cord. The currently available monitoring algorithms do not account for all anaesthetic drugs, including ketamine, nitrous oxide and halothane.

Generally, the limitations of the existing DoA monitors include unsatisfactory data filtering techniques, time delay and inflexibility. Efforts in solving or answering the above questions should be encouraged and promoted.

3. BIS SYSTEM CONFIGURATION AND EEG DATA ACQUISITION

The EEG data were collected from adult patients using BIS monitors. These raw EEG data files, binary files containing unfiltered EEG data, were exported to an USB drive from BIS monitors. The unfiltered EEG data were converted to signed numerical formula using MATLAB.

3.1. Data acquisition

The attending anaesthetist recorded the time, intravenous dosing and significant intraoperative events as indicated by the BIS monitor clock. The purposes and procedures of data collection were explained to all the patients. The agreement including all the ethics issues was made with all the patients. The study was approved by the University of Southern Queensland Human Research Ethics Committee (No: H09REA029) and the Toowoomba and Darling Downs Health Service District Human Research Ethics Committee (No: TDDHSD HREC 2009/016).

The EEG data were collected at Toowoomba St Vincent's Hospital from 37 adult patients (age 22-83 years, weight 55-130 kg, height 154-194cm, gender 15F/22M) by a senior anaesthetist. Their typical drug administration included earlier pharmaceuticals intravenous midazolam 0.05 mg/kg, fentanyl 1.5-3 μg/kg or alfentanil 15-30 μg/kg. The details are shown in Table 3.1 and Table 3.2.

Table 3.1: Patient demographics and intraoperative drug usage

Age (year)	22-83
Weight (kg)	55-130
Height(cm)	154-194
Gender (F/M)	15/22
Midazolam (mg)	2-5
Alfentanil (μg)	500,750,1000
Propofol (mg)	90-200
Parecoxib (mg)	40
Fentanyl (μg)	100,150

Table 3.2: Clinical notes

Time	**Patient**		**Time**	**Patient**		**Time**	**Patient**	
19/08/09	**3***		**31/08/09**	**17**		**02/09/09**	**25**	
09:22:00	midazo-lam	3	10:13:15	midazo-lam	3.5	07:07:15	midazo-lam	4
09:22:03	alfentanil	1000	10:13:35	alfentanil	1000	07:07:30	alfentanil	1000
09:25:53	propofol	120	10:14:53	propofol	150	07:08:45	propofol	150
09:25:55	start sevo/N2O		10:14:55	start des/N2O		07:08:50	start des/N2O	
09:30:00	parecoxib	40	10:16:30	intubate		07:11:00	intubate	
09:30:05	morphine	5	10:19:00	morphine	5	07:15:00	morphine	5
09:43:00	propofol	60	10:19:05	parecoxib	40	07:34:00	morphine	5
09:44:50	morphine	5	10:40:53	morphine	3	08:34:51	end des/N2O	
10:26:20	end sevo		10:53:46	end des/N2O				
			10:59:05	extubate				
***** SNAPSHOT CREATED *****			***** SNAPSHOT CREATED *****			***** SNAPSHOT CREATED *****		

* Take patients 3 and 17 and 25 as examples.

3.2. Equipment settings

The BIS VISTATM monitor (BIS VISTA Version 3.00, Algorithm Version BIS 4.1 (Johansen, 2006)) was used to collect raw EEG data.

The BIS VISTA monitoring system used is shown in Figure 3.1.

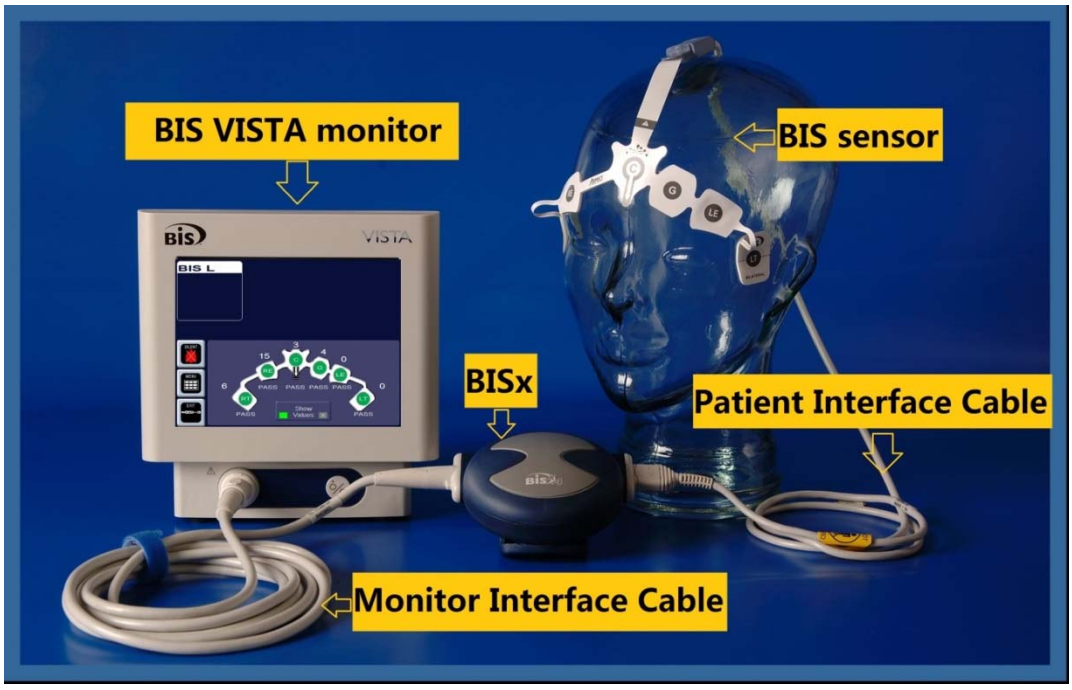

Figure 3.1: The BIS VISTA monitoring system ("Service information manual, Aspect Medical Systems, Inc.,")

The BIS VISTA Monitoring System consists of the following basic components:

• BIS VISTA Monitor (P/N 185-0151)

The BIS VISTA Monitor includes front panel, rear panel and integral battery. The front panel of the BIS VISTA monitor contains the Touch Screen, BISx port and the ON/Standby button. All controls (including ON/Standby button) are accessible by touching a designated area on the monitor screen. The ON/Standby button indicates whether the monitor is ON or in Standby mode. The rear panel includes two USB ports, the clamp shoe, an RS-232 port, the Reset button, the Battery/Power Supply cover, and the power cord receptacle. A rechargeable lithium ion battery inside the monitor provides approximately 45 minutes of back-up power when power cannot be supplied via the power cord.

• BISx (P/N 185-0145-AMS)

The BISx receives, filters, and processes patient EEG data. It is located close to the patient's head where the EEG signal is less subject to interference from other medical equipment.

• Patient Interface Cable (PIC) (P/N 186-0107)

Aspect's BIS sensor patient interface cable is used to connect the BISx to the BIS sensor.

• Monitor Interface Cable (MIC)

The monitor interface cable is long and flexible. It is used to connect the BISx to the front of the monitor.

• BIS Sensor

The sensor is the single use component of the BIS Monitoring System. It should be replaced after each use. All sensors, including the BIS Extend Sensor, utilize the monitor's saved settings (such as smoothing rate)("Service information manual, Aspect Medical Systems, Inc.,").

Four different types of electrodes are used in the EEG recording. They are extend sensor, quarto sensor, pediatric sensor and standard sensor.

Figure 3.2: Different types of electrodes ("BIS sensor for Aspect Medical Systems, Inc.,")

The EEG data were collected through the four adhesive forehead Quatro electrodes/sensors used clinically for BIS monitor. "The BIS Quatro Sensor offers enhanced performance in deep anaesthetic states and improved resistance to interference

from noise sources, such as high frequency/electromyography conditions, in the operating room and intensive care unit." ("BIS sensor for Aspect Medical Systems, Inc.,").

According to the BIS VISTA™ Monitoring System operating manual, cable connections, which include connecting the BISx to the monitor and connecting the PIC to the BISx, need to be done before hand. The initial menu settings include language selection, date and time and view/save settings. After that, the monitor can be switched on, and the system initiates a self-test to make sure that all parts are operating properly. The Quatro electrodes were placed diagonally on the forehead with electrode No. 1 at the centre of the forehead, approximate 2 inches (5 cm) above the bridge of the nose, electrode No. 4 directly above the eyebrow, No. 2 between No. 1 and No. 4, No. 3 on the temple, between the corner of the eye and hairline. The impedances of the electrodes should be below 5 Ω (Rezek et al., 2007).

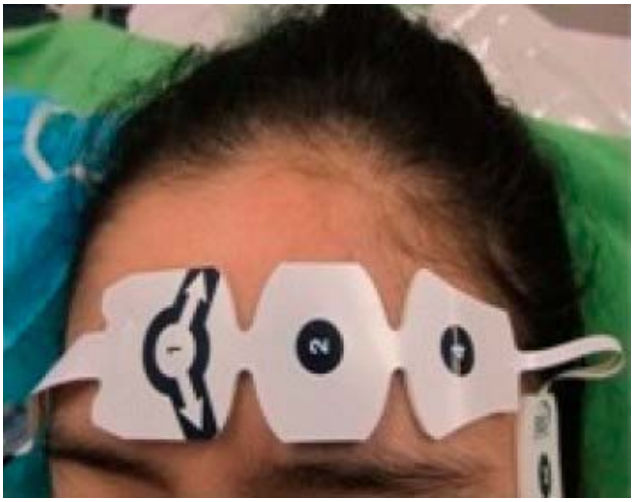

Figure 3.3: The electrode locations (Al-Kadi, Reaz, Ali, & Liu, 2014)

During the operation, the current numeric value of the BIS is displayed and continuously updated in the upper left corner of the screen as long as signal quality is sufficient. Three ports on the rear of the BIS VISTA monitor facilitate data transfer. The USB port is used to export data to a removable drive.

3.3. Data format and normalization

The collected data were transferred to a portable computer for off-line analysis through a USB drive. The exported EEG data files include the real time data (EEG, BIS and other processed variable information), BIS history data (BIS and other processed variables from the BISx) and monitor error logs (critical events and any monitor errors). The real time data is used as the raw EEG signals in this study.

The raw EEG data file named as filename.r2a is a binary file containing unfiltered EEG data from channel 1 and 2. It starts with the value of Channel 1, followed by the

value of Channel 2, and so on (Al-Kadi et al., 2014). The raw EEG signals were sampled at a frequency of 128 for each channel and each EEG sample was a 16-bit signed integer in unit of 0.05 μV. The recorded data were presented in an ASCII code format which cannot be opened or read by normal text editors. Therefore, they were converted to signed numbers using MATLAB code which was developed by our research group members.

The root filename for real time data is LMMDDHHMM, where MM is the month (01-12), DD is the day (01-31), HH is the hour (00-23), and MM is the minute (00-59). These files are stored in filename directory (LMMDDHHMM). The BIS index is presented as a single value and updated every second, which is calculated from gathered EEG data over the past 61.5 seconds. In addition, EMG and signal quantity Indicator (SQI) were also obtained at the same time.

3.4. Signal quality

The signal quality indicator is an index of the signal quality which is calculated based on impedance data, artifacts, and other variables. When SQI is lower than 15, the BIS index could not output a valid value on the screen. The EEG data from 37 adult patients were collected randomly. Because of poor signal quality, there are two main types of invalid BIS value appearing among the 37 patients' data.

For some cases, the invalid BIS values appear at the beginning of patients' wake states. One reason may be that the connection of sensors and patients' skin are not stable caused by the movements of patients. Another reason may be that the calculation of BIS needs a period of time to start the first valuable value. Some other reasons such as wrong operation, noise from the equipment or environment also may lead to these invalid BIS values. As a result, the beginning of BIS are a series of useless value (-3276.8 'excessive artifact detected in signal') or always 97.7 without change. Take patient 23 for an example, there is no valid BIS value at the wake states Figure 3.4.

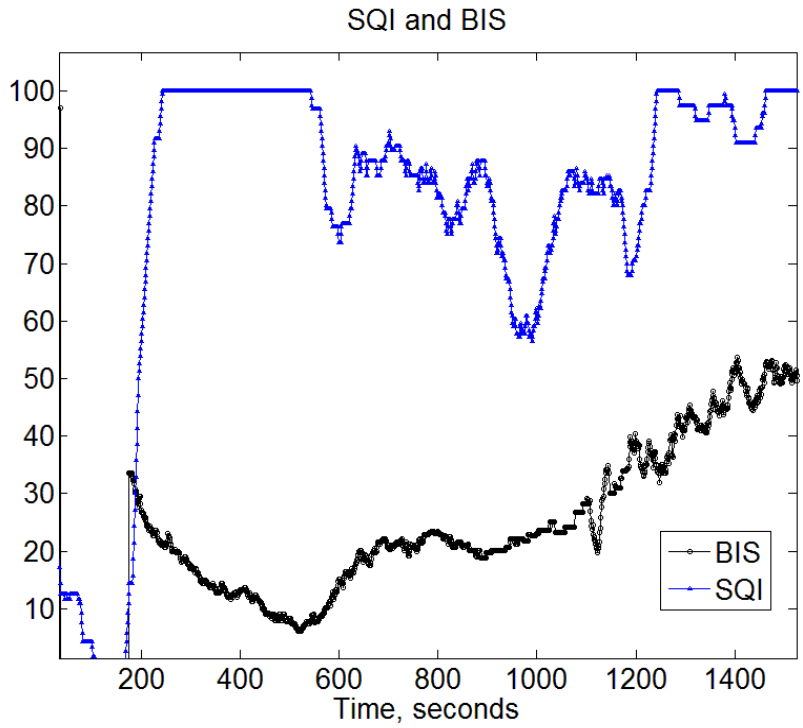

Figure 3.4: SQI and BIS of patient 23

The similar invalid BIS values also appear in other 11 cases (patient 1, patient 9, patient 10, patient 15, patient 16, patient 26, patient 27, patient 28, patient 33, patient 34, and patient 35) of the total 37 patients. There is only a short period of invalid BIS values appear at the beginning of awake states in most of these cases. However, some cases such as patient 23, it cannot be seen from the BIS index when patient's anaesthetic state changed from awake to anaesthetic state.

For some cases, the invalid BIS values appear at the middle of moderate anaesthetic state or deep anaesthetic state. Take patient 37 for an example, there is no valid BIS value at the middle of moderate anaesthetic state (see Figure 3.5).

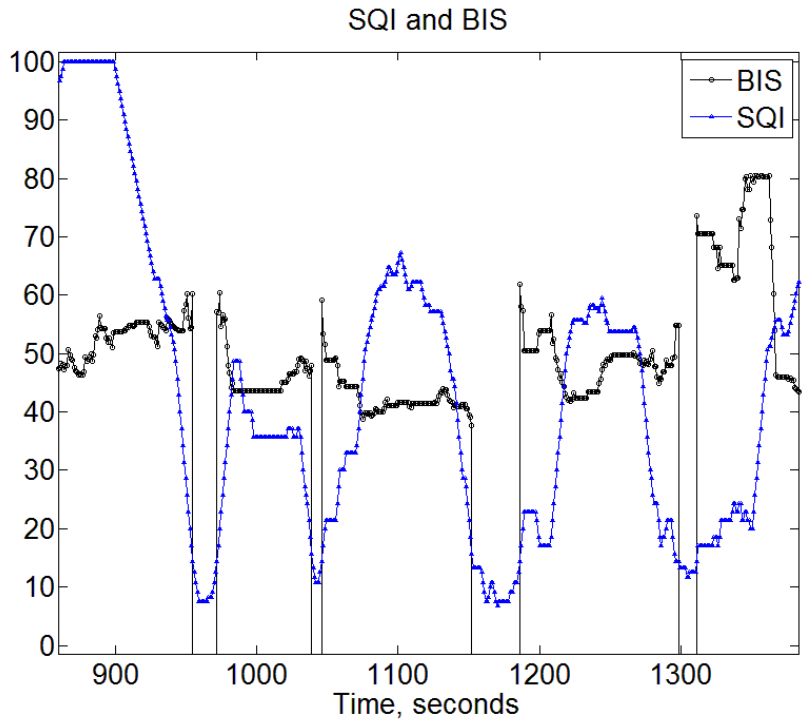

Figure 3.5: SQI and BIS of patient 37

The similar invalid BIS values also appear in other 2 cases (patient 22 and patient 36) of the total 37 patients.

These two types of invalid BIS values not only appear among the 37 cases of this study, but also appear in some other cases of our database in which some data are from other hospitals (such as Prince Charles hospital). Therefore, although BIS monitor is the most popular commercial DoA monitor, the performance is not satisfied in the case of poor signal quality.

In addition, the BIS monitor may show an incorrect DoA result because of poor signal quality.

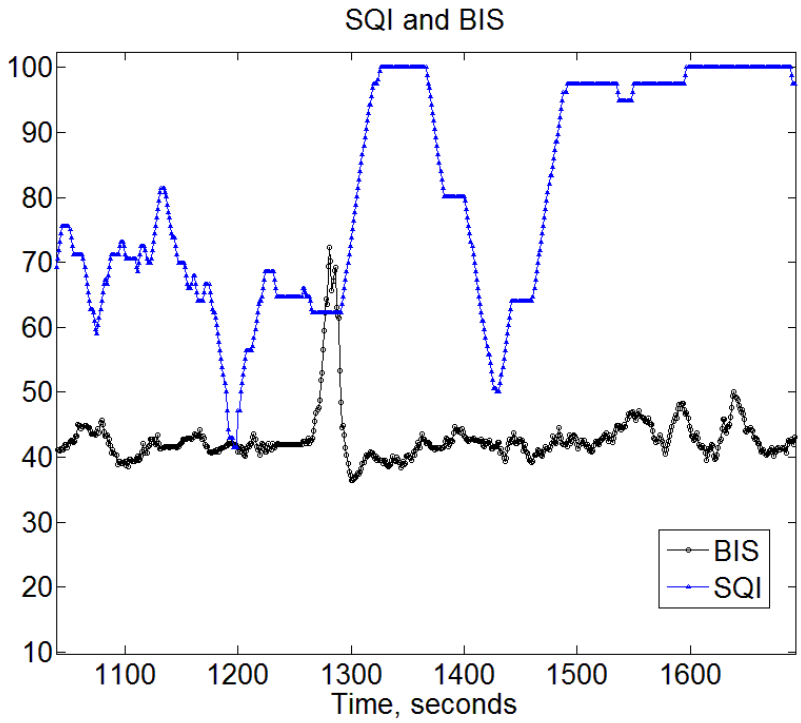

Figure 3.6: SQI and BIS of patient 21

Take patient 21 for an example, the BIS index shows a significant upward trend from about 1280 seconds to 1290 seconds and then a dramatic downward trend from about 1290 seconds to 1300 seconds in Figure 3.6. However, according to the anaesthetists' record, there was no recovery of consciousness (RoC) during this period. Because of the low SQI values about one and half minutes before these significant upward trends of the BIS, the BIS index might be influenced by noise and showed an incorrect BIS value.

The same situation also happened in other two cases (patient 15 and patient 29) of the total 37 patients. According to the facts mentioned above, it is reasonable to doubt that whether the BIS value is reliable or not when the corresponding signal quality indicator is lower than 50.

Therefore, to improve the DoA assessment results, it is of great significance to develop a robust DoA index which can show valid output in the case of poor signal quality.

3.5. Summary

The chapter presents the EEG data acquisition, patient demographics and intraoperative drug usage firstly. Then the equipment settings of BIS VISTATM monitors and the instructions of forehead Quatro electrodes are introduced. The raw EEG data were collected using BIS monitors and converted to signed numerical formula using

MATLAB. In addition, EMG and signal quantity Indicator (SQI) were also obtained from patients using BIS monitors.

The signal quality indicator is an index of the signal quality. When SQI is lower than 15, the BIS index could not output a valid value on the screen. Among the 37 patients' data, there are two main types of invalid BIS outputs including the values at the beginning of the wake state and the values at the middle of moderate anaesthetic state. In addition, the BIS monitor may show an incorrect DoA result which does not agree with clinical records because of noise.

4. NONLOCAL MEAN METHOD AND DENOISING

As a patch-based method, the NLM method calculates the weighted sum of a patch. The weight of each point is determined by the similarity between the points of the own patch and its neighbour. Based on the weighted sum, the noise is filtered out. In this study, the original NLM denoising method was improved then applied to EEG signals with additive Gaussian white, spiking and specific frequency noise.

4.1. Filtering and pre-processing

The main noise sources of EEG signals are the external (environmental) sources and physiological noise. The external sources include the AC power line noise and electromagnetic noise from the equipment in recording room. The physiological noise such as Electromyography, Electrocardiography, Electrooculography and skin potentials are hard to avoid during the recording (Repovš, 2010). Although there is no accurate description (traits and magnitude) of the noise in EEG signals, three typical of noises have been identified in previous studies (Repovš, 2010; Ryynanen et al., 2004; Zandi et al., 2011). They are the Gaussian white, spiking and specific frequency noises. Normally, the frequencies below 0.01Hz (caused by sweating and drifts in electrode impedance) and those above 100 Hz (caused by contraction of muscles) are filtered out (Repovš, 2010). The noise from electricity lines (50 or 60 Hz) can be eliminated by notch filters. Only the frequency band (0.01Hz to 64Hz) remains after filtering in this study, Then the pre-filtered EEG data was selected for the following denoising processing.

Conventionally, three steps are applied to obtain high quality denoised EEG signals. Firstly, external environmental sources noise should be eliminated using efficient methods during the data recording process (Repovš, 2010). Secondly, based on known EMG, ECG and EOG data, algorithms (e.g., adaptive filtering (He et al., 2004) and blind source separation (Romero et al., 2008)) are developed to remove these interferences from EEG signals. Thirdly, the other types of noise are eliminated using advanced denoising methods (e.g., signal averaging, filtering).

In this study, the nonlocal mean denoising method was developed and applied to EEG signal denoising. Firstly, the NLM is applied to simulated EEG signals with Gaussian white noise, spiking noise and specific frequency noise. Then it is applied to the pre-processed real EEG signal from hospitals.

4.2. Nonlocal mean denoising method

The nonlocal mean denoising method was first introduced by Buades et al. (Buades, Coll, & Morel, 2005) to address the edge degradation problem during denoising process. This method has been widely applied in one dimension (1-D) signal filtering and 2-D image denoising (Darbon, Cunha, Chan, Osher, & Jensen, 2008; Deledalle, Duval, & Salmon, 2012; Van De Ville & Kocher, 2009). Compared to Wavelet soft threshold algorithm, hybrid empirical mode decomposition and Wavelet denoising method, NLM showed better performance in biomedical signal ECG processing (Tracey & Miller, 2012).

Next, we briefly introduce the NLM algorithm.

Given, $v(n) = u(n) + n$, where $v(n)$ is the observed data, $u(n)$ is the real data and n is the noise. The NLM method is to calculate the weighted sum $\hat{u}(s)$ as its denoised value (Tracey & Miller, 2012).

$$\hat{u}(s) = \frac{1}{\sum_t w(s,t)} \sum_{t \in N(s)} w(s,t)v(t) \tag{4.1}$$

The weight ($w(s,t)$) of each neighbour point (t) depends on the similarity between the patch of the target point (s) and the patches of the neighbour (t). The weight is calculated as follows (Buades et al., 2005)：

$$w(s,t) = \exp\left(-\sum_{P \in \Delta} \frac{(v(s+P)-v(t+P))^2}{hP^2}\right) \tag{4.2}$$

Δ represents the patch size of the samples surrounding s or t and P is half of the patch size. h is the bandwidth which is a key parameter that controls the amount of smoothing applied. The value of h should not be too small (cause insufficient averaging) or too large (cause dissimilar patches to appear similar, resulting in blur) (Tracey & Miller, 2012). Figure 4.1 shows the basic patches in NLM method (T. Li, Wen, & Jayamaha, 2014).

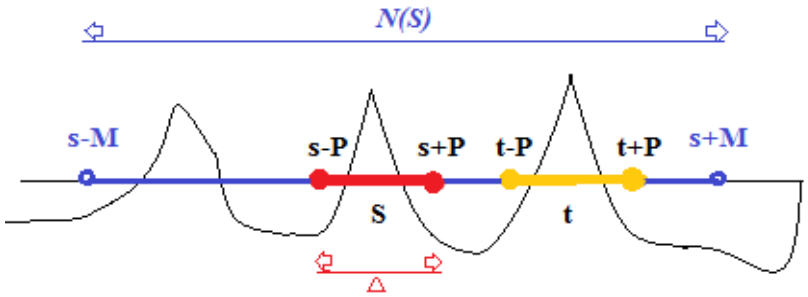

Figure 4.1: Illustration of NLM parameters.

The same patch centered on s is compared to patches centered on another point t in $N(s)$. Before applying the NLM denosing method on EEG signals, the value of three important parameters including patch size $\Delta(\Delta=2P+1)$, search neighbourhood $N(s)$ ($N(s)=2M+1$) and bandwidth h need to be selected based on maximum signal to noise ratio (SNR) standard (T. Li et al., 2014).

In this study, the same trend patches (STP) and moving adaptive shape patches (MASP) are developed for improving the NLM denoising method. For the same trend patches, before we use t point to calculate the $\hat{u}(s)$, a judgement about whether s patch and t patch have the same trend needs to be done. If they have the same trend (e.g., $v(s-p)<v(s)<v(s+p)$ and $v(t-p)<v(t)<v(t+p)$), the value of $v(t)$ can be used to calculate $\hat{u}(s)$, otherwise it is invalid. This method reduces the value of interference from diverse patches to improve the NLM denoise results.

For moving adaptive shape patches, a judgement about whether s patch and t patch has the same trend also needs to be made. If $0<v(s-p)-v(s)<v(s)-v(s+p)$ and $0<v(t-p)-v(t)<v(t)-v(t+p)$, the patches for t and s will be changed from $(-p,p)$ to $(0,2p)$, and then the new patches are adopted to calculate $\hat{u}(s)$ and vice versa. To sum up, the patches move to the bigger change side. In other cases, the calculation is the same as the basic NLM method.

To obtain better denoising results, two improved nonlocal mean methods are applied to the real EEG signals. The first is to combine the denoising results of NLM and MASP-NLM using uniformly weighted aggregation method. The new denoising results are equal to the average of the twos. The second is to combine the NLM methods and the WTD methods. The WTD is applied to decompose the raw EEG data into different levels of Wavelet coefficients. Then the Wavelet coefficients can be denoised using NLM and the filtered Wavelet coefficients are processed to reconstruct the noiseless EEG signals.

For assessing the performance of denoising methods, SNR improvement (SNRimp) in decibel, mean squared error (MSE), and percentage distortion (PRD) are employed (Tracey & Miller, 2012). To compare different denoising algorithms without the influence of noise, the MSE and PRD are improved as follows.

$$\mathrm{SNR} = 10\log_{10}\frac{\sum_{n=1}^{N} u(n)^2}{\sum_{n=1}^{N}(v(n)-u(n))^2} \tag{4.3}$$

$$\mathrm{SNRimp} = 10\log_{10}\frac{\sum_{n=1}^{N}(v(n)-u(n))^2}{\sum_{n=1}^{N}(\hat{u}(n)-u(n))^2} \tag{4.4}$$

$$\mathrm{MSE} = \frac{1}{N}\sum_{n=1}^{N}(\hat{u}(n)-u(n))^2 \tag{4.5}$$

$$\mathrm{MSEimp} = \left(\frac{1}{N}-\frac{1}{N^2}\sum_{n=1}^{N}\frac{(v(n)-u(n))^2}{u(n)^2}\right)*\sum_{n=1}^{N}(\hat{u}(n)-u(n))^2 \tag{4.6}$$

$$\mathrm{PRD} = 100\sqrt{\frac{\sum_{n=1}^{N}(\hat{u}(n)-u(n))^2}{\sum_{n=1}^{N}u^2(n)}} \tag{4.7}$$

$$\mathrm{PRDimp} = \left(100-\frac{100}{N}\sum_{n=1}^{N}\frac{(v(n)-u(n))^2}{u(n)^2}\right)*\sqrt{\frac{\sum_{n=1}^{N}(\hat{u}(n)-u(n))^2}{\sum_{n=1}^{N}u^2(n)}} \tag{4.8}$$

$u(n)$ is the value of simulated signal (assume they are pure data), $\hat{u}(s)$ is the denoised value and $v(n)$ is the value of signals with the additive noise. The improved MSE and PRD are adopted to assess the denosing results in this study.

4.3. EEG signal processing using nonlocal mean method

4.3.1. Parameter selection

The three important parameters of NLM are the search neighbourhood half-width M, the patch half-width P and the bandwidth h. In this study, they were selected based on the maximum SNR standard using testing signals with additive noise. In theory, the larger the M, the better the performance of NLM will be. However, a large M leads to highly computational complexity. Experiments show that results are good for M =>1000. The value of P is easy to be selected when the signal is regular (e.g., for sinusoidal signal, P/T (length of period) = 0.92). However, the experiments show that the best value of P for irregular EEG signals is not fixed. Our testing shows P=>50 is good enough. As it can be seen in Figure 4.2, the SNR increases slowly as the patch size increases when P>50. To reduce computation intensity, we choose P=50. The best bandwidth h is related to μ (the mean of absolute value of the amplitudes). The ratio of the μ/h is about 3.8. Therefore, the value h will be adjusted during the denoising process.

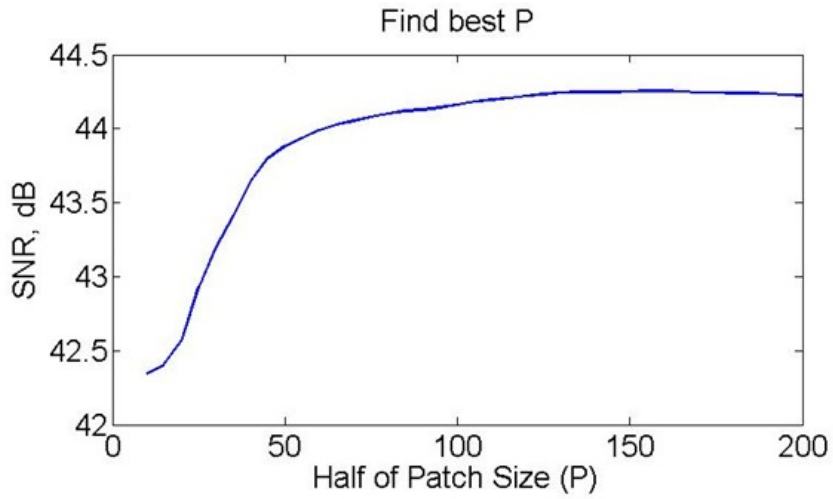

Figure 4.2: The SNR increase slowly as the patch size increase when the P>50.

4.3.2. Results for the simulated EEG signals

The NLM method is first evaluated using simulated EEG signals which include sinusoidal signals with noise and then the real EEG signals from our database. This database consists of both filtered and unfiltered raw EEG data which were obtained from hospitals in Toowoomba and Brisbane. These EEG signals were sampled at the frequency

of 128 for each channel (two channels) and each EEG sample was a 16-bit signed integer in units of 0.05μV.

Before applying the NLM method to real EEG signals, the simulated EEG signals which includes sinusoidal waves (60Hz) with additive Gaussian white noise, spiking noise and specific frequency noise (50Hz) respectively served as the testing signals. Therefore, three sets of experiments were done to evaluate the NLM method.

In each set of experiments, the NLM method, the best-practise WTD sym8 and db16 methods were applied to denoise the same testing signals to compare the performance.

The maximum amplitude of the Gaussian white noise was from 0 to 0.5μ (μ: the mean of absolute value of the signal amplitudes) in the first set of experiments. The noise level was distributed into 25 equal levels and the power of the additive noise was linearly rescaled from 1 to 25 units. The result in Figure 4.3 shows the SNRimp of NLM is much higher than those of sym8 and db16, the MSEimp of NLM is slightly lower than those of the other two methods. However, the PRDimp of NLM is higher than that of db16.

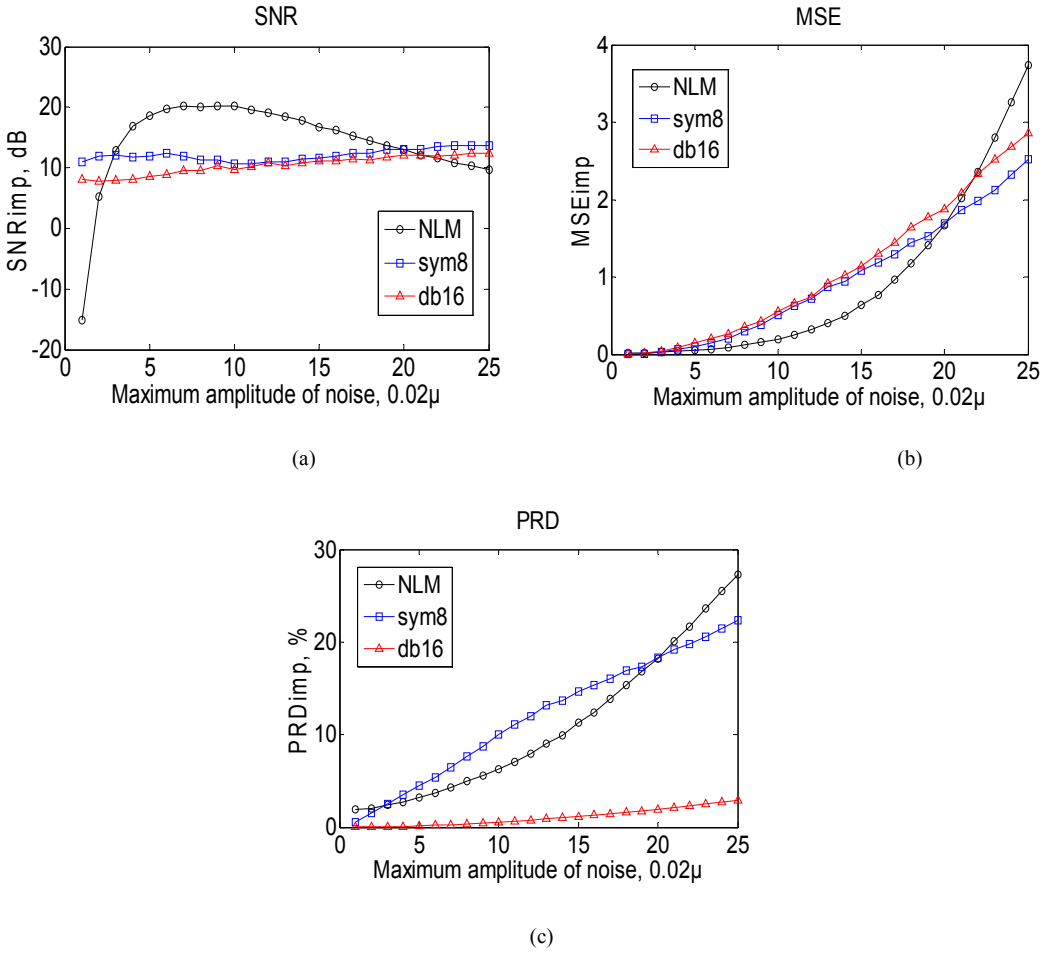

Figure 4.3: Denoising results: (a) improved signal to noise ratio, (b) improved mean squared error ratio and (c) improved percentage distortion ratio.

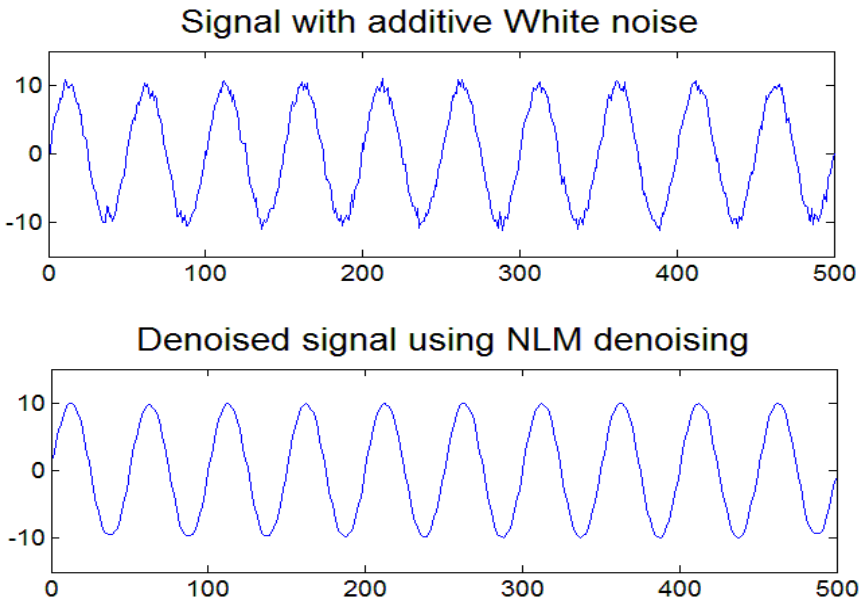
Signal with additive White noise
10
0
-10
0
100
200
300
400
500
Denoised signal using NLM denoising
10
0
-10
0
100
200
300
400
500

(a)

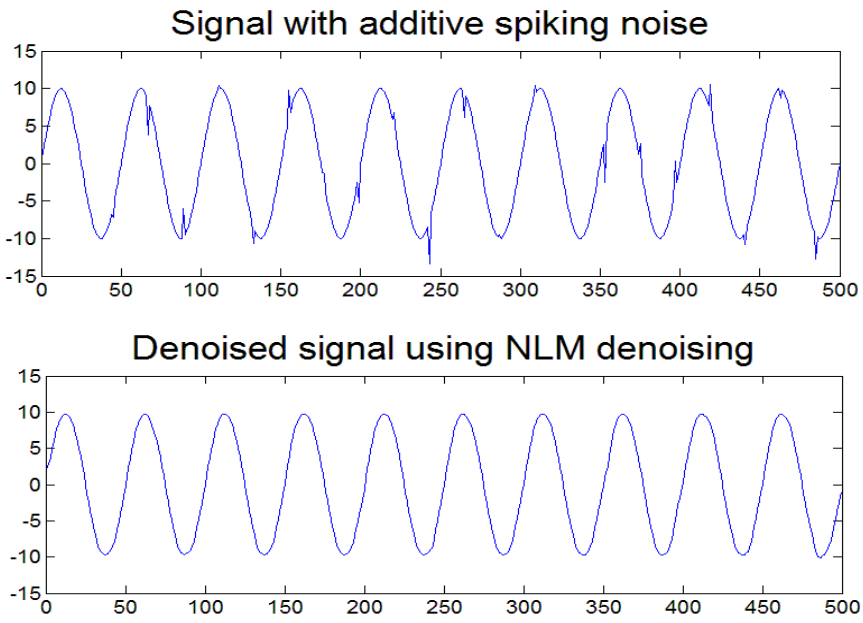
Signal with additive spiking noise
15
10
5
0
-5
-10
-15
0
50
100
150
200
250
300
350
400
450
500
Denoised signal using NLM denoising
15
10
5
0
-5
-10
-15
0
50
100
150
200
250
300
350
400
450
500

(b)

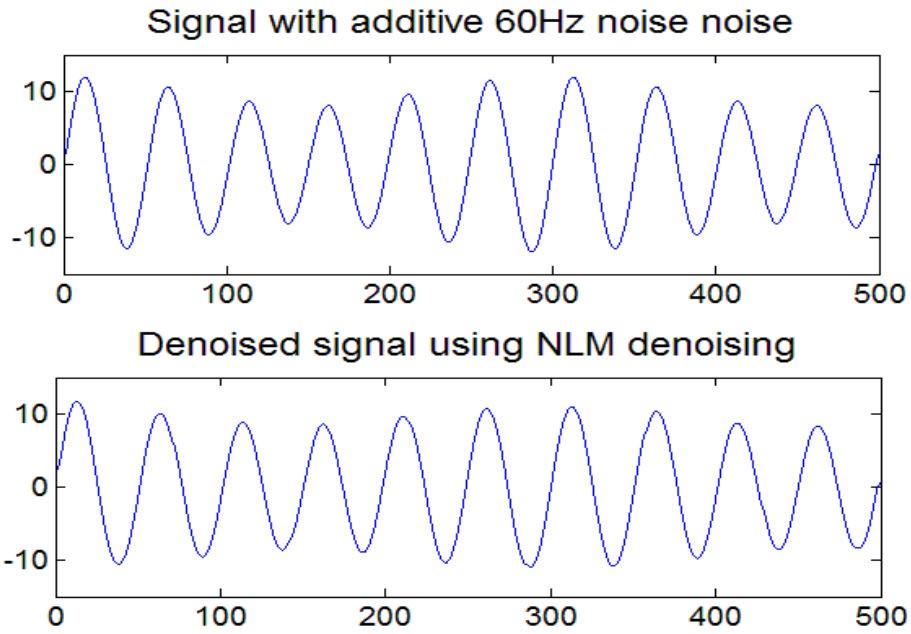

(c)

Figure 4.4: Comparison of signals with noise and denoised signals. Types of additive noise: (a) Gaussian white noise, (b) spiking noise and (c) additive 50Hz noise.

Figure 4.4(a) and Figure 4.4(b) show the results of the NLM denoising method with additive Gaussian white noise and spiking noise. It can be seen that the denoised signals are as smooth as the original sinusoidal signal. The denoising result on specific frequency noise is also satisfactory as shown in Figure 4.4(c). The NLM method reduces the disparities of two neighbour waveforms efficiently.

4.3.3. Results for the real EEG signals

The real EEG signals with additive noise are used as the measured raw EEG signals. These real EEG signals were obtained when patients were anaesthetised in the awake, the light and the deep anaesthetic states. It is difficult to know the exact components of noise in the EEG signals, so the testing additive noise is a mix of Gaussian white noise, spiking noise and specific frequency noise (50Hz). Since it is also not easy to know the magnitude of real noise, we use different noise levels for testing purposes. The maximum amplitude of the Gaussian white noise and additive 50Hz noise were from 0.01 to 0.49μ, and the maximum amplitude of spiking noise was from 0.05 to 2.45μ. The noise level was distributed into 24 equal levels and the power of the additive noise was linearly rescaled from 1 to 24 units.

As it can be seen from Figure 4.5, the EEG signals become lower in frequency and increasingly regular from awake to deep anaesthesia. Figure 4.6, Figure 4.7, and Figure

4.8 show the denoising results of EEG signals for the awake, the light and the deep anaesthetic state respectively.

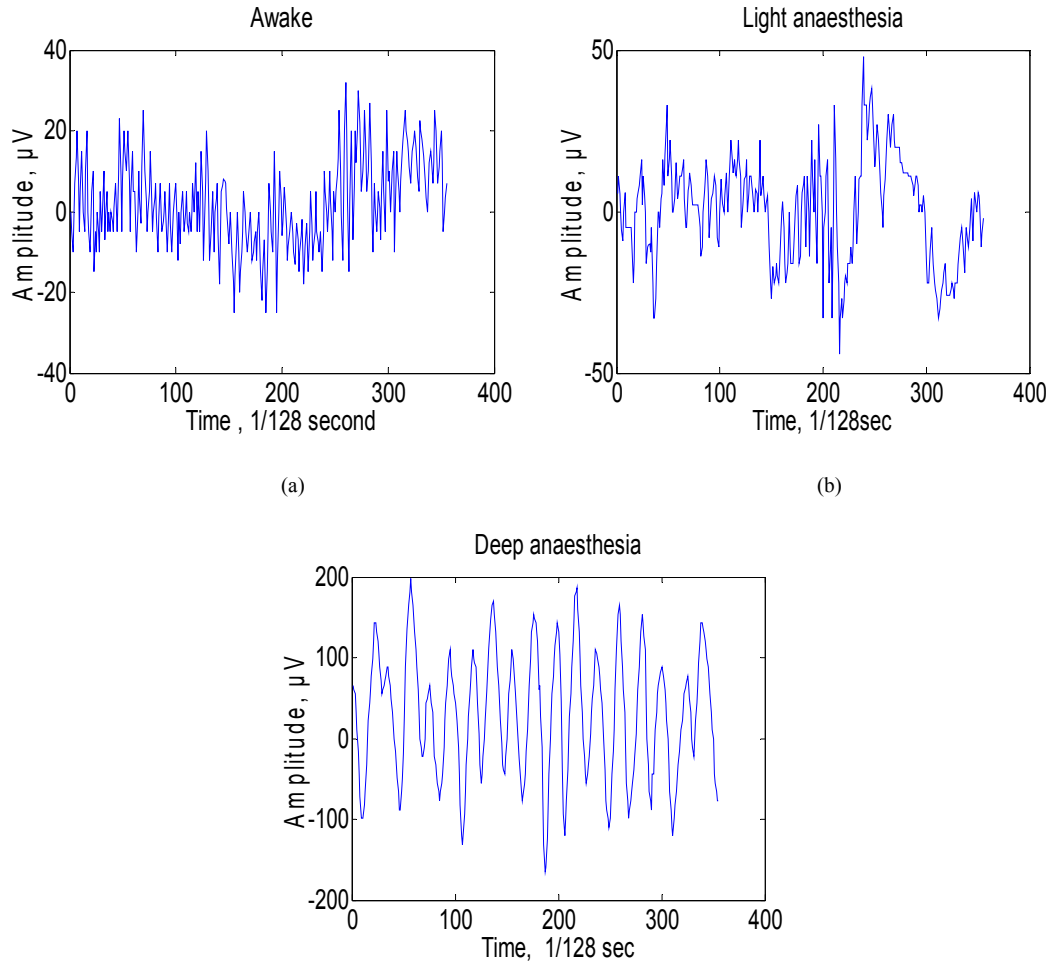

Figure 4.5: EEG signals at different anaesthetic states: (a) Awake state, (b) Light anaesthetic state and (c) Deep anaesthetic state.

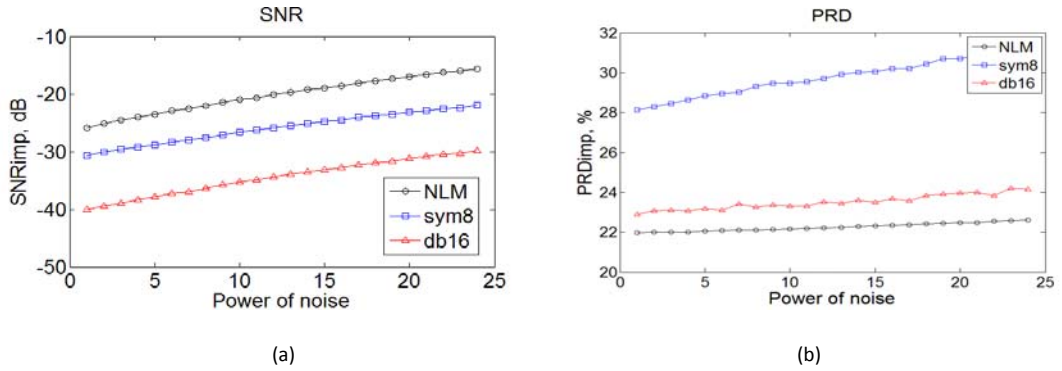

Figure 4.6: Denoising results of EEG signals at the awake state: (a) improved signal to noise ratio, and (b) improved percentage distortion ratio.

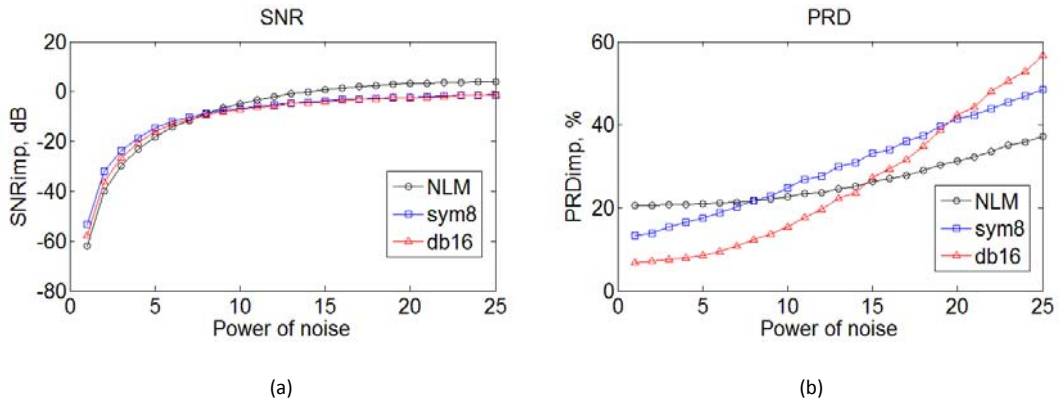

(a) (b)

Figure 4.7: Denoising results of EEG signals at the light anaesthetic state: (a) improved signal to noise ratio, and (b) improved percentage distortion ratio.

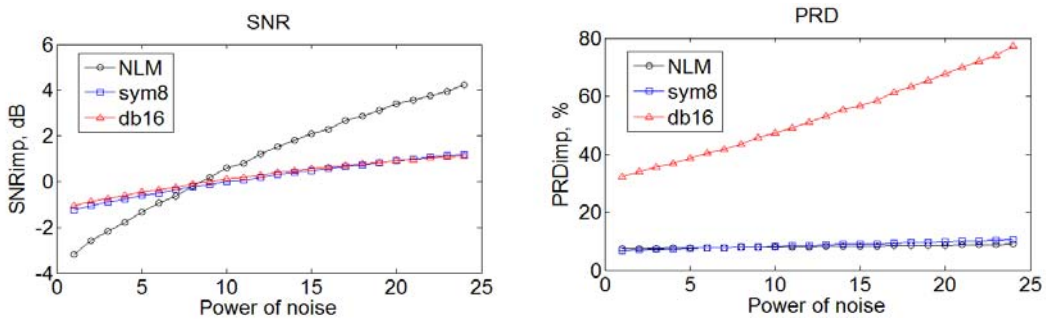

(a) (b)

Figure 4.8: Denoising results of EEG signals at the deep anaesthetic state: (a) improved signal to noise ratio, and (b) improved percentage distortion ratio.

For all EEG signals at different anaesthetic states, the SNRimp of NLM was about 0.93dB to 6.36dB higher than that of the WTD method when the power of noise was more than 11 units. Furthermore, the PRDimp of NLM was about 0% to 11.07% lower than that of WTD. On average, the SNRimps of NLM are 5.73dB, 1.55dB, and 0.81dB higher than those of WTD at awake, light anaesthetic and deep anaesthetic states respectively. The PRDimps of NLM are lower than those of WTD and the differences between NLM and WTD at different anaesthetic states are 1.26%, 0.61%, and 0.46% respectively.

It can also be seen from Figure 4.6 to Figure 4.8 that on average, the SNRimps of NLM for different anaesthetic states are approximately -20.18dB, -7.82dB and 1.05dB respectively. The PRDimps are about 22.07%, 21.4% and 7.80% respectively when the power of noise was less than 11 units.

Take patient 25 as an example, the denoising results are shown in Figure 4.9. It can be seen that the base line of denoised signal is much closer to X-axis than that of raw

signal in Figure 4.9(a). It means the low frequency noise (high amplitude) is eliminated efficiently. In addition, as shown in Figure 4.9(b), all the amplitudes of five basic frequency bands are in the normal range according to Table 5.1.

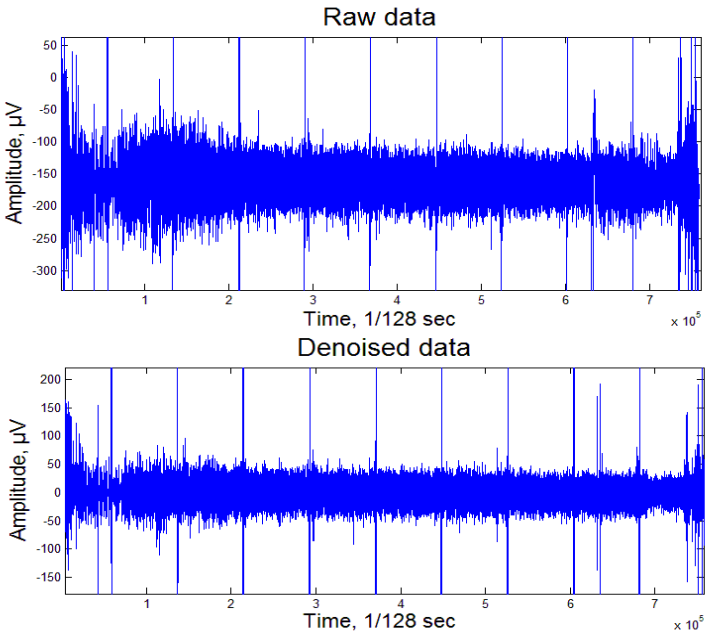

(a)

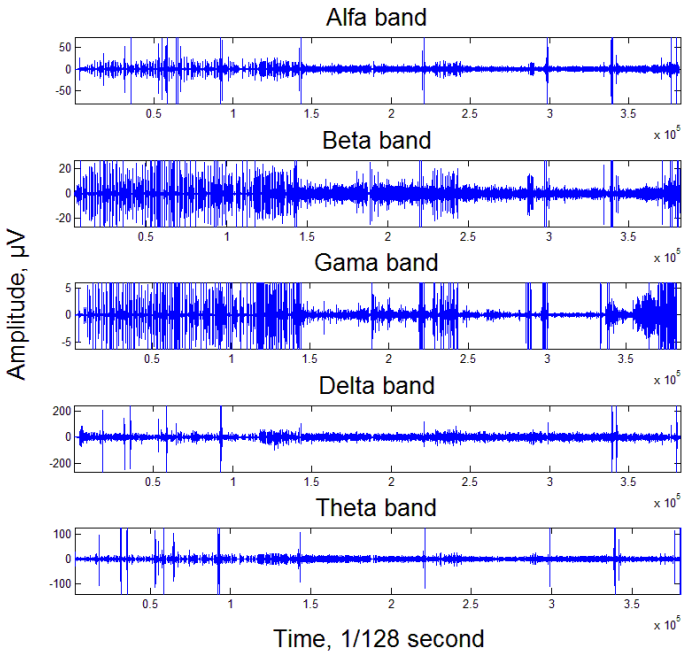

(b)

Figure 4.9: Denoising results, (a) A comparison between the raw data and denoised data, and (c) Denoised data of basic frequency bands.

4.3.3.1. Results using improved MASP-NLM method

As introduced in pervious sections, the NLM method is improved using STP and MASP. To evaluate STP-NLM and MASP-NLM methods, they were applied to de-noise the same EEG signals mentioned above. Compared with the best parameter bandwidth *h* of STP-NLM and MASP-NLM with those of the original NLM, MASP-NLM displayed a higher SNR when bandwidth was small (h<20) (see Figure 4.10(a)). It can be seen that MASP-NLM performs better when the signals change dramatically. In other words, MASP-NLM is more suitable for denoising signals with dramatic fluctuation. However, MASP-NLM is more sensitive to patch size than NLM as shown in Figure 4.10(b).

Further improvement of the denoising results was done by combining NLM and MASP-NLM denoising results using the uniformly weighted aggregation (UWA) method (Deledalle et al., 2012) to combine their strengths. Figure 4.11 shows that on average, the combined result is 0.99dB higher in SNRimp than that of original NLM and 1.30% lower in PRDimp than that of original NLM.

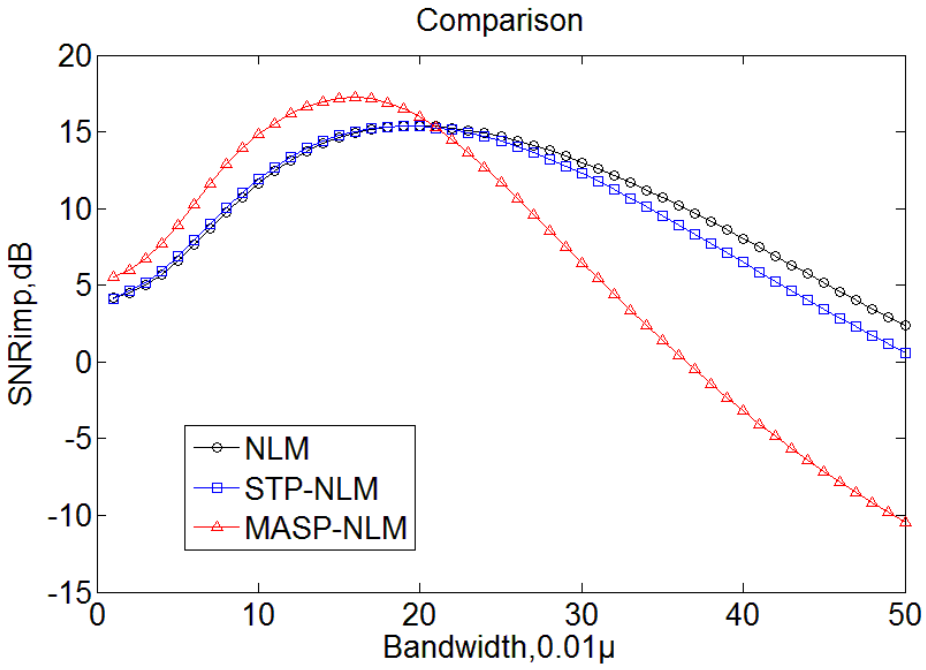

(a)

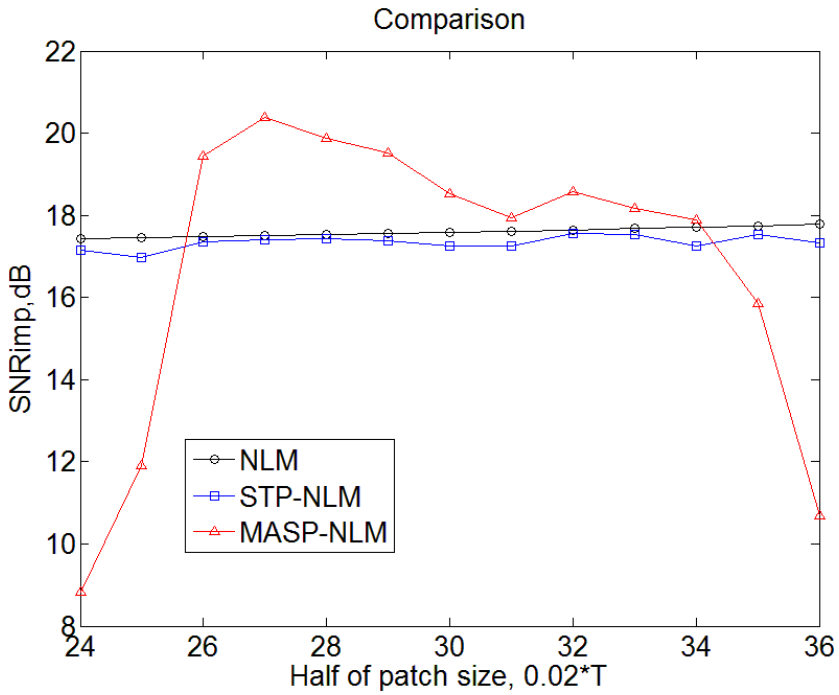

(b)

Figure 4.10: Comparison of NLM, STP and MASP: (a) Bandwidth *h* and (b) Patch *P*.

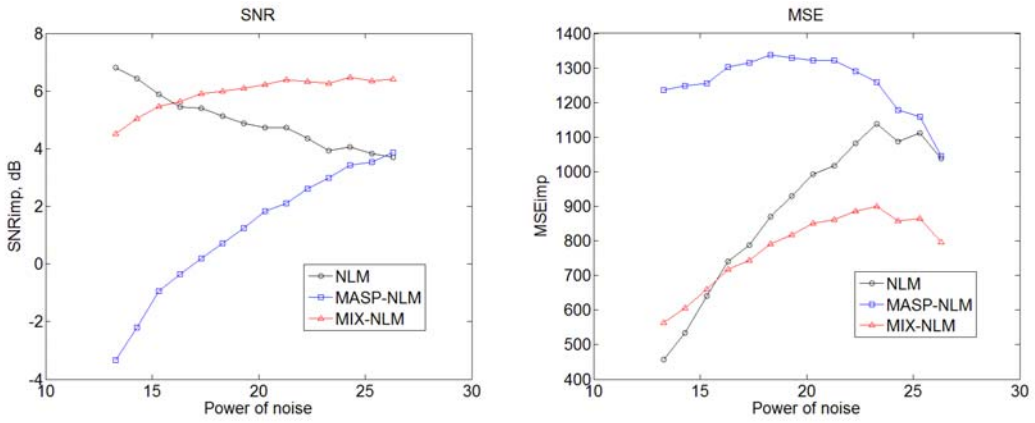

(a) (b)

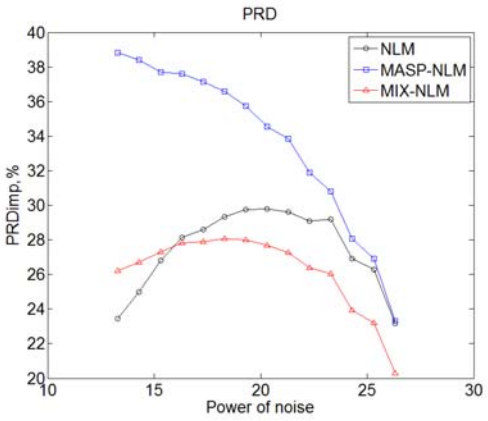

(c)

Figure 4.11: Comparison of NLM, MASP-NLM and MIX-NLM: (a) improved signal to noise ratio, (b) improved mean squared error ratio and (c) improved percentage distortion ratio.

4.3.3.2. Results using the combined NLMWTD denoising method

The NLM method is further improved using Wavelet transform to decompose the raw EEG signals so that relatively regular Wavelet coefficients can be filtered by NLM, then the noiseless EEG is reconstructed. Figure 4.12 shows the results of the combined NLMWTD denoising method. The results showed that when the power of noise was more than 11 units, the SNRimp of the combined NLMWTD was about 0.50dB to 4.89dB higher than that of the original WTD, and the PRDimp was about 9.07% to 18.44% lower than that of WTD.

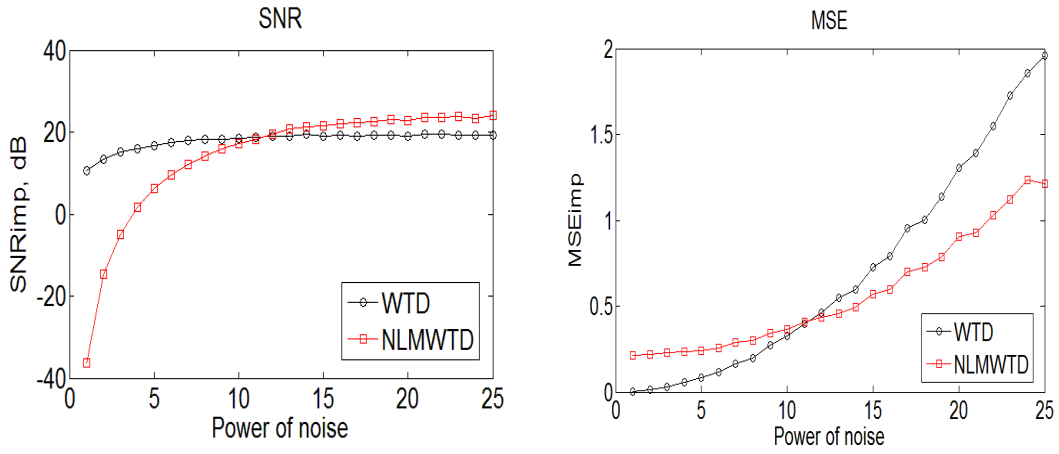

(a) (b)

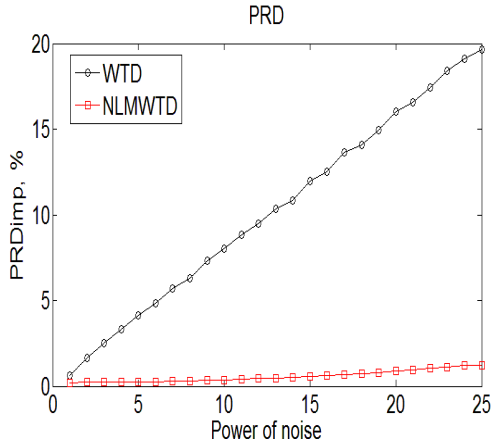

(c)

Figure 4.12: Comparison of NLMWTD and WTD: (a) improved signal to noise ratio, (b) improved mean squared error ratio and (c) improved percentage distortion ratio.

4.4. Summary

It is difficult to obtain pure EEG signals, and the exact noise components in EEG signals are also not clear. To test the performance of the NLM method, we first apply it to the simulated EEG signal which has known sinusoidal signal with additive noise to verify its performance. Three types of noise are added into sinusoidal signals to verify the performance of NLM. The results show that the NLM methods perform well in eliminating the added common Gaussian white, spiking and bases frequency noises (50Hz).

In the experiment using real EEG signals, the noise with different power is added as the magnitude of noise is unknown. The results shown in Figure 4.6 to Figure 4.8 are compared with those of the most popular WTD sym8 and db16 methods in the EEG filtering area. It can be seen clearly that the NLM performs better. In addition, it can also be observed from the tendency that the performance of NLM becomes better as the power of additive noise increases. The outcome indicates that on average, the SNRimp of NLM is about 2.70dB higher than that of WTD and the PRDimp was about 0.37% lower than that of WTD for real EEG signals.

In Figure 4.6 to Figure 4.8, the results also show that the SNRimp of the EEG signals in different anaesthetic states increases and the PRDimp decreases as the deepening of anaesthesia level. That means the NLM performs better for EEG signals at the deep anaesthetic state than those at the light anaesthesia, and the denoising results of EEG signals at awake state are the worst. Therefore, it is concluded that the more regular the signals, the better performance of the NLM denoising method is.

Compared among three different methods with the best bandwidth parameter h (the STP-NLM, the MASP-NLM and the original NLM), only MASP-NLM displayed a higher SNR. The results show that the NLM using MASP are more suitable for denoising the dramatic changes in EEG signals. The denoising results could be further

improved by combining NLM and MASP-NLM denoising results using the UWA method.

In addition, the results of the combined NLM and WTD methods also show that its performance is improved than that of the original WTD method (0.50 dB to 4.89dB higher in SNRimp, 0 to 0.79 lower in MSEimp and 9.07% to 18.44% lower in PRDimp), especially, while the signal quality is poor.

5. DOA ASSESSMENT BASED ON TIMING CHARACTERISTICS OF EEG BETA FREQUENCY BAND

The great nonlinearity and nonstationarity make the EEG signals hard to be processed. One effective way is to divide the EEG signals into a set of signals with different frequency bands, and then applying time domain methods to analyse them. In this Chapter, the most suitable frequency bands for DoA assessment using time domain methods are found. The proposed new DoA index is designed based on: the M parameters which are calculated from the amplitude of β Frequency band, the LZC parameters which are calculated from the power of β Frequency band and the PE parameters which are calculated from the amplitude of βb frequency band. The new DoA index is developed and evaluated using the measured EEG data and recorded BIS readings.

5.1. Frequency bands of EEG signals

The EEG signals are normally defined as the congregation of five basic frequency bands ($\alpha, \beta, \gamma, \delta$ and θ) (Rampil, 1998), These frequency bands are listed in the Table 5.1.

Table 5.1: Basic EEG frequency band (Rampil, 1998)

EEG frequency band	Frequency (Hz)	Amplitude (μV)
α (alfa)	7 - 13	20 – 60
β (beta)	13 - 30	2 – 20
γ (gama)	30 - 70	3 – 5
δ (delta)	0.5 - 3.5	20 – 200
θ (theta)	3.5 - 7	20 – 100

Most DoA algorithms are designed based on the EEG characteristics of different frequency bands. For the BIS monitor, the β-ratio is calculated based on the power spectrums of the frequency bands 30-47Hz and 11-20 Hz. Another important parameter, Synch-fast-slow from bispectral analysis, is based on the frequency bands of 0.5-47Hz and 40-47Hz. The frequency domain analysis of Narcotrend monitor is related to the α, β, δ and θ frequency bands. As for the AEP-monitor/2 monitor, the signals of 25-65Hz frequency band are used to autoregressive model with exogenous input (ARX).

Its undisclosed algorithm is applied to frequency band (3-47Hz). Burst suppression is also analyzed using the signals of 1-35Hz frequency band. The total frequency band from 0.5 to 50Hz is used for PSA 4000 monitor. The frequency domain analysis method of Cerebral state monitors includes α-ratio, β-ratio and (β-α)-ratio which are more relevant to low frequency bands than high frequency bands. For the Entropy-Module, the signals of frequency bands 0.8 to 32 Hz and 0.8 to 47Hz are filtered out using FFT method (Musizza & Ribaric, 2010).

The frequency bands of EEG signals for different DoA algorithms are not the same, and EEG channels obtained by different monitors are also different. For BIS monitors, Narcotrend monitors, Cerebral state monitors and Entropy-Module, only one channel EEG signal is used for their DoA algorithms. But the DoA assessment of PSA 4000 monitors is based on 4 channels EEG data.

In this study, the raw EEG data were obtained through BIS monitors. Therefore, two channels EEG data are available. The EEG data from both channels are calculated using different feature extraction methods. In this chapter, the middle and high frequency bands are divided into 14 small frequency bands to find a more accurate correlation between parameters and anaesthetic states:

Table 5.2: 14 small frequency bands

Basic frequency band	Small frequency band	Frequency (Hz)
α (alfa)	αa	7-10
	αb	10-13
β (beta)	$\beta 1$	13-17
	$\beta 2$	17-21.5
	$\beta 3$	21.5-26
	$\beta 4$	26-30
	βa	13-21.5
	βb	21.5-30
γ (gama)	$\gamma 1$	30-38.5
	$\gamma 2$	38.6-47
	$\gamma 3$	47-55.5
	$\gamma 4$	55.5-64
	γa	30-47
	γb	47-64

In this chapter, the Daubechies Wavelets with index number 16 and Sym8 Wavelet method are selected to transform the EEG signals into different Wavelet coefficients. For one episode of EEG signal, the number of Wavelet coefficients decrease as the level of Wavelet coefficients increase, totalling eight levels for Sym8 and 16 levels for the db16 Wavelet method. The amount of Wavelet coefficients above level five is too small to obtain reliable parameters, only the first five levels of approximately Wavelet coefficients and detail Wavelet coefficients are obtained from EEG signals.

5.2. Feature extraction methods

After dividing the denoised EEG signals into different frequency bands, time domain analysis methods are applied to extract the timing characteristics which are able to classify anaesthetic states. These time domain analysis methods should be low compute-intensive. Otherwise, they are not suitable for real-time applications as high compute-intensive leads to time delays. In addition, the parameters calculated using time domain analysis methods should have high correlations with different anaesthetic states. These correlations should also be robust for different patients. For these purpose, the mobility, permutation entropy and Lempel-Ziv complexity methods are proved valuable in this study.

5.2.1. Mobility

The mobility has shown that it is a promising method to extract the timing characteristics of EEG signals, as normal timing characteristics such as mean, standard deviation and differences of adjacent episodes of EEG signals have not an apparent relationship with different anaesthetic states (McBride et al., 2014). The mobility is defined as below:

$$M=\sqrt{\frac{\sigma_1}{\sigma_0}} \tag{5.1}$$

where σ_0 is the variance, and σ_1 is the variance of the first derivative. In this research, we select 56s as the window size and 55s as the overlap for the mobility calculation. To easily compare the different feature extraction methods in this research, the same window size (56s) is selected for all the feature extraction methods including the M, PE, LZC, SODP, IPE and ISODP methods.

5.2.2. Permutation entropy

Olofsen et al. developed a composite permutation entropy index (CPEI) which reliably tracked the anaesthetic-related EEG changes and showed a promising measurement of g-amino-butyric acid (GABA)-ergic anaesthetic drug effect (Olofsen, Sleigh, & Dahan, 2008). Other studies (Jordan, Stockmanns, Kochs, Pilge, & Schneider, 2008; Silva et al., 2011) also consistently showed that the permutation entropy could be used to efficiently discriminate different levels of consciousness during anaesthesia, and to provide an index for the anaesthetic drug effect.

The PE is calculated using the following algorithm. Firstly, define the EEG signal [$x(i)$,i=1,2,...] into a m-dimension space X[$x(i)$,$x(i+L)$,...,$x(i+(m-1)L)$], m is the number

of dimension, L is the time delay. Then sort the EEG series in the m dimension space in increasing sequence:

$$[x(i+(j_1-1)L) \leq x(i+(j_2-1)L) \leq .. \leq x(i+(j_m-1)L)] \quad (5.2)$$

j_1, j_2, …, and j_m show the new order of the series. For a m-dimension space, there are total $m!$ orders. Each $X[x(i),x(i+L),...,x(i+(m-1)L)]$ reflects one of these '$m!$'orders. Assume the probabilities of each order are P_1, P_2,..., P_K respectively. According to the Shannon Entropy, the permutation entropy $PE(m)$ is calculated as follows:

$$PE(m) = -\sum_{j=1}^{K} P_j \ln P_j \quad (5.3)$$

The smaller the $PE(m)$ *is,* the more regular the time series are. In this research, we select 56s as the window size and 55s as the overlap to calculate permutation entropy.

5.2.3. Lempel-Ziv complexity

As an effective method for characterising the randomness of signals, the Lempel-Ziv complexity (LZC) is a commonly used method for biomedical signals (McBride et al., 2014).

The LZC is calculated in the following steps. Firstly, the original signal (numerical sequence) need to be transformed into a 1/0 symbolic sequence S by comparing the signal to a threshold value. In this research, the median value of the signal is used as the threshold value. Whenever the signal is larger than the median value, one maps the signal to 1, otherwise, to 0.

After converting the whole signal into its symbolic 1/0 sequence, distinct "words" can be obtained by parsing this sequence and they can be encoded. The sequence $S = S1S2...Sn$ is rewritten as a concatenation $W = W1-W2...Wm$ of m "words" chosen such that $W1 = S1 = 0$ or 1 and Wj (j=2, 3…m) is the shortest "word" that has not appeared previously. Therefore, the number of the encoded distinct "words" (m) is decided by timing characteristics of the symbolic 1/0 sequence. The value of Lempel-Ziv complexity is relevant to the number of the encoded distinct "words" (m) and the length of the signal n. It is defined mathematically as

$$LZC = \frac{m(log_2^m + 1)}{n} \quad (5.4)$$

In this research, we select 56s as the window size and 55s as the overlap. Based on methods presented by previous researchers (Snaedal et al., 2010), the complexity features were computed using five-second small windows with 50% overlap. The LZC value for one 56s window size signals is the mean of LZCs of 21 small window size signals.

5.3. DoA index design based on time domain features

The mobility, Lempel-Ziv complexity and PE values are calculated from different frequency bands and all of them constitute the parameters pool. To find out the optimal parameter set for index designing, the regression technique is used to verify the correlation between the parameters and the anaesthetic states (referred to BIS value). The coefficient of determination (R squared) is used to evaluate the correlation between the parameters and BIS. To develop more reliable DoA algorithms, the correlation between parameters and different anaesthetic states are also analysed. The parameters which show the best performances of DoA assessment for different anaesthetic states are selected as the best parameter set. The new DoA index is designed based on the best parameter set.

5.4. Experimental simulation and result evaluation

5.4.1. Sample selection

To accurately measure the correlation between parameters and different anaesthetic states, the sample selected for parameter evaluation should be representative and diverse. As all of the data are collected from the anaesthetic patients, the period of anaesthetic state is usually much longer than the awake state. The data selected for the sample should balance both the anaesthetic states and awake states. In addition, the beginning of EEG data is not reliable in most cases. For example, at the beginning of the BIS monitor often displayed a series of useless values (-3276.8 'excessive artifact detected in signal') or always stayed at 97.7 without change and the SQI index values in some cases are even lower than 15 at the beginning. When we select the sample, we can choose the data whose SQI index values are high enough and the BIS values and raw EEG data are reasonably good at the beginning. Based on the consideration mentioned above, the data of Patient 2, Patient 3, Patient 4, Patient 5 and Patient 7 are selected to make up the sample (16693 seconds EEG data totally). Their data are shown in Figure 5.1, the lengths of different anaesthetic states are similar to with each other.

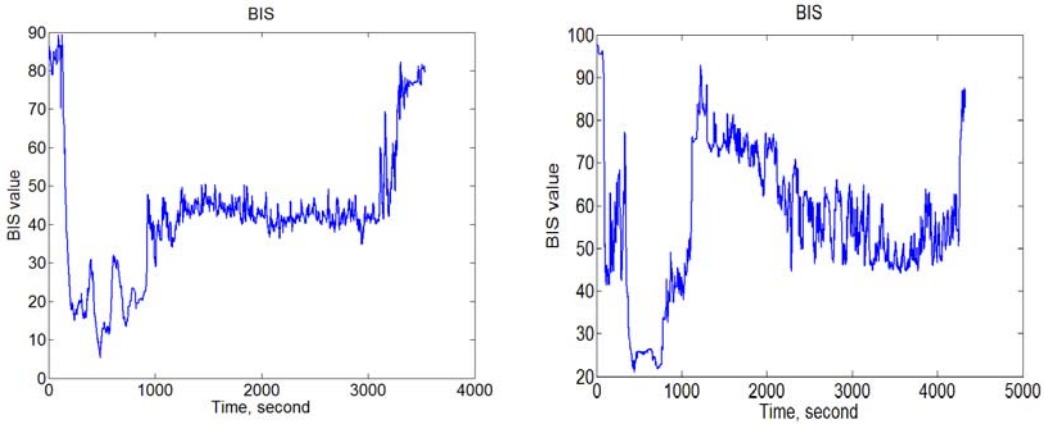

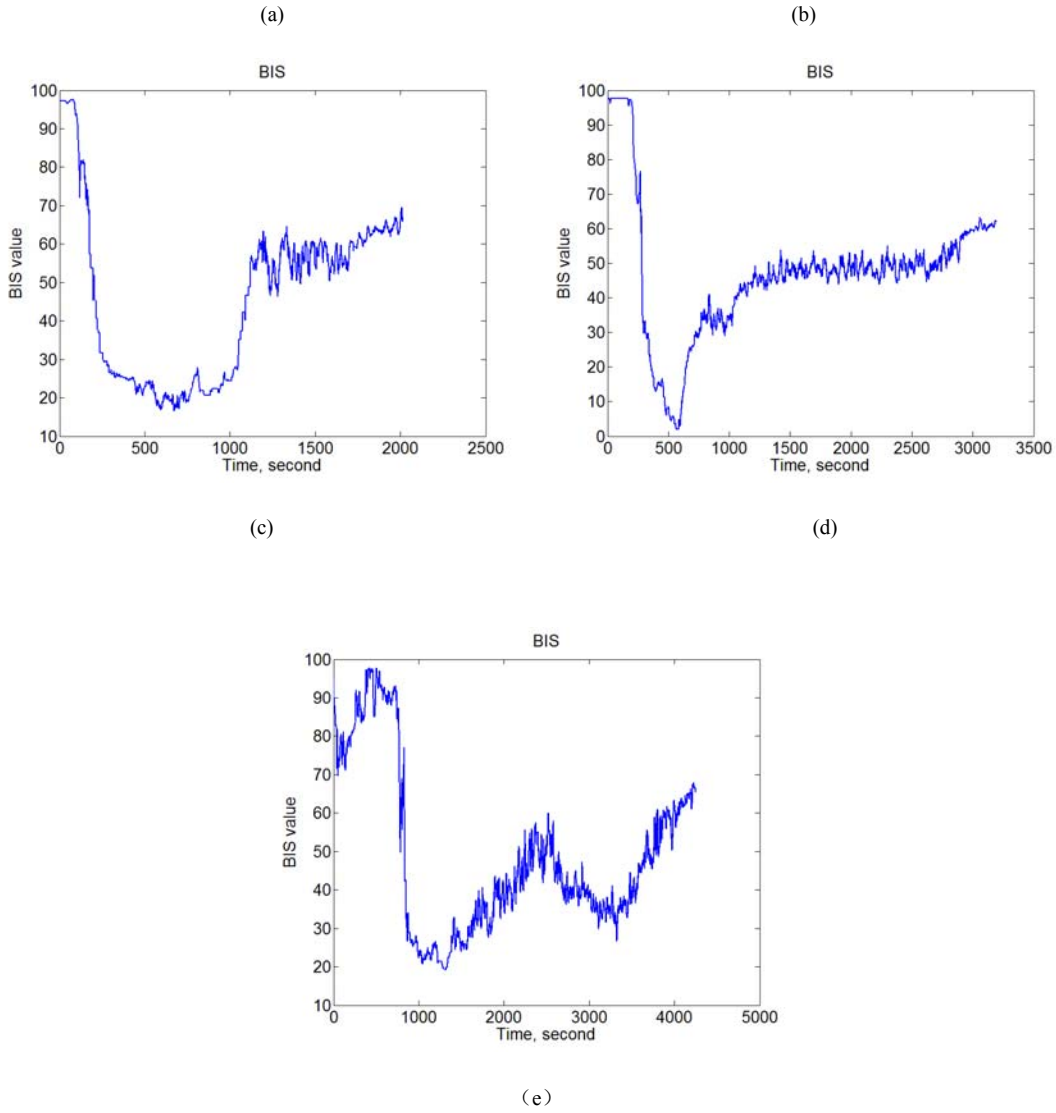

Figure 5.1: Sampled BIS data, (a) patient 2, (b) patient 3, (c) patient 4, (d) patient 5 and (e) patient 7.

5.4.2. Parameter selection

To evaluate the correlation between parameters and anaesthetic states, the coefficient of determination (R squared) is used.

In statistics, R squared (R^2), indicates how well data fit a statistical model. In our study, the statistical model should be a line or a curve. The definition of the coefficient of determination is given below

$$R^2 = 1 - \frac{\sum_i (y_i - f_i)^2}{\sum_i (y_i - \bar{y})^2} \tag{5.5}$$

where y_i is the BIS value. f_i is the modelled value which is calculated using the statistical model and parameters, i.e. $f_i = C1 + C2 * Parameter_i$, where *C1* and *C2* are constants. $\bar{y}$ is the mean of y_i, and the R squared ranges from 0 to 1. The greater the R squared is, the higher correlation between the parameter and BIS value is.

To calculate parameters for different frequency bands, the sym8 Wavelet method and db16 Wavelet method are applied to decompose the denoised EEG signals into Wavelet coefficients firstly. The R squared of different parameters is calculated for the level 5 sym8 Wavelet and db16 Wavelet coefficients respectively. The results are showed in Figure 5.2.

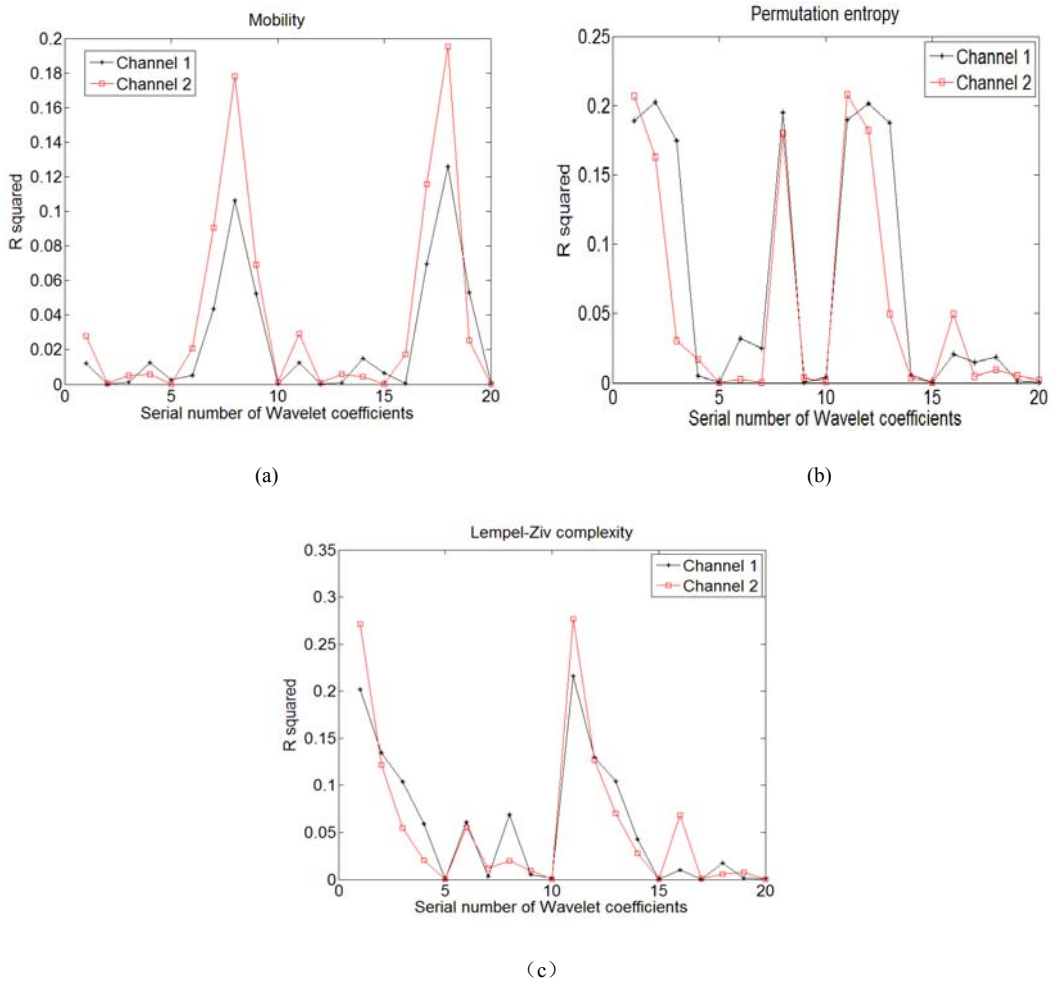

Figure 5.2: Comparisons of different Wavelet coefficients from Channel 1 and Channel 2 signals, (a) Mobility, (b) Permutation entropy and (c) Lempel-Ziv complexity. The No.1 to No.10 of Wavelet coefficients represent level 5 db16 Wavelet coefficients. They are level 1 to level 5 approximately Wavelet coefficients and then detail Wavelet coefficients respectively. The No.11 to No.20 of Wavelet coefficients represent level 5 Sym8 Wavelet coefficients.

As shown in Figure 5.2, the highest R squared of Channel 2 for mobility, permutation entropy and Lempel-Ziv complexity are always greater than those of Channel 1. It

means that the characteristics of EEG signals from Channel 2 are more correlated to DoA states than those from Channel 1. Overall, the R squared based on Wavelet coefficients is too small to be selected as the best parameters for new index design.

To further explore the relationship between the parameters and frequency bands, the EEG signals are divided into five basic frequency bands (α, β, γ, δ and θ), 14 small frequency bands mentioned in Table 5.2 and $\beta\gamma$ (21.5-38.5Hz). The original signal bands are also added as a reference. As a result, we finally obtained 5+15+1=21 sets of frequency bands from each episode of EEG signals. The mobility, Lempel-Ziv complexity and PE values are calculated based on both amplitude and power of each basic frequency band. The regression results of channel 1 and channel 2 are shown in Figure 5.3.

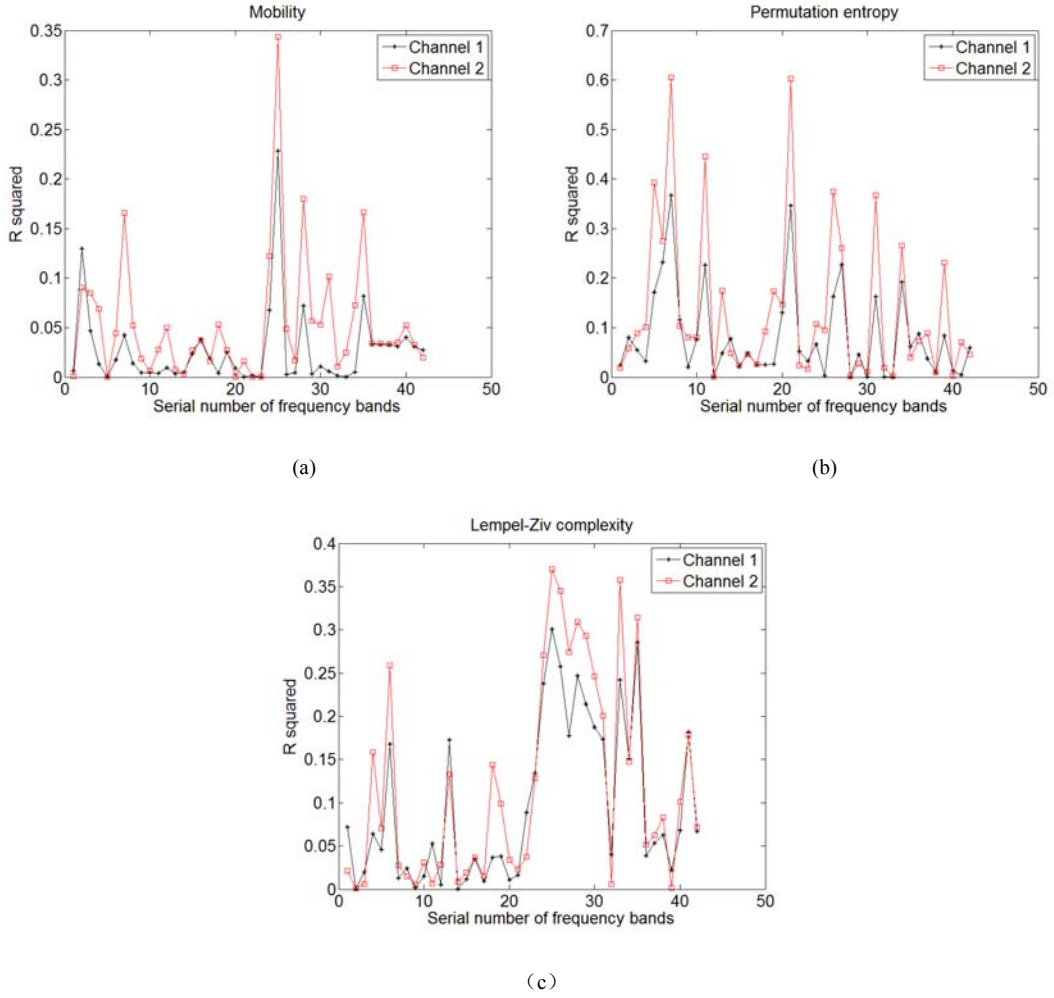

Figure 5.3: Comparisons of different frequency bands from Channel 1 and Channel 2, (a) Mobility, (b) Permutation entropy and (c) Lempel-Ziv complexity. The No.1 to No.21 of frequency bands represent the amplitude of δ (0.5- 3.5Hz), θ (3.5-7Hz), α (7-13Hz), β (13-30 Hz), γ (30-70 Hz), original signal (0.01-70Hz), βb (21.5-30Hz), $\gamma 1$ (30-38.5Hz), $\gamma 2$ (38.6-47Hz), $\gamma 3$ (47-55.5Hz), $\gamma 4$ (55.5-64Hz), γa (30-47Hz), γb (47-64Hz), βa (13-21.5Hz), αa(7-10Hz), αb(10-13Hz), $\beta 1$(13-17Hz), $\beta 2$(17-21.5Hz), $\beta 3$(21.5-26Hz), $\beta 4$(26-30Hz), and

$\beta\gamma$(21.5-38.5Hz) respectively. The No.22 to No.42 of frequency bands represent the power of the frequency bands mentioned above.

It can be seen from Figure 5.3, the results from Channel 2 are much better than those of Channel 1. For example, the highest R squared calculated from the power of β (13-30 Hz) is 0.3436 for Channel 2. However, the highest R squared for Channel 1 is only 0.2281. The difference is more apparent for permutation entropy parameters that the highest R for Channel 2 (0.6050) is 0.2376 higher than that for Channel 1 (0.3674). For the parameters of Lempel-Ziv complexity, the highest R squared calculated from the power of β (13-30 Hz) is 0.3702 for Channel 2 which is also higher than that for Channel 1 (0.3008). To sum up, based on the timing characteristics analysis methods and samples in this research, the parameters calculated from Channel 2 is much more valuable for doing DoA assessment than those from Channel 1.

The synchronization of Channel 1 and Channel 2 are also tested to find out a higher R squared for the parameters. Two kinds of cross features are calculated. One is based on the parameters calculated from two different channels, and the other one is based on the original EEG signals of two different channels. The results are showed in Table 5.3.

Table 5.3: The highest R squared based on cross features

The highest R squared	M	PE	LZC
Ch2P*-Ch1P	0.1317	0.2602	0.0566
(Ch1P+Ch2P)/2	0.3139	0.5874	0.3516
Absolute value of (Ch2P/Ch1P)	0.1257	0.2628	0.0605
Absolute value of (Ch2EEG-Ch1EEG)**	0.2503	0.3355	0.3625
(Ch1EEG + Ch2EEG)/2	0.1250	0.5883	0.4050
Absolute value of (Ch1EEG/Ch2EEG)**	0.0558	0.3290	0.2352

* Ch2P: The parameters calculated from Channel 2; **Ch2EEG: The amplitude of Channel 2 signals.

As shown in the table above, the best R squareds of cross features are always smaller than those from Channel 2. Therefore, we only use the parameters calculated from Channel 2 to design the new DoA index.

5.4.3. New DoA design

It can be seen from Figure 5.3, the parameters with the highest R squared are the mobility values which are calculated from the power of β (13-30 Hz) frequency band, the PE values which are calculated from the amplitude of βb (21.5-30Hz) frequency band and the Lempel-Ziv complexity values which are calculated from the power of β (13-30 Hz) frequency band. They are selected to make up the best parameters pool for new DoA design. In this research, we also analysed the relationship between the performances and the best parameters in different anaesthetic states. The original three best parameters are separated into different groups according to different anaesthetic ranges (referred to BIS value, for example, BIS value 70-99), and then the R squareds for three parameters are calculated for different anaesthetic ranges respectively. The results are shown in Figure 5.4.

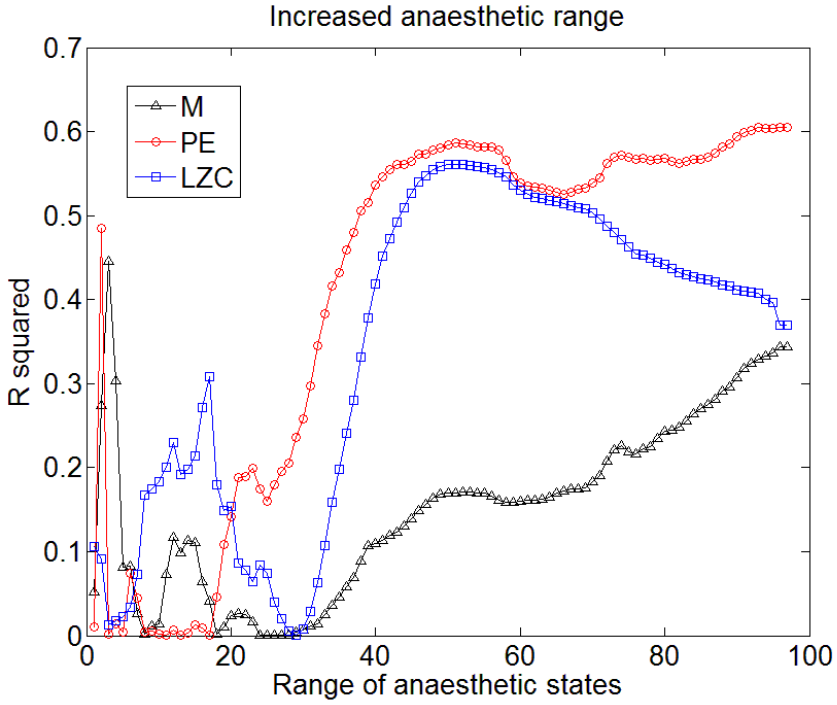

(a)

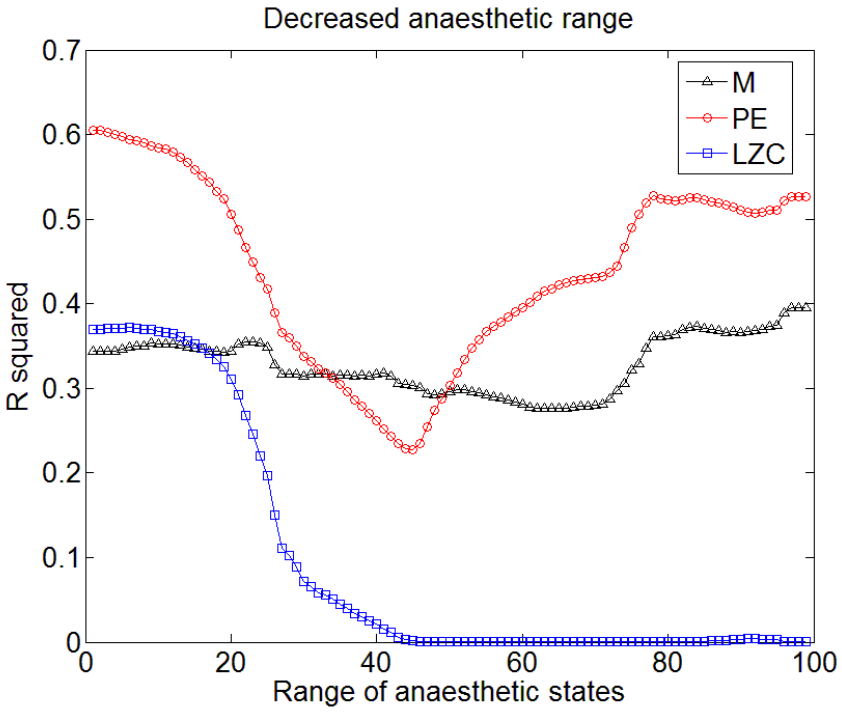

(b)

Figure 5.4: Performance of the three best parameters for different anaesthetic ranges, (a) Increased anaesthetic range, (b) Decreased anaesthetic range. Increased anaesthetic range: the anaesthetic range from BIS range (2-3), BIS range (2-4) to BIS range (2-99); Decreased anaesthetic range: from BIS range (1-99), BIS range (2-99) to BIS range (98-99).

It can be seen from Figure 5.4, the R squared of three parameters reaches the peak for the BIS range (2-53) and the R squared of three parameters becomes smallest for the BIS range (45-99). In this research, to further accurately assess the DoA for different anaesthetic states, the whole parameters pool are divided into two parts: the parameters refer to the BIS range (1-55) and the parameters refer to the BIS range (55-100). The linear regression analysis is done between the parameters and two different BIS range. The best R squared is shown in Table 5.4.

Table 5.4: The highest R squared based on different anaesthetic range

The highest R squared (Frequency band)	**BIS (1-55)**	**BIS (55-100)**	**BIS (1-100)**
M	0.4758 (power of α)	0.5957 (amplitude of β)	0.3436 (power of β)
PE	0.6548 (power of βa)	0.6878 (amplitude of β)	0.6050 (amplitude of βb)
LZC	0.5595 (power of β)	0.4425 (amplitude of $\gamma 4$)	0.3702 (power of β)

As shown in the table above, the performance of PE parameters is always better (R squared is higher than 60), however, only the M parameters calculated from the amplitude of β Frequency band show a high R squared (0.5957) for the BIS range (55-100), 5105 data points. As for LZC parameters, the best R squared calculated from power of β Frequency band is 0.5595 for the BIS range (1-55), 11868 data points. The linear relationship between these three parameters with the BIS value is shown in Figure 5.5.

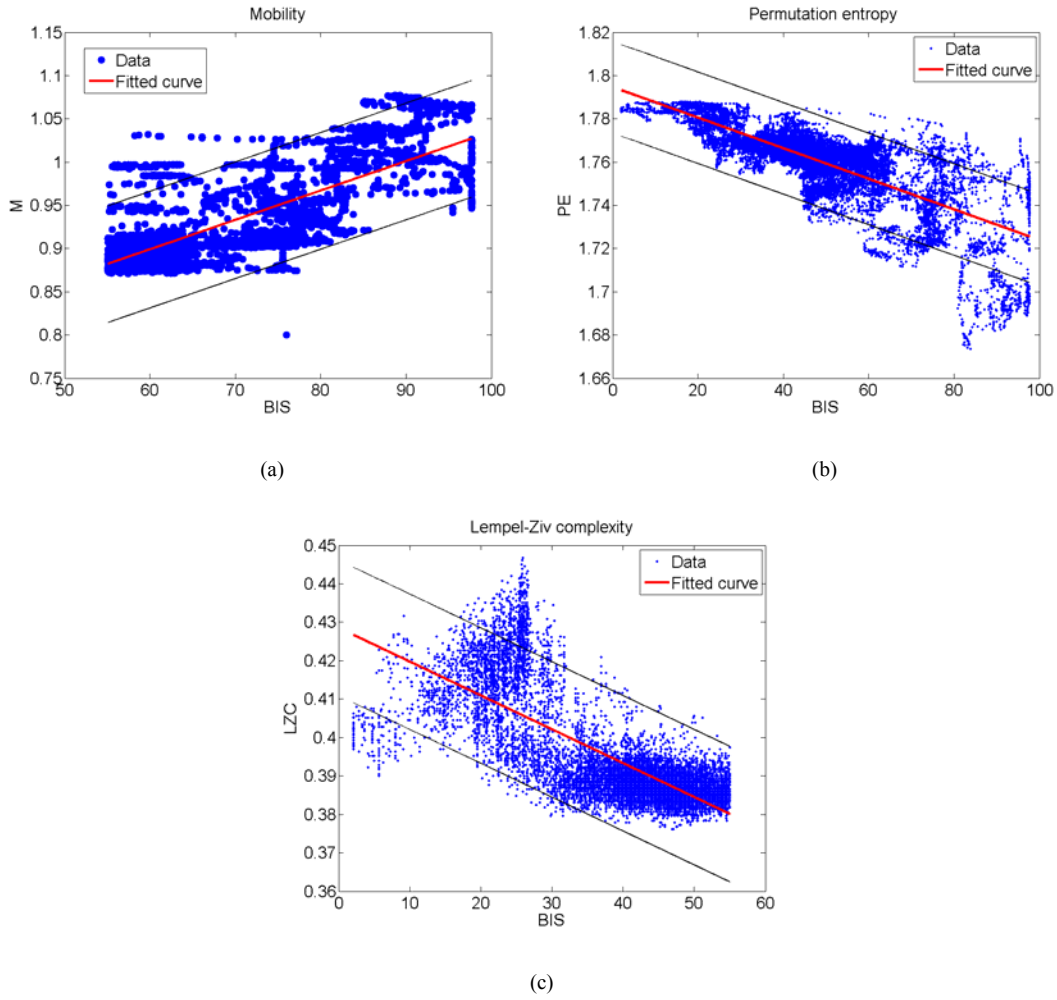

Figure 5.5: The linear relationship between parameters with BIS value, (a) Mobility, (b) Permutation entropy and (c) Lempel-Ziv complexity. The best-fit line is bold and black lines correspond to the 95% confidence boundaries. This fitted linear relation indicates that the two methods are extremely correlated.

The scatter plot graphs for the parameters and BIS are shown in Figure 5.5 for the sample (five patients, 16973 data points). Black line shows 95% confidence boundaries around the linear pink bold line. Few data points go beyond the 95%

confidence boundaries. As for the mobility, Linear equation is fitted to all data points during the BIS range (55-100) with the relation as BIS = -93.3097 + 175.3189 * M. As for the permutation entropy, Linear equation is fitted to all data points with the relation as BIS = 1553.2 - 854.9 * PE. As for the Lempel-Ziv complexity, Linear equation is fitted to all data points during the BIS range (1-55) with the relation as BIS = 289.0848 - 635.2348 * LZC.

It can be seen from Figure 5.5(b), the linear relationship between PE parameters with BIS values is weak during the BIS range (80-100), therefore, when we design the new DoA index, the mobility parameters are used to adjust the DoA assessment result of PE parameters during the awake and light anaesthetic states. In addition, the Lempel-Ziv complexity parameters are used to adjust the DoA assessment result of PE parameters during the deep anaesthetic states. The new Tindex is designed as follows:

$$\text{Tindex}=\frac{1553.2-854.9*PE+t_1*(-93.31+175.32*M)+t_2*(289.08-635.23*LZC)}{1+t_1+t_2} \quad (5.6)$$

According to BIS = 1553.2 - 854.9 * PE, When PE is equal to 1.7596, BIS is equal to 50. The 1.7596 of PE value is used as the threshold. According to BIS = -93.3097 + 175.3189 * M, When M is equal to 0.8459, BIS is equal to 55. When M is equal to 1.1026, BIS is equal to 100. If PE <= 1.7596 and 0.8459 < M < 1.1026, t_1=1, otherwise, t_1=0. According to BIS = 289.0848 - 635.2348 * LZC, When LZC is equal to 0.4535, BIS is equal to 1. When LZC is equal to 0.3685, BIS is equal to 55. If PE > 1.7596 and 0.3685 < LZC < 0.4535, t_2=1, otherwise, t_2=0.

The threshold is not 1.7561 (Corresponding BIS=55) because the DoA assessment for BIS=55 range will be inaccurate if the threshold is set as 1.7561. According to the tests on the sample, the Pearson correlation coefficients between the Tindex and the BIS index changes as the corresponding BIS values of the threshold increase. The relationship is shown in Figure 5.6. When the 1.7596 of PE value is used as the threshold, the Tindex show the highest corelation with BIS index.

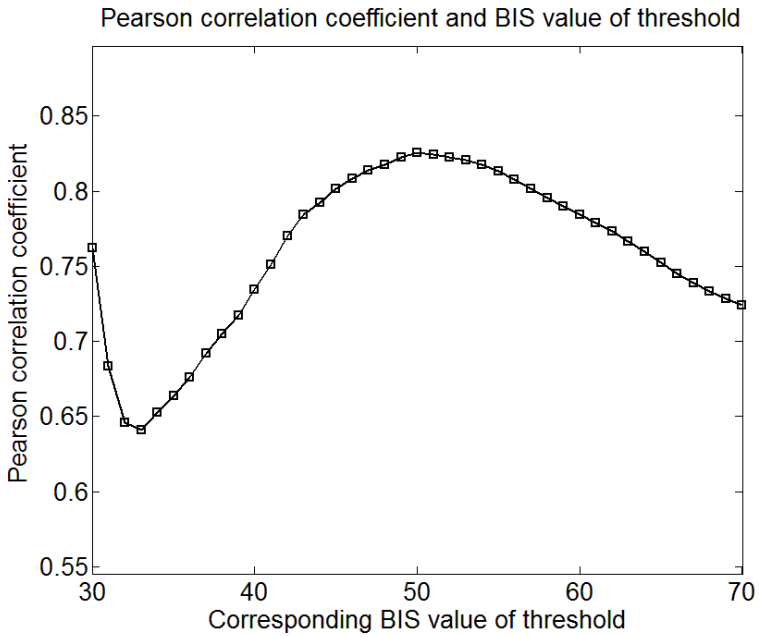

Figure 5.6: The Pearson correlation coefficient and the BIS value of threshold

The Tindex is normalised in the range of 0-100. If the Tindex value is more than 100, the Tindex value is equal to 100, and if the Tindex value is less than 0, the Tindex value is equal to 0.

5.4.4. New DoA evaluation

5.4.4.1. The correlation between Tindex and BIS index

The new Tindex is evaluated by comparing with the record BIS. The Pearson correlation method will be used to examine the correlation of Tindex and BIS index. It was widely applied for evaluating the correlation of new DoA index and BIS index (Shalbaf, Behnam, Sleigh, Steyn-Ross, & Steyn-Ross, 2014). The definition of the Pearson correlation coefficient is given below:

$$corr = \frac{\sum_N (x-\bar{x})(y-\bar{y})}{\sqrt{\sum_N (x-\bar{x})^2 \sum_N (y-\bar{y})^2}} \tag{5.7}$$

where the x is the new index value, the y is the corresponding BIS value. The $\bar{x}$ and $\bar{y}$ is the mean of x and y. The value of Pearson correlation coefficient is between 1 and -1. If the *corr* is closed to 1, it means that the two indexes are highly correlated. On the other hand, if the *corr* equals (-1), it means that there is no correlation at all between the indexes. If the *corr* equals 0, it means that there is a lack of correlation between two indexes.

The Tindex and BIS index are showed in Figure 5.7. The high Pearson correlation coefficient ($corr_{\text{Patient 2-5,7}}$=0.8227) show that there is a very close correlation between the proposed index and the BIS during different anaesthetic states.

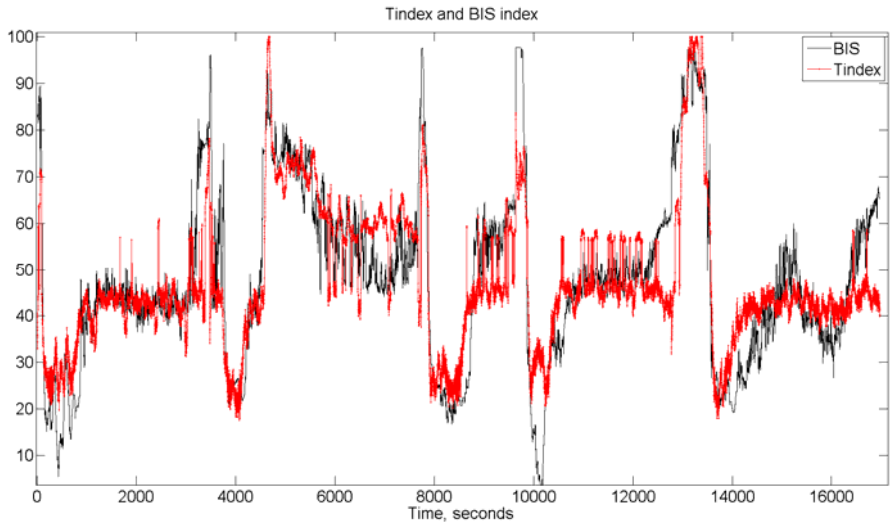

Figure 5.7: Tindex and BIS index

In addition to the sample, the performances of the new index for another random selected 12 patients (Patient 9 to Patient 20) are evaluated. The Pearson correlation coefficients for 12 cases are shown in Figure 5.8.

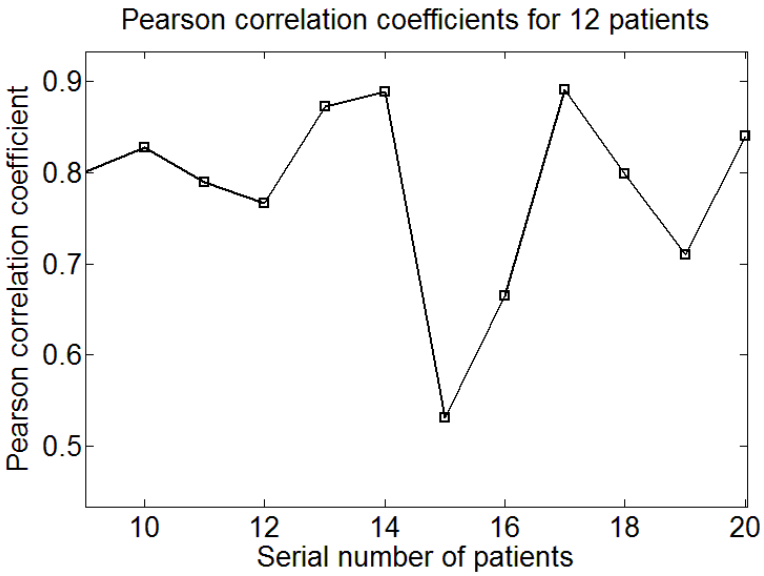

Figure 5.8: The Pearson correlation coefficients for 12 cases

The average Pearson correlation coefficient for 11 patients (No.9-14, No 16-20) is 0.8045. However, the performances of new Tindex are not good enough for Patient 15.

According to the SQI index of Patient 15, the signal quantity of Patient 15 is poor and the BIS did not have any valid outputs at the beginning of awake states. The unreliable BIS may cause the low Pearson correlation coefficient for Patient 15.

5.4.4.2. Patient's state in the case of poor signal quality

We also evaluated the performance of the new Tindex in poor signal quality cases (according to Signal Quality Indicator). When SQI is lower than 15, the BIS index could not output the valid values on the screen. In these cases, the value -3276.8 was labeled as a notice "excessive artifact detected in signal" (Nguyen-Ky et al., 2013a).

In our study, the Tindex shows the DoA values in most cases where the BIS index could not. In Figure 5.9(a), for patient 35, The BIS index is always -3276.8 from 556 to 574 seconds, but the Tindex has the assessed DoA value clearly during this period. In addition, where the BIS index shows significant upward trends from 532 to 538 seconds and from 582 to 588 seconds, but the Tindex is flat in general during this period. The same situation also happened during 1156 to 1311 seconds of patient 37 in Figure 5.9(b). According to the anesthetists' record, there was no recovery of consciousness during this period. According to the low SQI values about one minute before these significant upward trends of the BIS, the BIS index might be influenced by noise such as Electromyography. Therefore, the new Tindex is more reliable in this case.

The data of patient 37 is shown in Figure 5.9(b). The BIS index is always -3276.8 from 900 to 918 seconds, from 984 to 991 seconds, from 1097 to 1131 seconds, from 2340 to 2345 seconds and from 2368 to 2379 seconds. But the Tindex has the assessed DoA value clearly during this period. It can also be seen from the Figure 5.9(c), the Tindex has the assessed DoA value clearly from from 1269 to 1287 seconds but the BIS failed to output any useful result. According to the anesthetists' records, there was no change of patients' anesthestic states during this period. Based on that, the new value of Tindex is more reliable.

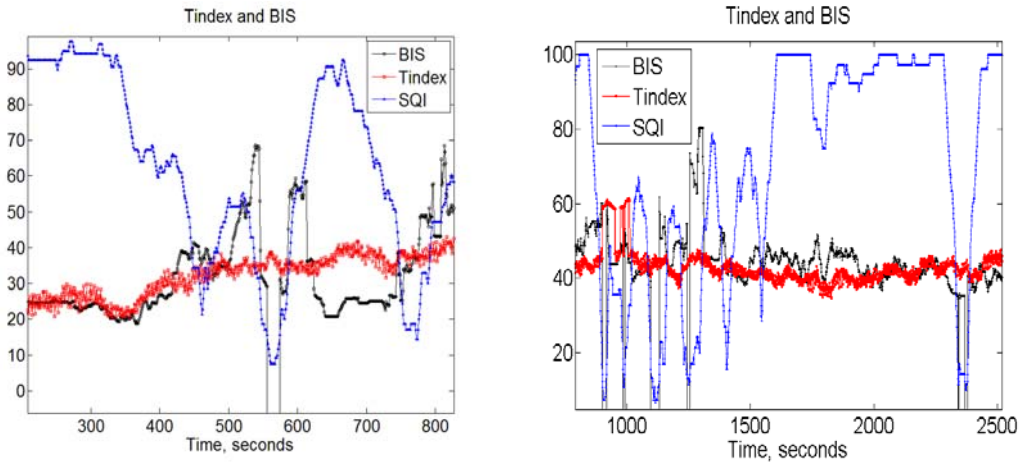

(a) (b)

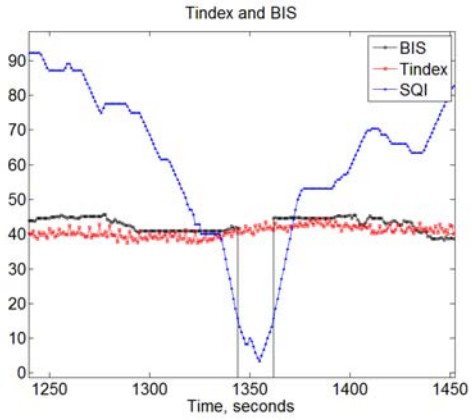

(c)

Figure 5.9: Comparison of the Tindex and BIS index, (a) patient 36, (b) patient 37 and (c) patient 22.

5.4.4.3. Time delay from deep anaesthesia to moderate anaesthesia

To evaluate the performance of the new Tindex, the time delay (deep anaesthesia to moderate anaesthesia) of both Tindex and BIS index are measured. The new index shows a very high correlation with BIS during the states of awake, light anesthesia and deep anaesthesia. However, the new Tindex shows an earlier reaction than BIS index when the patient from deep anaesthesia to moderate anaesthesia. Take patients 12 and 16 and 26 as examples, the comparison of the Tindex and BIS index is shown in Figure 5.10.

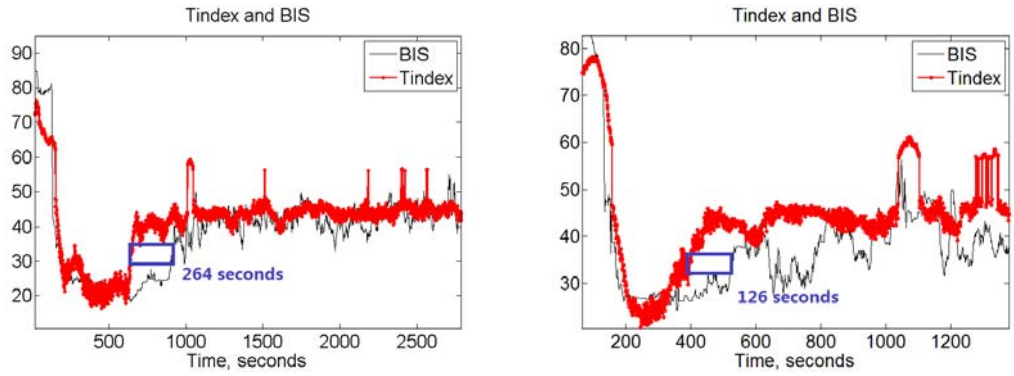

(a) (b)

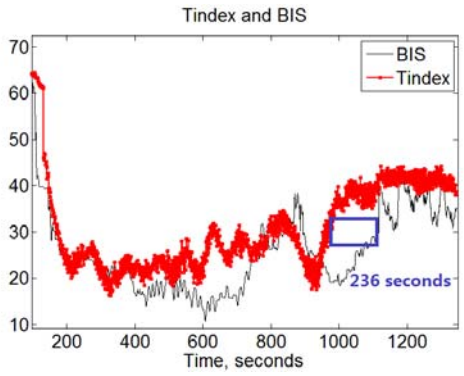

(c)

Figure 5.10: Comparison of the Tindex and BIS index, (a) patient 12, (b) patient 16 and (c) patient 26. The blue square frames show the earlier reaction of Tindex compared with the BIS.

This kind of earlier reaction appears in all the cases of the 12 patients. For the index value change (from 20 to 50), we assume that an index value of 35 corresponds to the inflection point where the patient's anaesthetic states changed from deep anaesthesia to moderate anaesthesia. In some cases, there is no significant upward trend near 35, so we compare the significant upward trends between BIS and Tindex. The time difference and Pearson correlation coefficients for 12 patients are indicated in Table 5.5.

Table 5.5: Pearson correlation and time response comparison between Tindex and BIS

Patients	**9**	**10**	**11**	**12**	**13**	**14**	**15**	**16**	**17**	**18**	**19**	**20**
Time difference (sec)	128	122	33	264	223	103	168	126	169	41	74	125
Pearson correlation	0.80	0.83	0.79	0.77	0.87	0.89	0.53	0.67	0.89	0.80	0.71	0.84

The time difference from deep anaesthesia to moderate anaesthesia is about 33 to 264 seconds. Although it is hard to assess the exact time when patients' anaesthetic states change from deep anaesthesia to moderate anaesthesia according to anaesthetists' records, the Tindex, Sindex (Chapter 6, Figure 6.2), Iindex (Chapter 7, Figure 7.3) all show the earlier reactions compared with BIS index. It also can be proved by the research outcomes of other members in our research group. It can be seen from Figure 5.11, the BIS index also shows a later reaction when patients' anaesthetic states change from deep anaesthesia to moderate anaesthesia compared with B_{DoA}. These types of later reactions for BIS index also appear in Fig. 13 and Fig.15 of Nguyen-Ky et al.'s paper (Nguyen-Ky et al., 2013a).

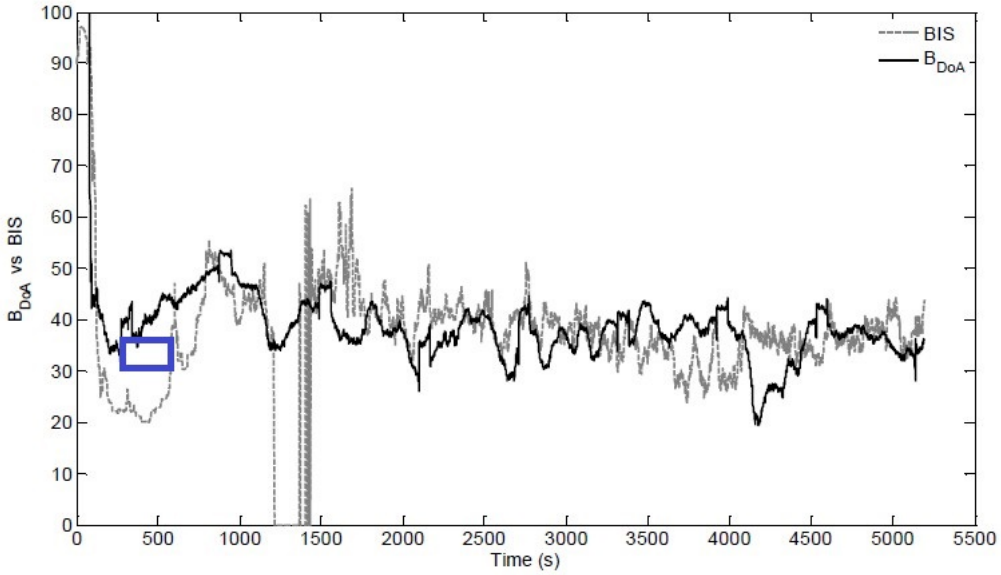

Figure 5.11: Comparison of the B_{DoA} and BIS index (Nguyen-Ky et al., 2013a).The blue square frame shows the later reaction of BIS index compared with the B_{DoA}.

Therefore, the Tindex is more reliable to show the change from deep anaesthesia to moderate anaesthesia. The early warning is useful for anesthesitics to control the time of surgical operation.

5.5. Summary

In this chapter, the mobility, Lempel-Ziv complexity and permutation entropy methods are applied to obtain the valuable parameters for DoA assessment. After the parameters are calculated from different frequency bands, the proposed new DoA index is designed based on: the M parameters which are calculated from the amplitude of β frequency band, the LZC parameters which are calculated from the power of β frequency band and the PE parameters which are calculated from the amplitude of βb frequency band. Then the new DoA index is evaluated in simulation using the measured EEG data and recorded BIS readings.

The results show that the average Pearson correlation coefficient for 11 patients is 0.8045. The results also show a 33-264 seconds earlier response than BIS during anaesthetic states changes. Furthermore, compared with BIS, the proposed new index can assess the DoA while the EEG is corrupted with noise. For example, even when the SQI value is below 15 and the BIS failed to output any valid value, the new DoA index works well. This means the proposed index can estimate the patient's anaesthetic states in poor signal quality.

6. MONITORING DOA USING SECOND ORDER DIFFERENCE PLOT METHOD

This chapter introduces the second order difference plot method and its application for EEG signal processing and DoA monitoring. First, a brief review about SODP method and its applications in EEG signal processing are provided. Then the SODP method is applied to identify different stages of anaesthesia. Finally, a new DoA Sindex is based on SODP method is developed and evaluated.

6.1. Second order difference plot method and EEG signal processing

As a graphical representation of successive rates against each other, the second order difference plot provides a rate of variability of data. The SODP method has been used for the analysis of EEGs and classification of epileptic signals (Pachori & Patidar, 2014). The SODP of intrinsic mode functions provides an elliptical structure, and the feature space formed using ellipse area parameters has given good classification performances. However, to our best knowledge, it has not been applied to assess DoA (T. Li, Wen, & Liu, 2015).

In this study, the SODP method is applied to design a new DoA index. Because the BIS index is an important reference or benchmark when developing a new DoA index, the performance of the new index is evaluated by comparing with the BIS index in the case of poor signal quality.

The denoised EEG signals, BIS values and signal quantity index were collected from 21 adult patients (Patient number:12, 13, 17-35, age 22-83 year, weight 60-130 kg. gender 9F/12M). In this study, the fast Fourier transform method is applied to divide the denoised signal into a set of signals with five basic frequency bands. We also divide the high frequency band into eight sub-frequency bands to find more useful parameters to design a new DoA index. The original denoised signal is also added in the test as a reference. As a result, a total number of 5+8+1=14 sets of frequency bands from each episode of the EEG signal are obtained.

A moving window technique is applied to calculate the SODP, mobility (M), LZC (McBride et al., 2014) and PE value. We select 56s as the window size and 55s as the

overlap in this study. The calculations based on this window size lead to a satisfactory DoA assessment results based on our study.

We calculate the SODP (Pachori & Patidar, 2014) for EEG each second. The SODP of signal *x(n)* is obtained by plotting $X(n)=x(n+1)-x(n)$ against $Y(n)=x(n+2)-x(n+1)$:

$$SX=\sqrt{\frac{\sum_{N=0}^{n-1} X(n)^2}{N}} \tag{6.1}$$

$$SY=\sqrt{\frac{\sum_{N=0}^{n-1} Y(n)^2}{N}} \tag{6.2}$$

$$SXY=\frac{1}{N}\sum X(n)\,Y(n) \tag{6.3}$$

$$D=\sqrt{(SX^2+SY^2)-4(SX^2SY^2-SXY^2)} \tag{6.4}$$

$$SODP=|\log(3\pi\sqrt{(SX^2+SY^2+D)(SX^2+SY^2-D)})| \tag{6.5}$$

The SODP value of one window is the mean of 56 SODP values. For each set of frequency band, we calculate the SODP, M, LZC and PE values based on the amplitude and power.

6.2. Parameter selection

To assess the effects of the SODP values and find out the optimal feature set for index designing, the regression technique is used to verify the correlation between the features extracted and the anaesthetic states (referred to the BIS values). Same as the previous chapter, the R squared is used to calculate the correlation between the SODP and the BIS.

In the following experiments, we calculate the SODP of the EEG signals from each patient and then combine them together. After assessing the correlation between the SODP sets and the BIS, we selected an optimal SODP set which shows the linear relationship with the Bispectral BIS. Finally, the R squared between the new DoA index with the BIS index for different patients are also calculated to show the performance of new DoA index.

To create a reliable sample set, we use 13221 seconds denoised signals from 5 patients (patient No. 12, No. 20, No. 24, No. 25 and No. 32). The denoised signals are divided into five basic frequency band and eight high frequency bands using fast Fourier transform. The SODP, M, LZC and PE values are calculated and compared with their corresponding BIS values using the following linear regression function:

$$f_i=C1+C2*Parameter_i. \tag{6.6}$$

where *C1* and *C2* are constants. They can be obtained using Matlab regression function. The SODP, M, LZC or PE values are calculated for each 56-second signal. The results of 14 frequency bands are shown in Figure 6.1.

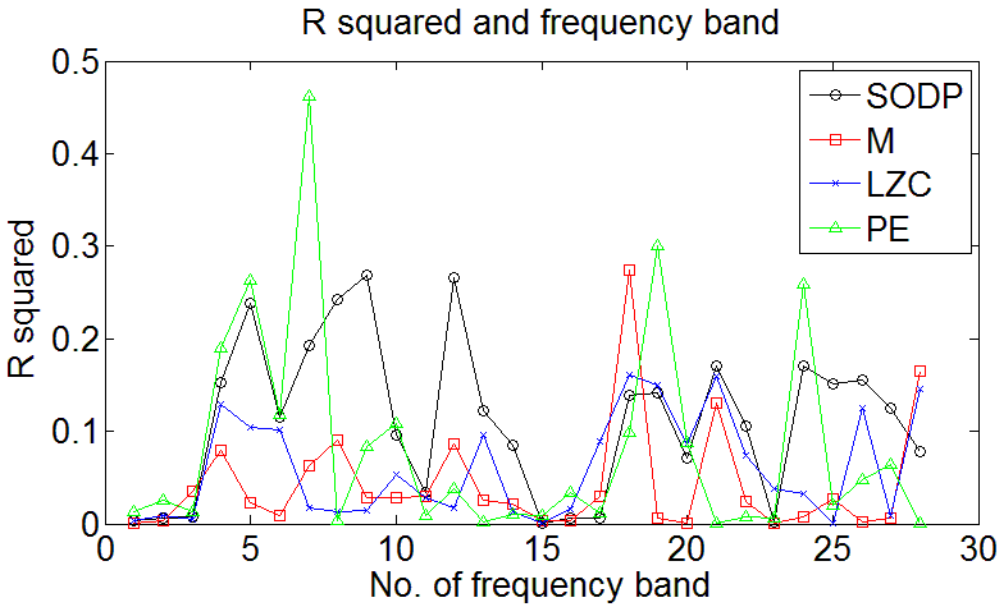

Figure 6.1: The R squared of 14 frequency bands for different feature extraction methods. The No.1 to No.14 of frequency bands represent the amplitude of δ (0.5- 3.5Hz), θ (3.5-7Hz), α (7-13Hz), β (13-30 Hz), γ (30-70 Hz), original signal (0.01-70Hz), βb (21.5-30Hz), $\gamma 1$ (30-38.5Hz), $\gamma 2$ (38.6-47Hz), $\gamma 3$ (47-55.5Hz), $\gamma 4$ (55.5-64Hz), γa (30-47Hz), γb (47-64Hz) and βa (13-21.5Hz) respectively. The No.15 to No.28 of frequency bands represent the power of the frequency bands mentioned above.

As it can be seen in Figure 6.1, the R squared of high frequency bands (γ, β) is much higher than that of low frequency bands (δ, θ and α). The average R squared of the SODP values is 0.1125 which is much higher than others (M: 0.0429, PE: 0.0818 and LZC: 0.0604). In addtion, the R squareds of SODP values for 16 different frenquency bands are more than 0.1. However, there are only eight different frenquency bands for LZC, three for M, and seven for PE with the R squared higher than 0.1. The premutation entropy and complexity measures are proved to be able to reliably track the anaesthetic-related EEG changes (Olofsen et al., 2008; X.-S. Zhang, Roy, & Jensen, 2001) and assess the different anaesthetic states (Silva et al., 2011). Therefore the SODP values can be used as measure for discriminating between different levels of consciousness during anesthesia depth assessment.

6.3. New index design

A new DoA index using the regression technique is designed as follows:

$$\text{Sindex}= C_0+\sum_n SODP_n^{K_n} * C_n \quad (6.7)$$

where C_0 to C_n are constants. The value of Kn is [-3, -2, -1, 2, 3]. The best SODP value calculated from the amplitude of $\gamma 2$ (38.6-47Hz), is selected as the $SODP_1$ and then we add other suitable SODP values. To reduce the redundancy and computation complexity of the new DoA algorithm, we only used the best seven SODP values to design the new index. In our experiments, the best SODP parameter set is from seven different frequency bands. The diversification can increase the robustness of the new Sindex. The seven SODP values ($SODP_1$ to $SODP_7$) are calculated from the amplitude of $\gamma 2$, the powers of γ, βb, $\gamma 3$, and original signals, the amplitude of α and the power of $\gamma 4$, respectively. The value of K_n is also decided by the best R squared. After tested with different K_n for the SODP set, the regression results only show a little difference. Therefore it is not very meaningful to find an optimatise K. Finally, the new index is defined as follows,

$$\text{Sindex} = 14.51+16.29*SODP_1-1.01*SODP_2-6.07*SODP_3-14.08*SODP_4 +21.10*SODP_5-8.63*SODP_6+6.65*SODP_7 \quad (6.8)$$

The Sindex is normalised at the range of 0-100. If the Sindex value is more than 100, it is set to 100. Likewise, if the Sindex value is less than 0, it is set to 0.

6.4. New DoA evaluation

The Sindex is evaluated by comparing with the recorded BIS. The average R squared between the new DoA index and the BIS index for 21 patients is 0.5375. In addition to the five patients (No. 12, No. 20, No. 24, No. 25 and No. 32) applied during the above experimental process, the performances of the Sindex for another 16 patients are also evaluated. Take patient 13, 19 and 34 as examples, the new index shown in Figure 6.2 has a very high correlation with the BIS during the states of awake, light anesthesia and deep anesthesia.

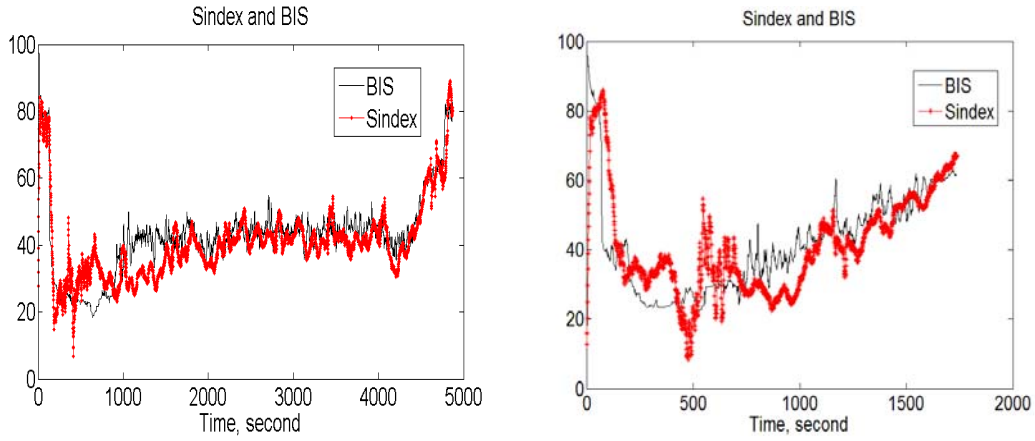

(a) (b)

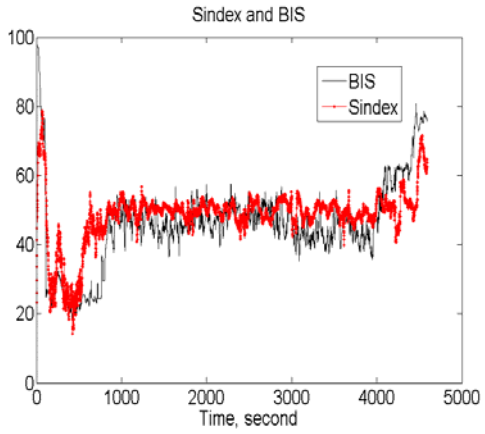

(c)

Figure 6.2: Comparisons of the Sindex and BIS index, (a) patient 13 (R squared =0.6593), (b) patient 19 (R squared =0.422), and (c) patient 34 (R squared =0.4954).

When SQI is lower than 15, the BIS index could not display the values on the screen. In this study, the Sindex shows valid index values in cases which the BIS index cannot. As it can be seen in Figure 6.3(a), for patient 22, the BIS index are always -3276.8 from 1328 to 1346 seconds, but the Sindex can assess the DoA during this period. Another similar case is also shown in Figure 6.3(c). The BIS index is always -3276.8 from 900 to 918 seconds, from 984 to 991 seconds and from 1097 to 1131 seconds. But the Sindex has the assessed DoA value clearly during this period. According to the BIS value before and after this period, the value of Sindex is reliable. In the case of patient 23, the comparison of the new proposed index, Sindex and the BIS values is showed in Figure 6.3(b). From 0 to 81 seconds, the invalid BIS values can not be displayed on the monitor screen. However, the Sindex shows the change from awake to deep anaesthesia state. This is consistent with the clinical observations according to the anesthetist's record (the Parecoxib (40 mg) and Propofol (160 mg) were used about 1 minute before the BIS index starting to show some valid values).

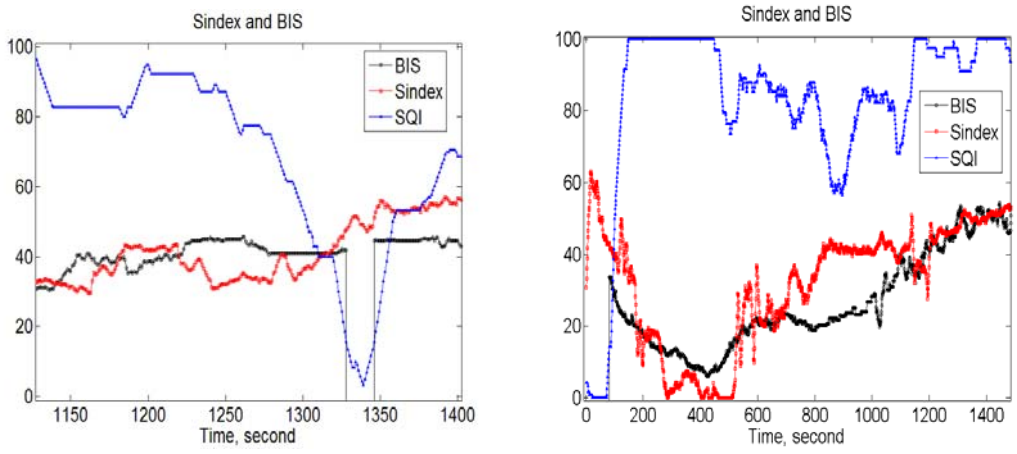

(a) (b)

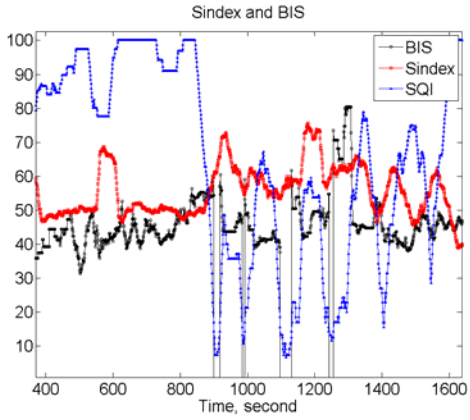

(c)

Figure 6.3: Comparison of Sindex and BIS index, (a) patient 22, (b) patient 23 and (b) patient 37.

6.5. Discussion

Comparing with BIS, the beginning of the new Sindex is not stable in some cases. One important reason is that when designing the new indexes, the regression technique is used to find the best coefficients which make the new index highly correlate to the BIS index. However, the beginning of BIS is not reliable in most cases because the calculation of BIS needs a period of time to start the first valuable value. It can be proved that the BIS values at the beginning of awake states are a series of useless value or always 97.7 without change. It is hard to know how many of them are useless, so we cannot delete them simply. Another reason is that all of the data are collected from the anaesthetic patients, thus the period of anaesthetic state is much longer than the awake state. As a result, the regression results from the sample can only obtain the high R squared in anaesthetic state, but small R squared in awake state. Not only the amount of the awake state data, but also the quality of the awake state data from the sample limit the outcome of regression technique. Although the optimization of samples has already been tried in Chapter 4, more work can be done in the future research. The larger sample size and higher quality samples are helpful to increase the robustness of the new indexes.

In addition, although R squared and Pearson correlation coefficients are widely used for assess the correlation among DoA researchers (Nguyen-Ky et al., 2013a; Shalbaf et al., 2014), the performance of them are not good for reflecting the real correlation in some cases from our study, especially, for the range with dramatic change of anaesthetic states. In future research, separating the different anaesthetic states for correlation evaluation or improve correlation evaluation method may lead to a more accurate correlation evaluation.

6.6. Summary

In this study, the SODP method is introduced and applied to assess DoA. The new DoA index is designed based on seven SODP parameters calculated from the amplitudes of *γ2* (38.6-47Hz) and *α* (7-13Hz), and the powers of *γ* (30-70Hz), *βb* (21.5-30Hz), *γ3* (47-55.5Hz), *γ4* (55.5-64Hz) and original signals. Compared with the BIS, the proposed Sindex shows a very close correlation during different anaesthesia states. In addition, the Sindex can assess the DoA while the signal quality is poor and the BIS has no valid output.

7. DEPTH OF ANAESTHESIA ASSESSMENT USING INTERVAL PERMUTATION ENTROPY AND INTERVAL SECOND ORDER DIFFERENCE PLOT TECHNIQUES

This chapter presents a new method to apply the interval permutation entropy and interval second order difference plot techniques to assess the depth of anaesthesia. Firstly, the denoised electroencephalograph signals are decomposed into 13 different frequency bands. The permutation entropy and second order difference plot values of each frequency band are calculated. The PE and SODP values of high frequency bands (21.5-47Hz) show the highest linear relationship with the anaesthesia states, therefore they are selected to form the parameter set. Then the SODP and PE parameters are fine tunned using interval feature (IF) technique. Finally, a new index is designed using the IPE and ISODP.

7.1. Interval feature extraction methods

Features derived from the signal over time segments of various lengths, called "interval features", have shown to lead to high classification accuracy (Rodríguez et al., 2005; Rodrıguez, Alonso, & Boström, 2001). Using interval feature method can not only extract more features from the same signals, but also obtain interval features from different lengths. The interval method is simple and intuitive compared to the other feature extraction methods. The simplicity is of significance in view of the large variability of the data. A more intricate and versatile model such as wavelets may overfit the noise. In addition, the interval extraction method is non-linear, which gives it additional flexibility (Kuncheva & Rodríguez, 2013). However, to our best knowledge, the interval extraction method has not been applied to assess DoA.

7.2. EEG signal processing based on Interval feature extraction method

The EEG data were collected from 23 adult patients (Patient1 to Patient 23, age 24-74 year, weight 55-110 kg. gender 11F/12M).

To obtain valuable parameters of denoised EEG signals, the fast Fourier transform method is applied to divide the denoised signal into five different frequency bands. We also divide the two high frequency bands into eight smaller frequency bands: *βa* (13-21.5Hz), *βb* (21.5-30Hz), *γ1* (30-38.5Hz), *γ2* (38.6-47Hz), *γ3* (47-55.5Hz), *γ4* (55.5-64Hz), *γa* (30-47Hz) and *γb* (47-64Hz). The original signal bands are also added as a reference. As a result, we totally obtained 5+8+1=14 sets of frequency bands from each episode of EEG signal.

7.2.1. SODP and PE parameters

A moving window technique is applied to calculate the PE and SODP parameters. The BIS monitor uses EEG segments up to 61.5s for index calculation and the window size is 60s as for Entropy-Module. As the Interval feature (IF) method shows the interval lengths are better to be the multiples of 2 (Kuncheva & Rodríguez, 2013), such as 2, 4, 8, we select 56s as the window size and the overlap is 55s. Therefore, as for every second, the PE and SODP are calculated based on the signals of its previous 56 seconds.

The second order difference plot (Pachori & Patidar, 2014) of each window size-signal is calculated. The SODP is calculated in seconds. The SODP of a 56-second EEG signal is the average of 56 SODPs.

As for each set of frequency band, we calculate their PEs and SODPs based on amplitude and power respectively. As a result, we obtained 28 sets of SODP and PE as the parameter pool.

To find out the optimal parameter set for index designing, the regression technique is used to test the correlation between the parameters and anaesthetic states (referred to the BIS value). The coefficient of determination (R squared) is used to evaluate the correlation between the parameter and BIS value.

7.2.2. Parameter set optimisation using interval feature

After comparing the correlation between the parameter and BIS value, the parameter which shows the highest linear relationship with the BIS value is selected to form the

optimal parameter set. Then the optimal parameter set is further improved using interval feature methods.

"Interval features" are derived from the signal over time segments of various lengths. Take one segment of the new DoA index as an example, denoted by *x(i)* the value of the signal at time *i*, where *i* =1, 2,..., *T* (*T* is dividable by 10). The signal segment is divided into 10 units equally, and the unit length is *u=T*/10. The first unit will be *U(1)*=[*x(1), x(2),..., x(u)*], the tenth unit will be *U(10)*=[*x(T-u+1), ...,x(T-1), x(T)*]. The interval length is varied as powers of two, so three kinds of point sets are two units, four units and eight units. While the starting point is kept at *j*, the first kind of interval at *j* is the point set [*U(j-1)*, *U(j)*], *j*∈ [*j*=2, ..., 10], the second kind of interval is [*U(j-3), U (j-2), U (j-1), U(j)*], *j*∈ [*j*=4, ..., 10], and the third kind of interval is [*U(j-7), U (j-6),..., U(j)*], *j*∈ [*j*=8, ..., 10]. For three kinds of interval length, there are totally 9+7+3=19 intervals.

In this study, three interval lengths are used to extract feature. The interval values calculated from each interval are: (1) the mean of the parameters μ, (2) the standard deviation σ, and (3) the covariance with the time variable (CTV). However, only the means of different interval lengths are useful to improve the optimal parameter set in this study. When we calculate the interval values, the window size is divided into eight equal units and each unit is equal to seven seconds. For each Interval parameter (Iparameter) value, Interval 2 is the mean of 14 parameter values (PE or SODP) from the previous 14 second period, Interval 4 is the mean of 28 parameter values from the previous 28 second period and Interval 8 is the mean of 56 parameter values from the previous 56 second period. The new Interval parameter (IPE, ISODP) are calculate as follows,

$$\text{Iparameter (IPE, ISODP)} = \text{Interval 2}^* \text{ Interval 4/ Interval 8} \qquad (7.1)$$

The new Iindex is designed based on the new Iparameters (IPE, ISODP) using regression technique.

7.3. Parameter estimation

42013 seconds denoised signals from 13 patients (patient 1 to patient 13) are randomly selected for the following experiments. Firstly, we calculated the parameters for each patient's EEG signals and then put these parameters from different patients together. After that we evaluated the correlation between the parameters of the whole sample with BIS values using a regression technique.

The denoised signals are divided into 5 basic frequency bands using the fast Fourier transform method. The SODP and PE value are calculated based on both amplitude and power of each basic frequency band. According to Liang et al. (Liang et al., 2009), *L*=6 seconds, *m*=3 are selected in this study for the best performance. Then the SODP

and PE for each second are compared with relevant BIS value using line regression technique. The results of five basic frequency bands are showed in Table 7.1.

Table 7.1: The regression results of Basic EEG frequency bands

R squared	Parameters	δ (delta)	θ (theta)	α (alfa)	β (beta)	γ (gama)	Denoisd data
Amplitude	SODP	0.0438	0.0339	0.0434	0.2494	0.3673	0.2560
	PE	0.0248	0.0670	0.1005	0.0713	0.3244	0.2321
Power	SODP	0.0311	0.0265	0.0321	0.2027	0.0838	0.2043
	PE	0.0347	0.0327	0.0825	0.0430	0.3098	0.2020

As shown in Table 7.1, the best R squared of SODP (0.3673) is higher than that of PE (0.3244). The premutation entropy is proved to be able to reliably track the anaesthetic-related EEG changes (Olofsen et al., 2008) and assess the different anaesthetic states(Silva et al., 2011). Therefore the SODP is treated as a promising parameter for discriminating between different levels of consciousness during anesthesia.

Table 7.1 also shows that the R squared of high frequency bands (γ, β) is much higher than that of low frequency bands (δ, θ and α). To find a more accurate correlation between parameters and BIS value, the high frequency bands are divided into eight small frequency bands: βa(13-21.5Hz), βb(21.5-30Hz), $\gamma 1$(30-38.5Hz), $\gamma 2$(38.6-47Hz), $\gamma 3$(47-55.5Hz), $\gamma 4$(55.5-64Hz), γa(30-47Hz) and γb(47-64Hz). The R squared of different frequence bands are listed as follows:

Table 7.2: The regression results of high EEG frequency bands

R squared	Parameters	βa	βb	$\gamma 1$	$\gamma 2$	$\gamma 3$	$\gamma 4$	γa	γb
Amplitude	SODP	0.2560	0.3182	0.3454	0.2709	0.1283	0.1119	0.3637	0.1759
	PE	0.0449	0.5529	0.0311	0.0611	0.1146	0.2806	0.0053	0.0839
Power	SODP	0.1285	0.1640	0.0472	0.0006	0.1733	0.1994	0.0787	0.1171
	PE	0.0341	0.0001	0.0007	0.0012	0.3434	0.0040	0.0169	0.1805

As for PE, the best R squared 0.5529 is in βb (21.5-30Hz). Therefore, according to Table 7.1 and Table 7.2, the PE value calculated from the amplitude of βb and the SODP value calculated from the amplitude of γ show the strongest linear correlation with BIS value. These two parameters are selected to form the optimal parameter set and they are futher improved using Interval feature method. According to equation

(6.1), the IPE values and ISODP values are obtained based on the original SODP and PE values.

To evaluate the performances of ISODP and IPE, we calculate the average values of ISODP, IPE, SODP and PE for different anaesthesia states respectively. As can be seen in Figure 7.1, the ISODP and IPE show stronger linear correlation with the BIS value than SODP and PE. Besides, unlike SODP and PE, ISODP and IPE make the new DoA index smoother than BIS index and clearly response to the change of index trends which can be seen from Figure 7.3(b), Figure 7.4(b) and Figure 7.6.

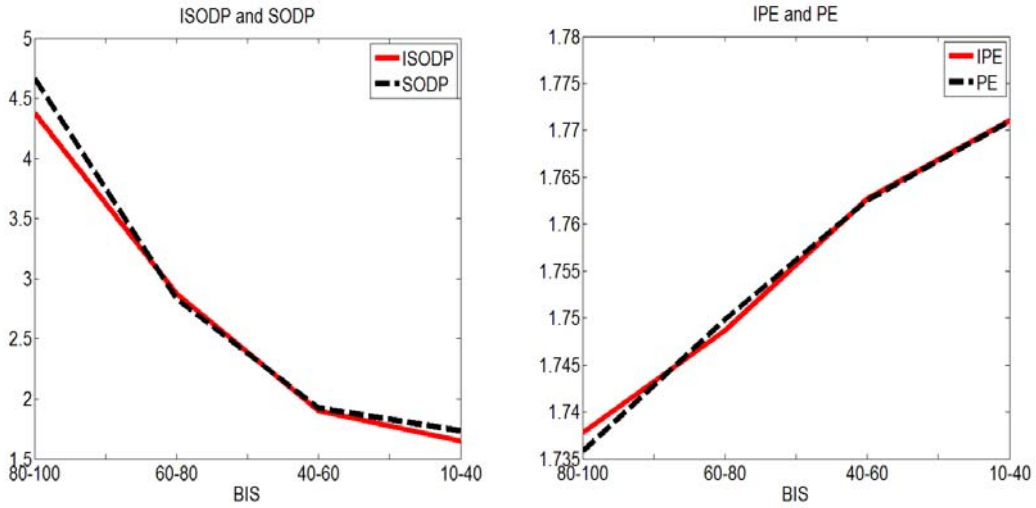

(a) (b)

Figure 7.1: The comparison of Iparameters and original parameters, (a) ISODP and SODP, (b) IPE and PE.

7.4. New Index Design and Evaluation

Table 7.3: The best parameter set

Anaesthesia states	**BIS value**	**Length**	**ISODP amplitude of γ (30-70 Hz)**	**IPE amplitude of βb (21.5-30Hz)**
Awake	80-100	1144s	4.3781±1.7636	1.7378±0.0221
Light anaesthesia	60-80	3227s	2.8777±1.0899	1.7486±0.0167
Moderare anaesthesia	40-60	18149s	1.9019±0.5907	1.7627±0.0074
Deep anaesthesia	10-40	18801s	1.6530±0.5323	1.7711±0.0096

Table 7.3 shows the best parameter set for new DoA design. We design the new DoA index using regression technique. The proposed new DoA index is designed as follows:

$$\text{Iindex} = C0 + C1*ISODP + C2*IPE \tag{7.2}$$

C0, C1 and *C2* are constants. They can be obtained using Matlab regression function. Based on 42013 seconds EEG data from 13 patients, the Iindex is calculated as follows,

$$\text{Iindex} = 1241.72 + 5.05*ISODP - 685.72*IPE \tag{7.3}$$

The Iindex is normalised in the range of 0-100. If the Iindex value is more than 100, the Iindex value is equal to 100, and if the Iindex value is less than 0, the Iindex value is equal to 0.

The new Iindex is compared with the BIS using realistic anesthetic EEG signals. In addition to the 13 patients applied as the sample during the above experimental process, the performances of the new index for another 10 patients (patient 14 to patient 23) are evaluated. A scatter plot for the Iindex and BIS is shown in Figure 7.2 for the 10 patients (31380 data points). Linear equation is fitted to all data points with the relation as Iindex = 0.5932*BIS+18.96. Black line shows 95% confidence boundaries around the linear pink bold line. Few data points go beyond the 95% confidence boundaries. The high Pearson correlation coefficient ($corr_{\text{Patient }14-23}$ =0.7773) for the 10 patients show that there is a very close correlation between the proposed index and the BIS during different anaesthetic states ($corr_{\text{Patient}1-13}$=0.7610).

Comparing with the BIS, the beginning of the Iindex is not close enough in some cases. One important reason is that when designing the new index, the regression technique is used to find the best coefficients which make the new index highly correlate to the anaesthetic states. To solve this problem, it is necessary to develop some methods to filter out the useless value of the awake state data and optimise the sample structure. The larger sample size and higher quality samples are helpful to increase the robustness of the new Iindex.

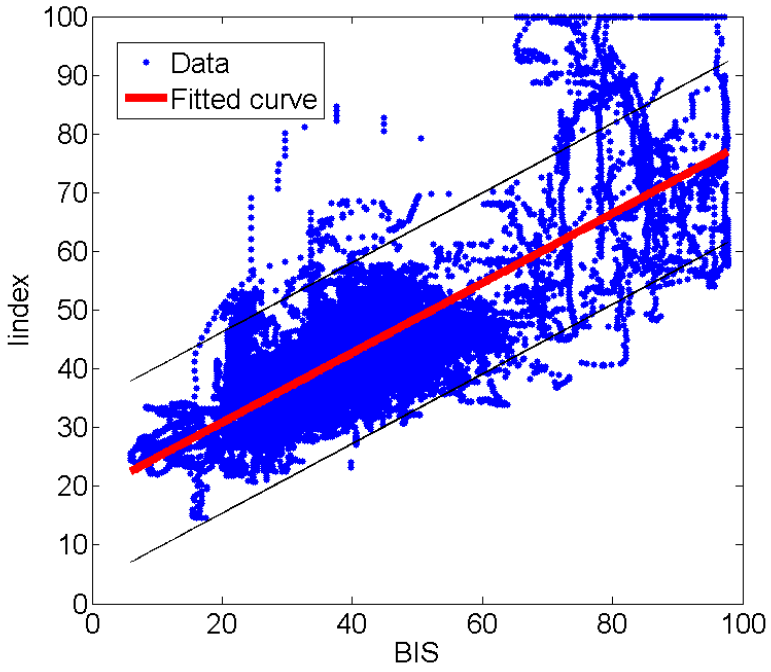

Figure 7.2: A scatter plot for the Iindex and BIS for 7 patients. The best-fit line is bold and black lines correspond to the 95% confidence boundaries. This fitted linear relation indicates that the two methods are extremely correlated.

7.4.1. Time delay from consciousness to unconsciousness

To evaluate the performance of the new Iindex, the time delay (awake to deep anaesthesia) of both Iindex and BIS index are measured. Take patients 14 and 18 as examples, in Figure 7.3 and Figure 7.4, the new index shows a very high correlation with BIS during the states of awake, light anaesthesia and deep anaesthesia. However, the new Iindex shows an earlier reaction than BIS index when the patient is from awake to deep anaesthesia.

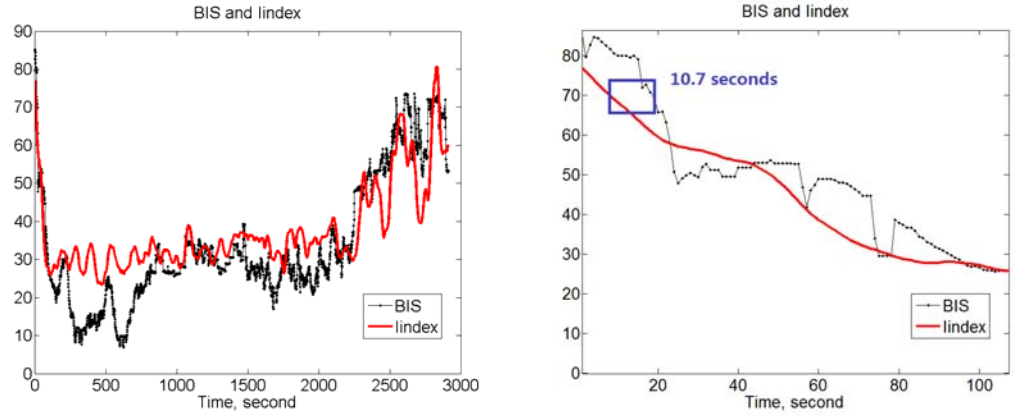

(a) (b)

Figure 7.3: Comparison of the Iindex and BIS index of patient 14, (a) all anaesthetic states, (b) the state from awake to deep anaesthesia. The blue square frames show the earlier reaction of Iindex compared with the BIS.

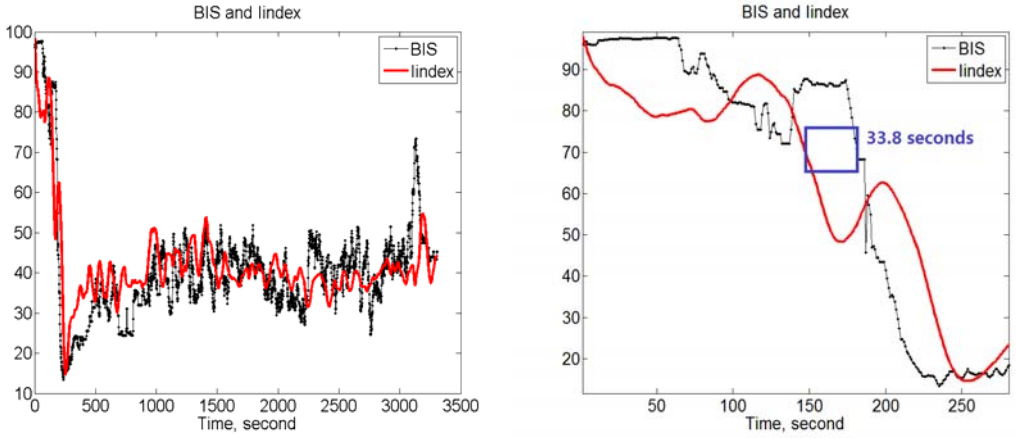

(a) (b)

Figure 7.4: Comparison of the Iindex and BIS index of patient 18, (a) all anaesthetic states, (b) the state from awake to deep anaesthesia. The blue square frames show the earlier reaction of Iindex compared with the BIS.

This kind of earlier reaction appears in nine cases of the 10 patients. According to Junbeom *et al.*'s paper (Kim et al., 2014), we assume that an index value of 70 corresponds to the inflection point where the patient starts to be anesthetized. In some cases, there is no significant downward trend near 70, so we compare the significant downward trends between BIS and Iindex. The time difference and Pearson correlation coefficients for 10 patients are indicated in Table 7.4. The time difference for loss of consciousness (LoC) is about 3.1 to 59.7 seconds. The early warning is useful for anaesthetics to control the time of surgical operation.

Table 7.4: Pearson correlation and time response comparison between Iindex and BIS

Patients	14	15	16	17	18	19	20	21	22	23
Time difference (sec)	10.7	3.1	59.7	5.9	33.8	8.0	37.5	36.4	16.9	No data*
Pearson correlation	0.7491	0.7431	0.7332	0.8189	0.7751	0.6761	0.7071	0.3983	0.5242	0.8531

* See Fig.6(b)

7.4.2. Patient's state in the case of poor signal quality

We also evaluated the performance of the new Iindex on poor quality data (according to Signal Quality Indicator). In our study, the Iindex shows the DoA values in most cases where the BIS index could not. In Figure 7.5(a), for patient 22, the BIS index is always -3276.8 from 1269 to 1287 seconds, but the Iindex has the assessed DoA value clearly during this period. The same situation also happened during 501 to 519 seconds and 1180 to 1191 seconds of patient 29 in Figure 7.6(c). According to the BIS value before and after this period, the value of Iindex is reliable.

The data of patient 23 is showed in Figure 7.5(b). It is observed from the 0 to 26 seconds, there are invalid BIS which were not displayed on the screen. However, the new Iindex shows all the changes from awake to deep anaesthesia all the time. This agreed with clinical observations recorded by attending anaesthetists, which said the Parecoxib (40 mg) and Propofol (160 mg) were administered about 1 minute before the BIS index starts to show some valid value.

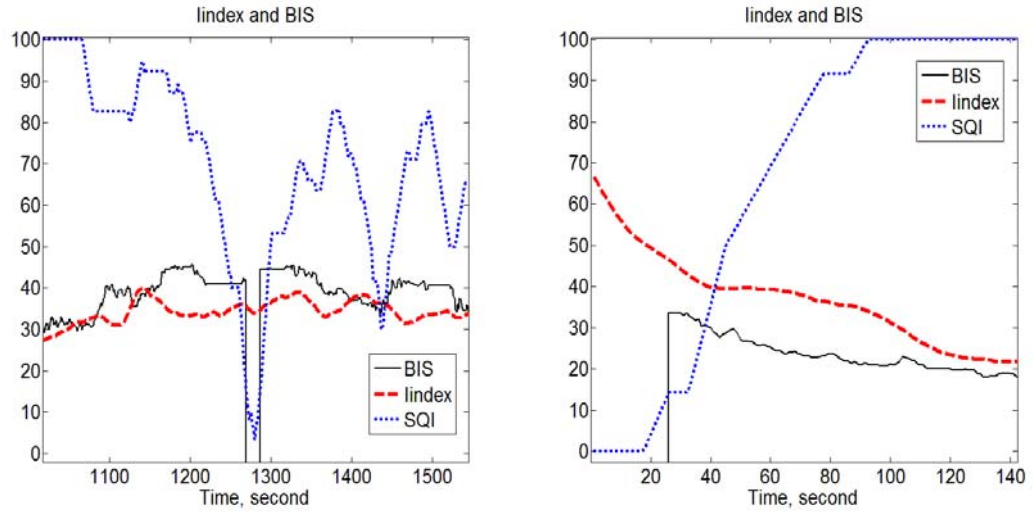

(a) (b)

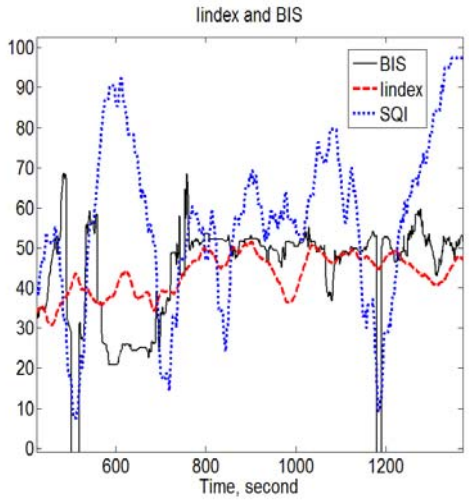

(c)

Figure 7.5: The comparison of Iindex and BIS index, (a) patient 22, (b) patient 23 and (c) patient 36.

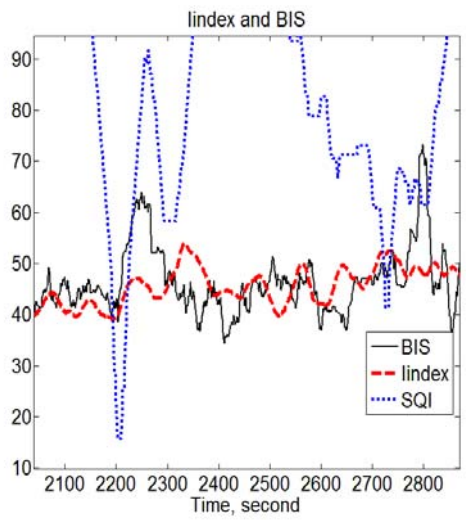

(a)

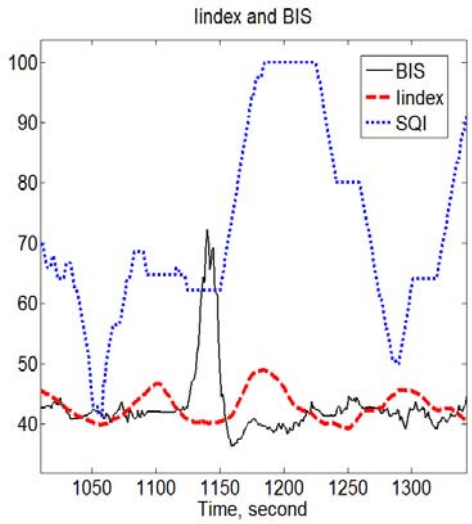

(b)

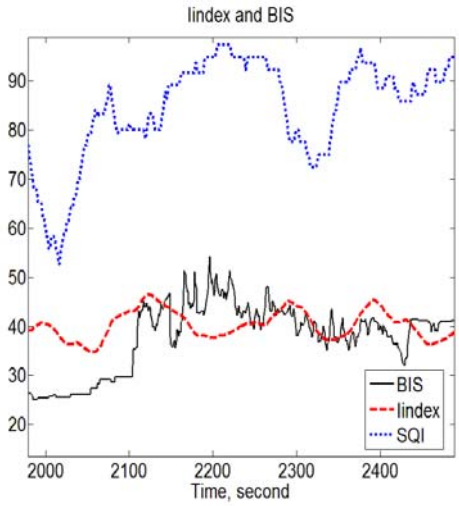

(c)

Figure 7.6: The comparison of Iindex and BIS index, (a) patient 15, (b) patient 21 and (c) patient 29.

The data of patient 15 is shown in Figure 7.6(a). Where the BIS index shows significant upward trends from 2200 to 2250 seconds and from 2790 to 2830 seconds, but the Iindex is flat in general during this period. According to the anaesthetists' record, there was no recovery of consciousness during this period. According to the low SQI values about one minute before these significant upward trends of the BIS, the BIS index might be influenced by noise such as Electromyography. Therefore, the new Iindex is more reliable in this case.

The same situation also happened during 1125 to 1135 seconds of patient 21 in Figure 7.6(b) and 2100 to 2200 seconds of patient 29 in Figure 7.6(c).

7.5. Summary

In this study, the second order difference plot and permutation entropy method are applied to obtain the valuable parameters for DoA assessment.

Using regression technique, the proposed new DoA index is designed based on two parameters: the IPE value calculated from the amplitude of βb (21.5-30Hz) and the ISODP value calculated from the amplitude of γ (30-70 Hz). The new DoA index is evaluated in simulation using measured EEG data and BIS recordings.

The results show a very close correlation with recorded BIS during different anaesthesia states. The Pearson correlation coefficient for 10 patients is 0.7771. The results also

show an earlier response (3.1-59.7 seconds) than BIS index during anaesthetic states changes.

Furthermore, compared with BIS, the proposed new index can assess the DoA even the SQI value is below 15, while the BIS failed to output any useful result. This means the proposed index can estimate the patient's anaesthetic states in poor signal quality.

8. DISCUSSION AND CONCLUSIONS

The focus of this study was to develop reliable DoA algorithms for accurate DoA assessment. Some novel signal processing techniques, which are better suited for non-stationary EEG signals than currently established methods, have been proposed and applied to monitor the DoA using simplified EEG signals. To sum up the whole research process, the realistic EEG data collected from hospitals are converted into decimal numbers and then the NLM denoising algorithms are applied to denoise the raw EEG signal. After that, we propose and develop three new DoA indexes for identifying, classifying and monitoring the DoA. Finally, the new indexes are evaluated by comparing to the most popular BIS index. The results show that the proposed indexes perform better in the cases of poor signal quality, time delay, and agreeing with the clinical records.

8.1. Work and main contributions

The significant achievements of this dissertation are presented in Chapters 4 to 7 which introduce one novel method to denoise raw anaesthetic EEG data and three novel methods to monitor the depth of anaesthesia. Details of the research contributions are summarized as follows:

To improve the data filtering results, the nonlocal mean method was applied to denoise the raw EEG data. The results show that the NLM, on average, achieves 2.70dB increase in improved signal to noise ratio and 0.37% drop in improved percentage distortion ratio compared to the popular sym8 and db16 Wavelet threshold denoising methods. Another two modified NLM methods also show satisfactory EEG denoising results. The improved moving adaptive shape patches-NLM performs better than the original NLM when the signals change dramatically. In addition, the performance of the combined NLMWTD denoising method is also better than the original WTD method (0.50dB to 4.89dB higher in SNRimp), especially, when the signal quality is poor.

To improve the time lag in DoA computation and flexibility of DoA algorithms, three new indexes (Tindex, Sindex and Iindex) are developed based on four parameters (M, PE, SODP and LZC) which are calculated from different frequency bands. To develop more reliable DoA indexes, the mobility, second order difference plot and interval feature extraction methods were applied to classify different anaesthetic states. As a result, all of the three indexes are not only able to clearly discriminate the awake state,

light anaesthesia, moderate anaesthesia and deep anaesthesia state, but also can continuously assess the DoA of patients while the quality of signal was poor. In some cases, the popular BIS index shows incorrect DoA values because of noise, but the new indexes can accurately assess the patients' anaesthetic states according to the clinical records.

The new Tindex shows a 33-264 seconds earlier time response than BIS from deep anaesthesia to moderate anaesthesia.

The proposed Iindex also shows an earlier time response (3.1-59.7seconds) than BIS during the change of anaesthetic states. The interval feature extraction method makes the new DoA index smoother than BIS index and clearly responds to the change of index trends which can be seen from most cases of this study.

To sum up, the main contributions are that a novel denoised method was developed to improve the filtering result of EEG signals; three new DoA indexes are designed to accurately assess DoA. The advancements of these new indexes are showing reliable results in the case of poor signal quality and earlier time response during the change of anaesthetic states.

8.2. Discussion

Compared with the Tindex and Sindex mentioned in pervious chapters, the trend of Iindex is smoother than those of Tindex and Sindex. Therefore, it is suggested that Tindex and Sindex can be used to reflect the patient's changes of anaesthetic states; and Iindex can be used to monitor the steady state during general anaesthesia.

In addition, The Tindex shows a 33-264 seconds earlier time response than BIS during the change from deep anaesthesia to moderate anaesthesia. However, the Iindex shows a 3.1-59.7 seconds earlier time response than BIS during the change from awake to light anaesthesia. Therefore, Iindex and Tindex can be coordinated by their weighted sum. Another option is that the Iindex is used for the DoA assessment from awake to light anaesthetic states of the patients. After the patients reach the deep anaesthetic states, the Tindex is used for the DoA assessment instead of Iindex. Therefore, the time delay can be reduced to the maximum extent by the combined Tindex and Iindex. However, these combinations are based on the assumptions that we can detect or predict the transient and the steady state.

8.3. Future work and direction

During the course of this study, many improvements in DoA index design were explored for improvement. Despite these attempts, there is still much room for further improvements.

As for general DoA indexes, the performance for one patient is good but for another one, it may not be satisfactory. Not only Tindex, Sindex, Iindex, but also BIS index is

influenced by the physical characteristics of different patients. Therefore, the performances of DoA indexes are different in different cases. One promising option for improvement is to develop an individualized DoA index which can be adjusted according to each individual patient.

In future research, by increasing the number of patients, these parameters (M, PE, LZC, SODP) in Chapters 5, 6, and 7 may become a function of patients' physical characteristics. Accurately assessing the relationship between these parameters with the characteristics of patients will help in developing a more robust individualized DoA index.

In addition, the patients in this study are all adults. The age range is from 22 to 83 years old. However, the DoA assessment based on EEG signals for children is very different from that of adults because the children's brains are still developing. Therefore, the individualized DoA index development for different age groups is of great significance.

In future research, EEG, ECG, blood pressure and other standard measures will be combined as the input signals which may be advantageous to increase the validity of the depth of anaesthesia assessment. The ECG, blood pressure and other standard measures of individual patients can be considered when an individualized DoA index is designed.

In this study, the DoA assessment is based on the single channel EEG signals. All the PE, SODP, M and LZC parameters are calculated based on the Channel 2 EEG signals obtained from BIS monitors. There are experiments in Chapter 5 proving that the PE, SODP, M and LZC parameters calculated from Channel 2 EEG signals are more useful for new DoA index than those calculated from Channel 1. It also shows that the front temporal synchronization of EEG signals is helpful for DoA assessment in other research. For example, an index named order pattern laminarity (OPL) was designed based on the order patterns cross recurrence plot method to successfully assess changes in long-range frontal-temporal synchronization as the mechanism forming the foundation of conscious perception (Shalbaf et al., 2014). Therefore, the work about multichannel electroencephalogram analysis for different parameters can be done to improve the assessment of depth of anaesthesia in the future.

REFERENCES

Al-Kadi, M. I., Reaz, M. B. I., Ali, M. A. M., & Liu, C. Y. (2014). Reduction of the Dimensionality of the EEG Channels during Scoliosis Correction Surgeries Using a Wavelet Decomposition Technique. *Sensors, 14*(7), 13046-13069.

Alfeeli, B., & Agah, M. (2009). MEMS-based selective preconcentration of trace level breath analytes. *Sensors Journal, IEEE, 9*(9), 1068-1075.

Antognini, J. F., Carstens, E., & Raines, D. E. (2003). *Neural mechanisms of anesthesia*: Springer.

Arianos, S., & Carbone, A. (2007). Detrending moving average algorithm: A closed-form approximation of the scaling law. *Physica A: Statistical Mechanics and its Applications, 382*(1), 9-15.

Aspect. (2013). Analysis of the competitors of BIS 2013, from http://www.docin.com/p-511924648.html

Atwood, H. L., & MacKay, W. A. (1989). *Essentials of neurophysiology*: Decker.

Bøggild-Madsen, N., & Cargnelli, T. (1978). Accidental over-dose of alfathesin under general anaesthesia: case report. *Canadian Anaesthetists' Society Journal, 25*(3), 245-246.

Bandt, C., & Pompe, B. (2002). Permutation entropy: a natural complexity measure for time series. *Physical Review Letters, 88*(17), 174102.

Bein, B. (2006). Entropy. *Best Practice & Research Clinical Anaesthesiology, 20*(1), 101-109.

Bibian, S., Zikov, T., Dumont, G. A., Ries, C. R., Puil, E., Ahmadi, H., . . . MacLeod, B. A. (2001). *Estimation of the anesthetic depth using wavelet analysis of electroencephalogram.* Paper presented at the Engineering in Medicine and Biology Society, 2001. Proceedings of the 23rd Annual International Conference of the IEEE.

BIS sensor for Aspect Medical Systems, Inc.

Bischoff, P., Schmidt, G. N., & am Esch, J. S. (2000). Assessment of depth of anaesthesia. *Best Practice & Research Clinical Anaesthesiology, 14*(2), 321-334.

Bowdle, T. A. (2006). Depth of anesthesia monitoring. *Anesthesiology clinics, 24*(4), 793.

Brice, D., Hetherington, R., & Utting, J. (1970). A simple study of awareness and dreaming during anaesthesia. *British journal of anaesthesia, 42*(6), 535-542.

Bruhn, J., Lehmann, L. E., Röpcke, H., Bouillon, T. W., & Hoeft, A. (2001). Shannon entropy applied to the measurement of the electroencephalographic effects of desflurane. *Anesthesiology, 95*(1), 30-35.

Bruhn, J., Röpcke, H., Rehberg, B., Bouillon, T., & Hoeft, A. (2000). Electroencephalogram approximate entropy correctly classifies the occurrence of burst suppression pattern as increasing anesthetic drug effect. *Anesthesiology, 93*(4), 981.

Buades, A., Coll, B., & Morel, J.-M. (2005). A review of image denoising algorithms, with a new one. *Multiscale Modeling & Simulation, 4*(2), 490-530.

Cao, Y., Tung, W.-w., Gao, J. B., Protopopescu, V. A., & Hively, L. M. (2004). Detecting dynamical changes in time series using the permutation entropy. *PHYSICAL REVIEW-SERIES E-, 70*(4; PART 2), 046217-046217.

Castro, A., Almeida, F. G., Amorim, P., & Nunes, C. S. (2009). *A wavelet based method for steady-state detection in anesthesia.* Paper presented at the Engineering in Medicine and Biology Society, 2009. EMBC 2009. Annual International Conference of the IEEE.

Chen, D., Li, D., Xiong, M., Bao, H., & Li, X. (2010). GPGPU-aided ensemble empirical-mode decomposition for EEG analysis during anesthesia. *Information Technology in Biomedicine, IEEE Transactions on, 14*(6), 1417-1427.

Cutillo, L., Jung, Y. Y., Ruggeri, F., & Vidakovic, B. (2008). Larger posterior mode wavelet thresholding and applications. *Journal of Statistical Planning and Inference, 138*(12), 3758-3773.

Darbon, J., Cunha, A., Chan, T. F., Osher, S., & Jensen, G. J. (2008). *Fast nonlocal filtering applied to electron cryomicroscopy.* Paper presented at the Biomedical Imaging: From Nano to Macro, 2008. ISBI 2008. 5th IEEE International Symposium on.

Daubechies, I. (1992). *Ten lectures on wavelets* (Vol. 61): SIAM.

Davidson, A. J., Huang, G. H., Czarnecki, C., Gibson, M. A., Stewart, S. A., Jamsen, K., & Stargatt, R. (2005). Awareness during anesthesia in children: a prospective cohort study. *Anesthesia & Analgesia, 100*(3), 653-661.

Deledalle, C., Duval, V., & Salmon, J. (2012). Non-local methods with shape-adaptive patches (NLM-SAP). *Journal of Mathematical Imaging and Vision, 43*(2), 103-120.

Fan, S., Yeh, J., Chen, B., & Shieh, J. (2011). Comparison of eeg approximate entropy and complexity measures of depth of anaesthesia during inhalational general anaesthesia. *J. Med. Biol. Eng, 31*, 359-366.

Fell, J., Röschke, J., Mann, K., & Schäffner, C. (1996). Discrimination of sleep stages: a comparison between spectral and nonlinear EEG measures. *Electroencephalography and Clinical Neurophysiology, 98*(5), 401-410.

Gelb, A. W., Leslie, K., Stanski, D. R., & Shafer, S. (2010). Monitoring the depth of anesthesia. *Millers Anesthesia. 7th Ed. Philadelphia: Churchill Livingstone*, 1251-1253.

Ghanatbari, M., Mehridehnavi, A., Rabbani, H., Mahoori, A., & Mehrjoo, M. (2010). *A comparative study of the output correlations between wavelet transform, neural and neuro fuzzy networks and BIS index for depth of anesthesia.* Paper presented at the 2010 IEEE Symposium on Industrial Electronics & Applications (ISIEA).

Ghoneim, M., & Block, R. I. (1997). Learning and memory during general anesthesia: an update. *Anesthesiology, 87*(2), 387-410.

Gifani, P., Rabiee, H., Hashemi, M., & Ghanbari, M. (2005). *Extraction of anesthesia depth using self similarity and fluctuation analysis on the wavelet coefficients of EEG.* Paper presented at the The 3rd IEE International Seminar on Medical Applications of Signal Processing (Ref. No. 2005-1119).

Hall, J., & Lockwood, G. (1998). Bispectral index: comparison of two montages. *British journal of anaesthesia, 80*(3), 342-344.

He, P., Wilson, G., & Russell, C. (2004). Removal of ocular artifacts from electro-encephalogram by adaptive filtering. *Medical and biological engineering and computing, 42*(3), 407-412.

Jensen, E. (2005). Cerebral state monitoring and pharmacodynamic modelling by advanced fuzzy inferencestate of the art. *Präsentation vorgestellt auf: AMCA*.

Johansen, J. W. (2006). Update on bispectral index monitoring. *Best Practice & Research Clinical Anaesthesiology, 20*(1), 81-99.

Johansen, J. W., Sebel, P. S., & Sigl, J. C. (2000). Clinical impact of hypnotic-titration guidelines based on EEG bispectral index (BIS) monitoring during routine anesthetic care. *Journal of clinical anesthesia, 12*(6), 433-443.

John, E. R. (2001). A field theory of consciousness. *Consciousness and Cognition, 10*(2), 184-213.

Jones, J., & Aggarwal, S. (2001). Monitoring the depth of anesthesia. *Awareness during anesthesia, 1*, 69-91.

Jordan, D., Stockmanns, G., Kochs, E. F., Pilge, S., & Schneider, G. (2008). Electroencephalographic order pattern analysis for the separation of consciousness and

unconsciousness: an analysis of approximate entropy, permutation entropy, recurrence rate, and phase coupling of order recurrence plots. *Anesthesiology, 109*(6), 1014-1022.

Kim, J., Hyub, H., Yoon, S. Z., Choi, H., Kim, K. M., & Park, S. (2014). *Analysis of EEG to quantify depth of anesthesia using Hidden Markov Model.* Paper presented at the Engineering in Medicine and Biology Society (EMBC), 2014 36th Annual International Conference of the IEEE.

Kortelainen, J., Koskinen, M., Mustola, S., & Seppanen, T. (2008). Time–frequency properties of electroencephalogram during induction of anesthesia. *Neuroscience letters, 446*(2), 70-74.

Kortelainen, J., Vayrynen, E., & Seppanen, T. (2011a). Isomap approach to EEG-based assessment of neurophysiological changes during anesthesia. *Neural Systems and Rehabilitation Engineering, IEEE Transactions on, 19*(2), 113-120.

Kortelainen, J., Vayrynen, E., Jia, X., Seppanen, T., & Thakor, N. (2012). *EEG-based detection of awakening from isoflurane anesthesia in rats.* Paper presented at the Engineering in Medicine and Biology Society (EMBC), 2012 Annual International Conference of the IEEE.

Kortelainen, J., Vayrynen, E., & Seppanen, T. (2011b). Depth of anesthesia during multidrug infusion: separating the effects of propofol and remifentanil using the spectral features of EEG. *Biomedical Engineering, IEEE Transactions on, 58*(5), 1216-1223.

Kuizenga, K., Wierda, J., & Kalkman, C. (2001). Biphasic EEG changes in relation to loss of consciousness during induction with thiopental, propofol, etomidate, midazolam or sevoflurane. *British journal of anaesthesia, 86*(3), 354-360.

Kuncheva, L. I., & Rodríguez, J. J. (2013). Interval feature extraction for classification of event-related potentials (ERP) in EEG data analysis. *Progress in Artificial Intelligence*, 1-8.

Lennmarken, C., Bildfors, K., Enlund, G., Samuelsson, P., & Sandin, R. (2002). Victims of awareness. *Acta anaesthesiologica scandinavica, 46*(3), 229-231.

Li, T.-N., & Li, Y. (2014). Depth of anaesthesia monitors and the latest algorithms. *Asian Pacific journal of tropical medicine, 7*(6), 429-437.

Li, T., Wen, P., & Jayamaha, S. (2014). Anaesthetic EEG signal denoise using improved nonlocal mean methods. *Australasian Physical & Engineering Sciences in Medicine, 37*(2), 431-437.

Li, T., Wen, P., & Liu, G. (2015). *Depth of Anaesthesia Assessment using the second order different plot technique and feature evaluation method.* Paper presented at the 2nd International Conference on Mechanical, Electronics and Computer Engineering, 24-26 Jan 2015, Zhuhai, China.

Li, X., Li, D., Liang, Z., Voss, L. J., & Sleigh, J. W. (2008). Analysis of depth of anesthesia with Hilbert–Huang spectral entropy. *Clinical Neurophysiology, 119*(11), 2465-2475.

Li, X., Sleigh, J., Voss, L., & Ouyang, G. (2007). Interpretation of anesthetic drug effect using recurrent dynamics of EEG recordings. *Neurosci Lett, 424*, 47-50.

Liang, Z., Li, D., & Li, X. (2009). *Comparison of permutation entropy index and Bispectral Index for monitoring effects of anesthetic drugs to brain activity.* Paper presented at the Biomedical Engineering and Informatics, 2009. BMEI'09. 2nd International Conference.

Liang, Z., Li, D., Ouyang, G., Wang, Y., Voss, L. J., Sleigh, J. W., & Li, X. (2012). Multiscale rescaled range analysis of EEG recordings in sevoflurane anesthesia. *Clinical Neurophysiology, 123*(4), 681-688.

Liu, Q., Wei, Q., Fan, S.-Z., Lu, C.-W., Lin, T.-Y., Abbod, M. F., & Shieh, J.-S. (2012). Adaptive computation of multiscale entropy and its application in EEG signals for monitoring depth of anesthesia during surgery. *Entropy, 14*(6), 978-992.

Mallat, S. (1999). *A wavelet tour of signal processing*: Academic press.

Mathews, D., Rahman, S., Cirullo, P., & Malik, R. (2005). Increases in bispectral index lead to interventions that prevent possible intraoperative awareness. *British journal of anaesthesia, 95*(2), 193-196.

Maynard, D., & Jenkinson, J. (1984). The cerebral function analysing monitor Initial clinical experience, application and further development. *Anaesthesia, 39*(7), 678-690.

McBride, J. C., Zhao, X., Munro, N. B., Smith, C. D., Jicha, G. A., Hively, L., . . . Jiang, Y. (2014). Spectral and complexity analysis of scalp EEG characteristics for mild cognitive impairment and early Alzheimer's disease. *Computer methods and programs in biomedicine, 114*(2), 153-163.

Mertins, A. Signal analysis: wavelets, filter banks, time-frequency transforms and applications. 1999: John Wiley & Sons Ltd, New York.

Moerman, N., Bonke, B., & Oosting, J. (1993). Awareness and recall during general anesthesia: facts and feelings. *ANESTHESIOLOGY-PHILADELPHIA THEN HAGERSTOWN-, 79*, 454-454.

Musizza, B., & Ribaric, S. (2010). Monitoring the depth of anaesthesia. *Sensors, 10*(12), 10896-10935.

Musshoff, F., Padosch, S., & Madea, B. (2005). Death during patient-controlled analgesia: piritramide overdose and tissue distribution of the drug. *Forensic science international, 154*(2), 247-251.

Myles, P., Leslie, K., McNeil, J., Forbes, A., Chan, M., & Group, B.-A. T. (2004). Bispectral index monitoring to prevent awareness during anaesthesia: the B-Aware randomised controlled trial. *The Lancet, 363*(9423), 1757-1763.

Nakamura, M., Sanjo, Y., & Ikeda, K. (1999). Predicted sevoflurane partial pressure in the brain with an uptake and distribution model: Comparison with the measured value in internal jugular vein blood. *Journal of clinical monitoring and computing, 15*(5), 299-305.

Nguyen-Ky, T. (2011). *Monitoring the depth of anaesthesia using simplified electroencephalogram (EEG).* University of Southern Queensland.

Nguyen-Ky, T., Wen, P., & Li, Y. (2010). An improved detrended moving-average method for monitoring the depth of anesthesia. *Biomedical Engineering, IEEE Transactions on, 57*(10), 2369-2378.

Nguyen-Ky, T., Wen, P., & Li, Y. (2013a). Consciousness and Depth of Anesthesia Assessment Based on Bayesian Analysis of EEG Signals. *IEEE Journals & Magazines, 60*(6), 1488-1498.

Nguyen-ky, T., Wen, P., & Li, Y. (2013b). *An improved Chaos method for monitoring the depth of anaesthesia.* Paper presented at the 2013 International Conference on Computing, Management and Telecommunications (ComManTel)

Nguyen-Ky, T., Wen, P., Li, Y., & Gray, R. (2011). Measuring and reflecting depth of anesthesia using wavelet and power spectral density. *Information Technology in Biomedicine, IEEE Transactions on, 15*(4), 630-639.

Olofsen, E., Sleigh, J., & Dahan, A. (2008). Permutation entropy of the electroencephalogram: a measure of anaesthetic drug effect. *British journal of anaesthesia, 101*(6), 810-821.

Pachori, R. B., & Patidar, S. (2014). Epileptic seizure classification in EEG signals using second-order difference plot of intrinsic mode functions. *Computer methods and programs in biomedicine, 113*(2), 494-502.

Pomfrett, C., & Pearson, A. (1998). EEG monitoring using bispectral analysis. *Engineering Science and Education Journal, 7*(4), 155-157.

Rampil, I. J. (1998). A primer for EEG signal processing in anesthesia. *Anesthesiology, 89*(4), 980-1002.

Repovš, G. (2010). *Dealing with Noise in EEG Recording and Data Analysis.* Paper presented at the Informatica Medica Slovenica.

Rezek, I., Roberts, S. J., & Conradt, R. (2007). Increasing the depth of anesthesia assessment. *Engineering in Medicine and Biology Magazine, IEEE, 26*(2), 64-73.

Rezek, I., Roberts, S. J., Siva, E., & Conradt, R. (2005). *Depth of anaesthesia assessment with generative polyspectral models.* Paper presented at the Fourth International Conference on Machine Learning and Applications.

Rodríguez, J. J., Alonso, C. J., & Maestro, J. A. (2005). Support vector machines of interval-based features for time series classification. *Knowledge-Based Systems, 18*(4), 171-178.

Rodrıguez, J. J., Alonso, C. J., & Boström, H. (2001). Boosting interval based literals. *Intelligent Data Analysis, 5*(3), 245-262.

Romero, S., Mañanas, M. A., & Barbanoj, M. J. (2008). A comparative study of automatic techniques for ocular artifact reduction in spontaneous EEG signals based on clinical target variables: a simulation case. *Computers in biology and medicine, 38*(3), 348-360.

Ryynanen, O., Hyttinen, J., & Malmivuo, J. (2004). *Study on the spatial resolution of EEG-effect of electrode density and measurement noise.* Paper presented at the Engineering in Medicine and Biology Society, 2004. IEMBS'04. 26th Annual International Conference of the IEEE.

Saeid, S., & Chambers, J. (2007). EEG signal processing. *Chichester: John Willey & Sons. Ltd*.

Sandhu, K., & Dash, H. (2009). Awareness during anaesthesia. *Indian journal of anaesthesia, 53*(2), 148.

Sandin, R. H., Enlund, G., Samuelsson, P., & Lennmarken, C. (2000). Awareness during anaesthesia: a prospective case study. *The Lancet, 355*(9205), 707-711.

Sanei, S., & Chambers, J. A. (2008). *EEG signal processing*: Wiley-Interscience.

Schmidt, G. N., Bischoff, P., Standl, T., Jensen, K., Voigt, M., & Esch, J. S. (2003). Narcotrend® and Bispectral Index® monitor are superior to classic electroencephalographic parameters for the assessment of anesthetic states during propofol-remifentanil anesthesia. *Anesthesiology, 99*(5), 1072-1077.

Schmidt, R., & Franks, R. (1986). Multiple source DF signal processing: an experimental system. *Antennas and Propagation, IEEE Transactions on, 34*(3), 281-290.

Schneider, G., Schöniger, S., & Kochs, E. (2004). Does bispectral analysis add anything but complexity? BIS sub-components may be superior to BIS for detection of awareness. *British journal of anaesthesia, 93*(4), 596-597.

Sebel, P. S., Bowdle, T. A., Ghoneim, M. M., Rampil, I. J., Padilla, R. E., Gan, T. J., & Domino, K. B. (2004). The incidence of awareness during anesthesia: a multicenter United States study. *Anesthesia & Analgesia, 99*(3), 833-839.

Service information manual, Aspect Medical Systems, Inc.

Shalbaf, R., Behnam, H., Sleigh, J. W., Steyn-Ross, D. A., & Steyn-Ross, M. L. (2014). Frontal-Temporal Synchronization of EEG Signals Quantified by Order Patterns Cross Recurrence Analysis During Propofol Anesthesia.

Silva, A., Campos, S., Monteiro, J., Venâncio, C., Costa, B., de Pinho, P. G., & Antunes, L. (2011). Performance of anesthetic depth indexes in rabbits under propofol anesthesia: prediction probabilities and concentration-effect relations. *Anesthesiology, 115*(2), 303-314.

Snaedal, J., Johannesson, G. H., Gudmundsson, T. E., Gudmundsson, S., Pajdak, T., & Johnsen, K. (2010). The use of EEG in Alzheimer's disease, with and without scopolamine–A pilot study. *Clinical Neurophysiology, 121*(6), 836-841.

Sweeney-Reed, C., & Nasuto, S. (2007). A novel approach to the detection of synchronisation in EEG based on empirical mode decomposition. *Journal of Computational Neuroscience, 23*(1), 79-111.

Takamatsu, I., Ozaki, M., & Kazama, T. (2006). Entropy indices vs the bispectral index™ for estimating nociception during sevoflurane anaesthesia. *British journal of anaesthesia, 96*(5), 620-626.

Taslimi, P., Rabiee, H. R., & Shakouri, G. (2009). *An empirical centre assignment in RBF network for quantification of anaesthesia using wavelet-domain features.* Paper presented at the NER'09. 4th International IEEE/EMBS Conference on Neural Engineering.

Thuraisingham, R. A., Tran, Y., Boord, P., & Craig, A. (2007). Analysis of eyes open, eye closed EEG signals using second-order difference plot. *Medical & biological engineering & computing, 45*(12), 1243-1249.

Tonner, P., & Bein, B. (2006). Classic electroencephalographic parameters: median frequency, spectral edge frequency etc. *Best Practice & Research Clinical Anaesthesiology, 20*(1), 147-159.

Tracey, B. H., & Miller, E. L. (2012). Nonlocal Means Denoising of ECG Signals. *Biomedical Engineering, IEEE Transactions on, 59*(9), 2383-2386.

Urban, B., & Bleckwenn, M. (2002). Concepts and correlations relevant to general anaesthesia. *British journal of anaesthesia, 89*(1), 3-16.

Van De Ville, D., & Kocher, M. (2009). SURE-based non-local means. *Signal Processing Letters, IEEE, 16*(11), 973-976.

Vanluchene, A., Struys, M., Heyse, B., & Mortier, E. (2004). Spectral entropy measurement of patient responsiveness during propofol and remifentanil. A comparison with the bispectral index. *British journal of anaesthesia, 93*(5), 645-654.

Vetterli, M., & Herley, C. (1992). Wavelets and filter banks: Theory and design. *Signal Processing, IEEE Transactions on, 40*(9), 2207-2232.

Viertiö‐Oja, H., Maja, V., Särkelä, M., Talja, P., Tenkanen, N., Tolvanen‐Laakso, H., . . . Meriläinen, P. (2004). Description of the Entropy™ algorithm as applied in the Datex‐Ohmeda S/5™ Entropy Module. *Acta anaesthesiologica scandinavica, 48*(2), 154-161.

Wei, Q., Liu, Q., Fan, S.-Z., Lu, C.-W., Lin, T.-Y., Abbod, M. F., & Shieh, J.-S. (2013). Analysis of EEG via multivariate empirical mode decomposition for depth of anesthesia based on sample entropy. *Entropy, 15*(9), 3458-3470.

Willmann, K., Springman, S., Rusy, D., & Daily, E. (2002). A preliminary evaluation of a new derived EEG index monitor in anesthetized patients. *Journal of clinical monitoring and computing, 17*(6), 345-350.

Wong, K. F. K., Smith, A. C., Pierce, E. T., Harrell, P. G., Walsh, J. L., Salazar, A. F., . . . Mukamel, E. A. (2011). *Bayesian analysis of trinomial data in behavioral experiments and its application to human studies of general anesthesia.* Paper presented at the Engineering in Medicine and Biology Society, EMBC, 2011 Annual International Conference of the IEEE.

Xu, L., Ivanov, P. C., Hu, K., Chen, Z., Carbone, A., & Stanley, H. E. (2005). Quantifying signals with power-law correlations: A comparative study of detrended fluctuation analysis and detrended moving average techniques. *Physical Review E, 71*(5), 051101.

Ye, Z., Tian, F., & Weng, J. (2006). *EEG signal processing in anesthesia-using wavelet-based informational tools.* Paper presented at the 27th Annual International Conference on Engineering in Medicine and Biology Society. IEEE-EMBS

Yu, L. (2009). *EEG De-Noising Based on Wavelet Transformation.* Paper presented at the 3rd International Conference on Bioinformatics and Biomedical Engineering. ICBBE

Zandi, A. S., Dumont, G. A., Yedlin, M. J., Lapeyrie, P., Sudre, C., & Gaffet, S. (2011). Scalp EEG Acquisition in a Low-Noise Environment: A Quantitative Assessment. *Biomedical Engineering, IEEE Transactions on, 58*(8), 2407-2417.

Zhang, L., Wu, D., & Zhi, L. (2009). *Method of removing noise from EEG signals based on HHT method.* Paper presented at the 2009 1st International Conference on Information Science and Engineering (ICISE)

Zhang, X.-S., Roy, R. J., & Jensen, E. W. (2001). EEG complexity as a measure of depth of anesthesia for patients. *Biomedical Engineering, IEEE Transactions on, 48*(12), 1424-1433.

Zikov, T., Bibian, S., Dumont, G. A., Huzmezan, M., & Ries, C. R. (2006). Quantifying cortical activity during general anesthesia using wavelet analysis. *Biomedical Engineering, IEEE Transactions on, 53*(4), 617-632.